Trafficking and endocytosis of BRI1 and SERK receptors

Josephina Catharina Maria Aker

Trafficking and endocytosis of BRI1 and SERK receptors

Josephina Catharina Maria Aker

Proefschrift
ter verkrijging van de graad van doctor
op gezag van de rector magnificus
van Wageningen Universiteit,
Prof. Dr. M.J. Kropff,
in het openbaar te verdedigen
op woensdag 8 oktober 2008
des namiddags te half twee in de Aula

Voor Ed, Sanne en Nienke

Contents

Chapter 1

Regulation of cell-surface receptors

Abstract

Membrane receptors are important proteins to relay a signal, by perception of a chemical or physical signal. This usually takes place from the outside of the cell to the inside and ultimately leads to activation or inhibition of transcription and therefore genetic control of a cell. Degradation regulates the level and activity of membrane receptor proteins, using two processes: endocytosis after mono-ubiquitination, leading to signaling, sorting and either recycling or finally to degradation in the lysosomes or vacuoles, or endocytosis after poly-ubiquitination that leads directly to degradation in the proteasome.

Receptors involved in brassinosteroid signaling

Brassinosteroids (BRs) are plant hormones recognized by the Brassinosteroid receptor like kinase BRI1 (Brassinosteroid Insensitive1), a member of the leucine rich repeat receptor like kinase (LRR-RLK) family in Arabidopsis. BRI1 contains 25 LRRs, separated by a 70 amino acid island domain between LRR 21 and 22, a single transmembrane domain (TM), and an intracellular kinase domain. Its co-receptor, SERK3 (Somatic Embryogenesis Receptor like Kinase) or BAK1 (BRI associated kinase1) was identified based on genetic and yeast two-hybrid screens (Li et al., 2002; Nam and Li, 2002). SERK3 comprises a short, 5 LRR containing extracellular domain, a TM domain and a kinase domain. Together they function in stimulation of cell elongation, leaf unrolling, xylem differentiation and cell division, and in inhibition of root elongation, radial stem expansion and anthocyan biosynthesis. Other processes involving BRs are male sterility, timing of flowering and senescence and leaf development (Altmann, 1999; Kauschmann et al., 1996; Li and Chory, 1997; Nam and Li, 2002; Szekeres et al., 1996). Brassinosteroid mutants, lacking the ability to synthesize or perceive BRs, exhibit a dwarfed stature, round leaves and reduced male fertility.

The model for BRI1's activation is derived from the work of Wang et al. (Wang et al., 2005). BRI1 in the absence of BRs is in a homodimeric state. The BRI1- receptors are kept in an auto-inhibitory conformation by the C-terminal (CT) domain of BRI1 due to hyperphosphorylation of the kinase-domains. Upon binding of BL, the most active brassinosteroid, to the extracellular domain of BRI1, a conformational change of the kinase domain is induced and leads to phosphorylation of the CT domain that releases auto-inhibition and enhances autophosphorylation further. The fully activated receptor then forms a multimeric complex with its co-receptors which transduces the BR signal. After steroid binding to the extracellular domain of the BRI1-kinase, BKI1, an inhibiting substrate of BRI1 kinase is released from the PM, which increases the affinity of BRI1 for BAK1/SERK3 (Wang and Chory, 2006). Oligomerization of the BRI1/BAK1 receptors and transphosphorylation of the kinase domains takes place (Wang et al., 2005). This inhibits, via an unknown pathway, the phosphorylation of BZR1 (Brassinazole resistant 1), by the BIN2 (BR insensitive 2) kinase, and when phosphorylated, is translocated to and retained in the cytoplasm via the 14-3-3λ protein (Gampala et al., 2007). Moreover BR activates the phosphatase BSU1 (BRI1 suppressor protein1), that dephosphorylates BES1 (BRI1 EMS Suppressor 1). Subsequently, accumulation of BSU1- mediated dephosphorylated nuclear-localized BES1 and BZR1 transcription factors induces gene transcription (Vert and Chory, 2006). (Fig. 1)
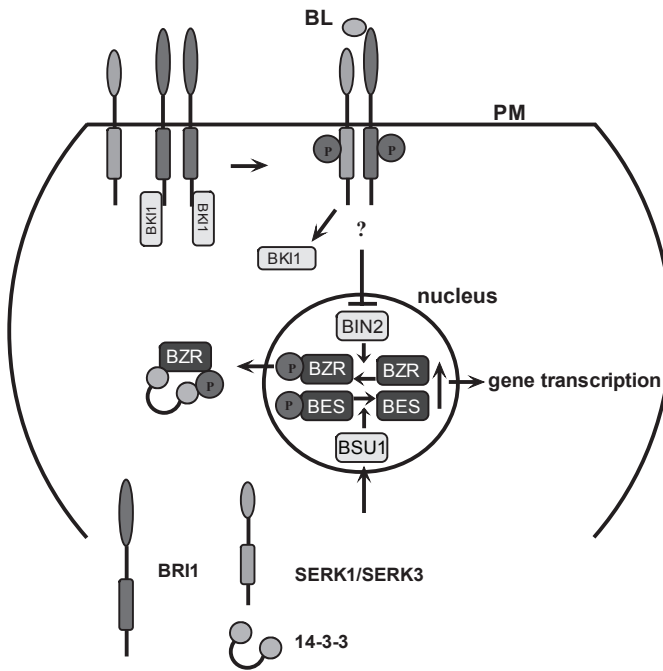
Figure 1. The brassinosteroid signaling pathway (Aker and de Vries, 2008).
Upon hetero-dimerization of the receptors, transphosphorylation of the kinase domains takes place, resulting in dephosphorylation of the nuclear-localized BES1 and BZR1 transcription factors that control gene transcription, by BIN2 and BSU1. A 14-3-3 protein retains phosphorylated BZR1 in the cytoplasm.

Recent evidence suggests that BAK1/SERK3 is not the only co-receptor of BRI1. Another family member of SERK3, SERK1 also interacts with BRI1 (Karlova et al., 2006). The SERK1 complex was immuno-precipitated from transgenic seedlings and found to contain both the BRI1 and SERK3 proteins. In addition, were identified the KAPP (Kinase Associated Protein Phosphatase) protein, a member of the 14-3-3 family, and the AAA ATPase CDC48A (Cell Division Cycle protein A), as well as two putative transcriptional regulators. Of these the KAPP, 14-3-3, and CDC48A proteins were previously also found in a yeast two-hybrid screening (Rienties et al., 2005), suggesting a direct interaction with the SERK1 receptor. For SERK1, SERK3, and BRI1, it was shown that they localize to the PM as well as in to endosomes and co-localize there with the phosphatase KAPP (Russinova et al., 2004; Shah et al., 2002).

BAK1/SERK3 was also found to interact with the LRR-RLK FLS2 (Flagellin Sensitive 2) that is involved in plant defense (Chinchilla et al., 2007). Furthermore BAK1 participates in

FLS2-independent PAMP (pathogen-associated molecular patterns) recognition, possibly via interaction with other receptors, and together with SERK4/BKK1 (BAK like 1) regulates BR dependent growth and BR independent cell death (He et al., 2007).

The binding of a ligand to their extracellular part activates receptors. But how are the levels and activities of membrane receptor proteins regulated? After dimerization and trans-phosphorylation the signal is ultimately transduced to proteins in the nucleus that regulate transcriptional activation. After triggering, the receptors need to be de-activated and degraded, or recycled to the PM. The CDC48A protein could function in degradation of the SERK1 protein. It has been shown to function in ERAD (Endoplasmic Reticulum-associated degradation) for the barley (Hordeum vulgare) MLO-1 receptor (Müller et al., 2005), and could likewise play a role in targeting of misfolded SERK1 proteins to the proteasomal pathway. Another function could be the inactivation of plasma membrane receptors after endocytosis. The proteasomal pathway as well as the endosomal pathway will be described in the following sections. The signal for degradation of receptors in the proteasome is ubiquitination, and aberrations in this process lead to several serious diseases in animals (Mukhopadhyay and Riezman, 2007). Ubiquitination is also the signal for receptors to enter into the endosomal pathway.

Ubiquitination as a signal for de-activation of receptors

For animal receptors, after ligand binding and subsequent phosphorylation, ubiquitination is used as a sorting signal for translocation into endosomes or to the proteasomal machinery. Phosphorylation itself is probably the signal for post-translational modification by the small molecule ubiquitin (Tang et al., 2003). Ubiquitin is a 76-amino acid protein that binds covalently to mostly lysine residues on the substrate protein. Ubiquitin binding is a three-step process, involving an E1 ubiquitin-activating enzyme, an E2 ubiquitin-conjugating enzyme and an E3 ubiquitin-ligase, which determines the specificity (Figure 2, and reviewed in (Hicke and Dunn, 2003). Among the E3-ligases, the Skp (in plants ASK1), Cullin and F-box containing SCF complex is the best understood. The F-box is responsible for target recognition, and Cul1 and ASK1 together with a fourth protein, RBX1, form the active E3-ligase (Jurado et al., 2008).

Proteins can be modified by a single ubiquitin (mono-ubiquitination), more single ubiquitins at different places (multi-ubiquitination), or by polymeric ubiquitin chains (poly-ubiquitination). The kind of ubiquitin modification determines the fate of the substrate protein. Mono-ubiquitination serves as a signal for endocytosis of PM proteins, sorting of proteins to the MVBs, budding of retroviruses, DNA-repair and transcriptional activation. Poly-ubiquitination has mainly been associated with targeting substrates to the proteasome. However, other functions, like DNA repair, inflammatory response, the endocytic pathway and ribosomal protein synthesis are also described. Different linkages between the single ubiquitins are possible between each of the seven internal lysines in one, and the C-terminal glycine in another ubiquitin molecule. Linkage through Lys48 seems to be important for targeting to

the proteasome, while linkage through Lys63 leads to other functions (reviewed in (Haglund et al., 2003).

Many lines of evidence showed that different ubiquitin-dependent processes occur in animal cells as well as in plant cells. The best-characterized function of ubiquitin is its role as a signal for the entry of endocytic cargo into vesicles both at the PM and at the late endosome. In the yeast Saccharomyces cerevisiae, ubiquitin appears to be the major signal to recruit G-protein coupled receptors (GPRCs) and other cargo into vesicles budding form either the PM or the MVB (Reggiori and Pelham, 2001). Signal transducing receptors are one class of proteins that undergo regulated internalization after receptor stimulation. Animal Receptor tyrosine kinases (RTKs) like the EGF receptor (Shtiegman and Yarden, 2003) use ubiquitination as a signal to promote internalization into early endosomes and to sort the receptors for delivery into the MVB or lysosomes. Unlike the yeast GPCRs and the RTKs, the known mammalian GPCRs appear to require ubiquitination only as a sorting signal at the MVB level, not at the PM. Although then at the PM, other ubiquitinated proteins, like β-arrestin, bind to the tail of GPCRs to recruit the receptor after ligand stimulation to the clathrin-dependent endocytic machinery. So lysine residues in the receptor itself are not required for ubiquitination, but β-arrestin-ubiquitination promotes rapid endocytosis (Shenoy and Lefkowitz, 2003).

Signaling receptors of the immune system are also regulated by ubiquitination. Ubiquitination-dependent endocytosis has also been co-opted by viruses to down-regulate the host immune system as an evasion system. Virus encoded E3-ligases modify normally stable PM proteins like the MHC class 1 (major histocompatability class1) molecules, functioning in antigen presentation, with an ubiquitin signal that directs them to lysosomes for irreversible inactivation and degradation (Coscoy et al., 2001; Hewitt et al., 2002).

Transporters and channels account for another large class of molecules that undergo ubiquitin-mediated endocytosis. In yeast, peptide and sugar transporters are ubiquitinated and use the signal for internalization and endosomal sorting (Katzmann et al., 2002). In mammalian cells, ion channels are down regulated by lysosomal degradation after ubiquitination (Staub O et al., 1997).

As ubiquitination is a post-translational modification so widely used to regulate cellular processes, aberrations in ubiquitination can lead to various diseases. Inhibition of degradation of the epidermal growth factor receptor family member ERBB2 has emerged in a variety of cancers (reviewed (Warren and Landgraf, 2006). On the other hand, enhanced degradation of tumor suppressor proteins has the same effect. In plants, much less is known about the role of ubiquitination in regulation of receptors. Recently, a multidimensional Protein identification technology (Mudpit) was employed to analyze ubiquitinated proteins in Arabidopsis (Maor et al., 2007). The authors could, amongst other proteins, identify several plant receptors; a putative ethylene receptor ETR2, a LRR-transmembrane protein kinase, and a Toll-like receptor involved in plant disease resistance TIR-NBS-LRR (Toll/Interleukin1 receptor-nucleotide binding site-LRR), showing that ubiquitination also plays a role in regulation of plant receptors. The receptors mentioned were all found to be mono-ubiquitinated. Poly-ubiquitination also plays a role in regulation the levels of plant receptors. The barley stem rust-resistance

protein Rpg1, a receptor-like protein kinase, is degraded in the proteasome after poly-ubiqui-tination, upon infection with the stem rust fungus Puccinia graminis. It is proposed that the degradation process itself, or the products, activate a signaling pathway that results in disease resistance (Nirmala et al., 2007). How the plant proteasome functions will be discussed in the next section.
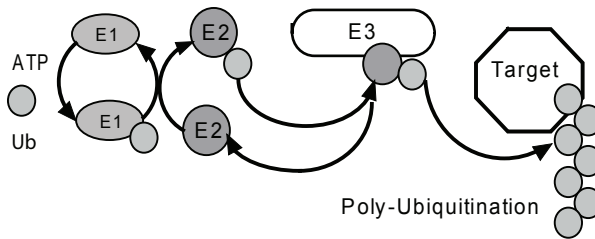
The plant proteasome

In eukaryotes the proteasome serves as the proteolytic component in the Ubiquitin Protea-some System (UPS), which controls the degradation of misfolded and damaged proteins. In the Arabidopsis genome about 5% of the genome encodes proteins with a function or homol-ogy to proteins of the UPS system. The UPS system recognizes two classes of proteins; first the misfolded and damaged proteins that are recognized by their loss of tertiary structure. The second class comprises functional proteins that carry specific degradation signals; sec-ondary modifications like phosphorylation or dephosphorylation that changes the protein's stability after signaling and promotes interaction with an E3 ligase. As a consequence, two general functions of the UPS can be distinguished: first, the quality control of misfolded and damaged proteins and second, the cellular regulation through degradation of regulatory pro-teins (Kurepa and Smalle, 2008).

The Arabidopsis 26S proteasome consists of the 20S core particle (CP) and the 19S regulatory particle (RP) that contains a base and a lid (Fig. 2). In the CP, proteins are degraded, while the RP base contains RPT proteins; mostly ATPases necessary for ATP hydrolysis to unfold target proteins and to open the entrance to the core proteolysis compartment. The RP base also contains non-ATPase proteins (RPNs) for docking of ubiquitinated proteins. The RP lid contains RPN proteins for assembly and integrity of this subunit and 1 RPN that harbors de-ubiquitination activity.

The role of proteasomal degradation in plants

Proteasomal degradation plays an important role in many processes including plant develop-ment. Developmental responses to the phytohormone auxin are controlled by the activity of the auxin-inducible genes. Without auxin, transcription is repressed by the AUX/IAA transcriptional repressors. In response to auxin, AUX/IAA repressors are degraded, thereby inducing gene expression. The F-box protein TIR1 (conferring E3 ligase specificity), which was identified as the auxin receptor in plants (Dharmasari et al., 2005; Kepinski and Leyser, 2005), binds to these proteins in an auxin-dependent manner, thereby controlling this process (Gray et al., 2001).

Protein ubiquitination
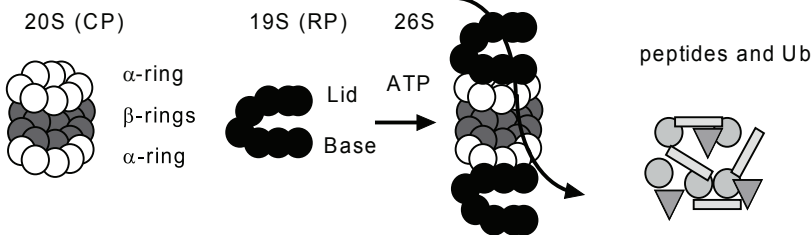
Figure 2. The plant UPS system.
Ubiquitin binding is a three-step process, involving a ubiquitin-activating enzyme (E1), a ubiquitin-conjugating enzyme (E2) and a ubiquitin-ligase (E3), which determines the specificity. Poly-ubiquitination leads to degradation in the proteasome, consisting of the 20S core particle (CP) and the 19S regulatory particle (RP) that contains a base and a lid. (J Aker, adapted from Kurepa and Smalle, 2008).

The ubiquitin-specific protease AtUBP14 is essential for disassembly of multi-ubiquitin chains. Mutants of AtUBP14 cause an embryo-lethal phenotype, and arrested seeds contain increased levels of multi-ubiquitin chains, showing that the proteasomal pathway and UBP14 in particular is essential for early embryo development (Doelling et al., 2001). Mutations in CUL4, one of 11 cullin proteins in Arabidopsis that functions in a protein-complex as an E3 ligase, severely affect various aspects of development (Bernhardt et al., 2006).

Secondly, proteasomal degradation plays a role in transcriptional regulation. An example in plants is the involvement of an SCF E3 Ub ligase in the degradation of DELLA proteins, the transcriptional repressors of gibberelin (GA) responsive growth. GA binds to the soluble Gibberelin receptor GID1 (GIBBERELIN-INSENSITIVE DWARF1). Upon binding of GA to GID1, the formation of a GID1-DELLA complex enhances the interaction with the SLEEPY1 (SLY1) SCF E3 ligase and promotes poly-ubiquitination and degradation of the DELLAs (Griffiths et al., 2006).

Proteasomal activity also plays a role in regulation of the amount of cell cycle regulators and rapid degradation of the spindle apparatus and phragmoplast. The proteasome subunits expression is highly upregulated in actively dividing cells, showing that it plays an important role in cell division (reviewed in (Kurepa and Smalle, 2008).

Another function is the reprogramming of the cellular metabolism after developmental changes that involve dramatic changes in reorganization of cells and tissues, as e.g. after artificially induced somatic embryogenesis (Stasolla et al., 2004).

Proteasomal regulation also plays a role in programmed cell death (PCD), although evidence seems to be somewhat contradictionary. Several studies have shown that suppression of proteasome activity leads to PCD in plants (Kurepa and Smalle, 2008), but a recent report states that proteasome activity is required for the PCD in heat-shocked tobacco cells (Vacca et al., 2007).

Furthermore, proteasomes where shown to be involved in the defense responses in a number of plant species. A key component of the plant defense response system is the formation of Reactive Oxygen Species (ROS), which suppresses directly pathogen viability and movement to other cells. The expression of 3 din (defense induced) subunits of the 20S CP is correlated with the induction of ROS (Suty et al., 2003).

To conclude, proteolysis is essential for cell survival and helps to regulate the cell's response to the changing environment.

Proteasomal degradation of membrane-proteins; the role of CDC48 proteins

A way to control the levels of receptors is degradation in the proteasome. Poly-ubiquitinated substrates are delivered to the proteasome via ubiquitin receptors that bind to the ubiquitin moiety and the proteasome. The AAA family of proteins (ATPases Associated with various cellular activities) plays a role in this targeting. The yeast and animal AAA ATPases Cdc48 or p97/VCP are involved in various activities as diverse as cell cycle regulation, transcriptional activation, membrane fusion and ERAD of misfolded proteins (Müller et al., 2005; Woodman, 2003). AtCDC48A is a member of this family and was found in a protein-complex immuno-precipitated from Arabidopsis seedlings together with SERK1. Although the ATPases are also involved in proteasome-independent functions, many substrates of CDC48 proteins are eventually degraded in the proteasome. The physiological role of AAA ATPases is to generate mechanical force to disrupt or fuse molecular structures by means of ATP binding and hydrolysis. AAA proteins are comprised of an N-domain, two stacked hexameric rings; the domains D1 and D2 that are connected by a linker and are responsible for binding and hydrolysis of ATP and a C-terminal tail.

P97/VCP or Cdc48p proteins participate in the fusion of the ER-membrane (Latterich et al., 1995; Zhang et al., 1994), via stable binding to the cofactor p47 (Shp1), which together interact with syntaxin 5. Syntaxin 5 is a membrane-localized p47-receptor and a family member of the t-SNARE proteins (target soluble NSF (N-ethylmaleimide-sensitive) attachment protein receptors (Rabouille et al., 1998). Syntaxin 5 proteins on two close membranes pair to form a complex, resulting in fusion of these membranes. The p97/p47 complex is suggested to act as a chaperone in this process. P47 recruits p97 via its ubiquitin regulatory X (UBX) domain and mediates post-mitotic fusion of Golgi and ER-membranes. Halawani and Latterich (Halawani and Latterich, 2006) propose a more active role for p97 in substrate recognition and presenta-

tion to ubiquitin ligases, in contrast to the commonly accepted model where substrates are recognized after being processed by the ubiquitination machinery.

Apart from the cofactor p47, other proteins like Ufd1/NP14 were found having ubiquitin binding capacity. There is a difference in the recognition of mono- or poly-ubiquitinated substrates. P47 binds preferentially to mono-ubiquitinated proteins, linking to non-degradative functions of p97 in membrane fusions while Ufd1/Np14 bind to poly-ubiquitinated substrates, required for p97 functions related to the ubiquitin/proteasome pathway (Dai et al., 1998; Meyer et al., 2002). The interaction between the mentioned cofactors and p97 takes place at the N-terminus of the hexamer (Dreveny et al., 2004; Meyer et al., 2000). Other ubiquitin binding cofactors, like Ufd2 and Ufd3, dock at the C-terminal domain of a substrate-occupied p97 complex (Rumpf and Jentsch, 2006).

Furthermore, for both VCP as well as for Cdc48p, de-ubiquitination enzymes (VCIP135 and Otu1) where found to be associated, and this appeared to be important for organelle membrane fusion (Rumpf and Jentsch, 2006; Uchiyama and Kondo, 2005).

AAA ATPases also facilitate the translocation of misfolded proteins over the ER-membrane via interaction with cofactors that recognize and bind ubiquitinated substrates (Fig. 3). In yeast an integral ER membrane UBX protein, Ubx2, was found that recruits Cdc48 to the ER. Ubx2 mediates binding of Cdc48 to the E3 ligases Hrd1 and Doa10 and to ERAD substrates.

Figure 3. The ERAD-system in yeast
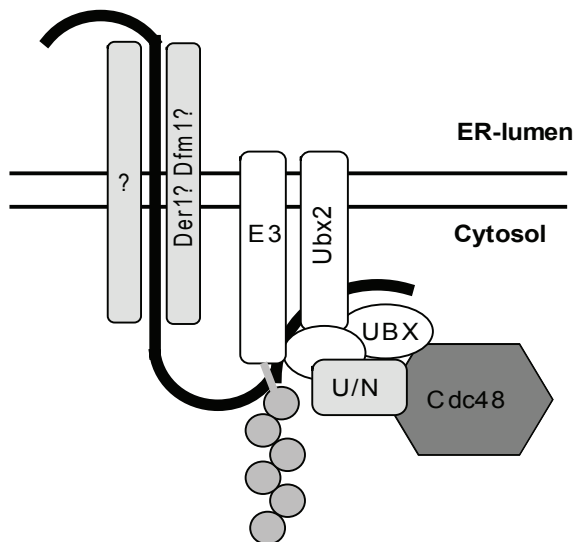ERAD substrate emerging from a dislocation pore in the ER-membrane speculatively composed of Der1, Dfm1, and/or other pore proteins ('?') is recognized by an ERAD ubiquitin ligase (E3) and covalently modified with a ubiquitin chain (circles). The ubiquitinated substrate is bound by Cdc48 in complex with its cofactors Ufd1−Npl4 (U/N) (J Aker, adapted from (Schuberth and Buchberger, 2005).

To conclude, all these different functions make the AAA ATPase p97/VCP/Cdc48p or CDC48A an intriguing membrane complex protein involved in recognizing ubiquitinated membrane proteins. Because evidence in animal receptor biology suggest that ubiquitination is one of the first events after receptor activation (Hicke, 1997; Lowe et al., 2006; Shenoy, 2007), CDC48 proteins in plants may be involved both in the initiation and the termination of signaling pathways.

Endocytosis

Endocytosis, the invagination of membrane compartments leading to small vesicles called endosomes, can occur by several mechanisms. Endocytic pathways in mammals involve clathrin-mediated, caveolae or lipid raft mediated, or caveolin independent endocytosis, fluid-phase endocytosis and phagocytosis. The nature of the internalized cargo, the size of the vesicles and the associated proteins determine the different mechanisms of endocytosis (Samaj et al., 2005).

Clathrin-mediated endocytosis in animal cells is the best-understood; after the assembly of clathrin coats on membranes, vesicle invagination and fission takes place, followed by movement of vesicles into the cytoplasm. Subsequently the vesicle is uncoated and fusion takes place with the early endosome. Adaptor proteins like Epsins and Adaptins AP2 and AP180 bind to cytoplasmic domains of receptors and recruit clathrin to form a clathrin coat on the inner side of the PM. Endophilin is involved in invagination, and the GTPase Dynamin is required for the fission of clathrin coated vesicles (CCVs) from the PM. SH3-domain containing proteins provide scaffolding for various proteins of CCV trafficking. In plants several components involved in clathrin-dependent endocytosis have been identified. These include clathrin itself (Blackbourn and Jackson, 1996), adaptor proteins like AP180, adaptins (Barth and Holstein, 2004) and SH3P proteins involved in the fission and uncoating of clathrin-coated vesicles (Lam et al., 2001). Dhonukshe et al (Dhonushke et al., 2007) showed clathrin and clathrin-coated pits at the PM of Arabidopsis cells, and co-localization of clathrin vesicles with PIN1 and PIN2-GFP containing endosomes.

The classical view on receptor endocytosis has long been a mechanism to inactivate receptors and down-regulate signaling. This view has been changed based on observations that endosomes contain large amounts of receptors and key signaling components. This led to the suggestion that endocytosis is required to bring the components for signaling to the activated receptors and to the hypotheses that 1) endocytosis adds an additional layer of specificity to signaling pathways through compartmentalization; and 2) endocytosis is required for trafficking of signaling complexes to specific cellular locations (reviewed in (Lei and Martinez-Moczygemba, 2008; McPherson et al., 2001; Varghese et al., 2008).

The role of endocytosis in plants

Several lines of evidence suggest a role for regulated endocytosis in plant development. For example, it was shown in growing root hairs and pollen tubes that FM4-64, a membrane-dye extensively used to track endomembrane compartments, accumulated strongly in the apex of growing root hairs and pollen tubes, soon after application (Samaj et al., 2006).

Endocytosis and endosomes play an important role in cell wall morphogenesis. Baluska et al. (Baluska et al., 2002) showed that cell wall pectins were internalized and that these endosomal pectins serve as preformed building blocks for the formation of new cell walls. These would also provide the cell plate that is established within minutes, with new building material (Baluska et al., 2002; Dhonukshe et al., 2005).

Another function of endocytosis is the internalization of plant specific auxin efflux carriers (PIN proteins) necessary for the regulation of auxin efflux (Geldner et al., 2003). Fast recycling of PIN proteins is necessary for polar transport of auxin, therefore continuous cycling of PIN between the PM and the endosomal compartment takes place. It was shown that auxin promotes its own efflux by regulating endocytic activity of carrier proteins like PIN1 (Paciorek et al., 2005) and PIN2 (Abas et al., 2006).

Endocytosis also plays a role in the regulation of ion channels and transporters. An example in Arabidopsis is the boron transporter AtBor1, which accumulates in the PM under low boron conditions, whereas it gets internalized and degraded after boron concentrations rises to toxic levels (Takano et al., 2005).

Endocytosis regulates activities and levels of receptors. The first example of receptor- mediated endocytosis (RME) in plants is the ligand-dependent internalization of the Flagellin Sensitive2 (FLS2) receptor in Arabidopsis (Robatzek et al., 2006). The FLS2 receptor localizes to the PM and gets internalized into endosomal compartments upon stimulation with flg22, a 22 amino acid (AA) bacterial flagellin peptide, a known elicitor of basal defense response (Gomez-Gomez et al., 2001). Prolonged stimulation of FLS2 fused to GFP led to a complete loss of GFP fluorescence in epidermal and mesophyll cells, suggesting a degradation of the FLS2 receptor. For Arabidopsis CRINKLY4 (ACR4) it was shown that the protein's function and internalization are linked to a rapid protein turnover (Gifford et al., 2005).

Compartments, markers and molecules of the plant endomembrane system

The endomembrane system in plants, like in animals, comprises membrane-derived organelles of which the function is defined by the presence of specific resident proteins (Müller et al., 2007).

Receptors or other membrane proteins that are internalized, first show up in early endosomes (EE). Proteins determined for recycling either go back to the PM immediately or first pass the recycling or sorting endosomes (RE/SE). From the EEs they can also be transported to the trans golgi-network (TGN). Proteins destined for degradation are packed and delivered to multivesicular bodies (MVBs), also called prevacuolar compartments (PVCs). From these PVCs, proteins can be degraded in lytic vacuoles or returned to the TGN, from which early
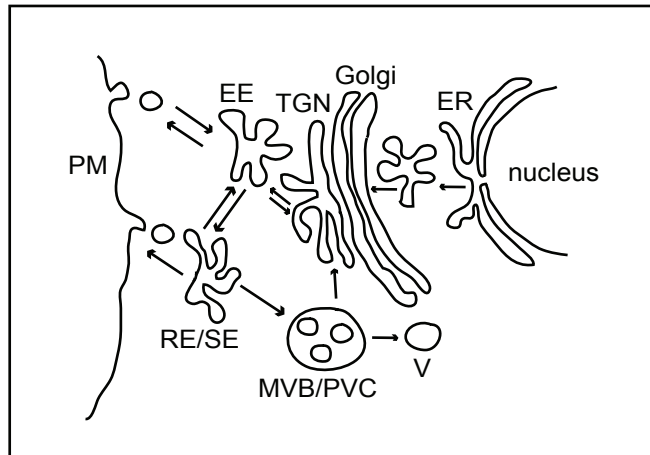
Figure 4. The plant endomembrane system.
Receptors or other membrane proteins that are internalized, first show up in early endosomes (EE). Proteins determined for recycling either go back to the PM immediately or first pass the recycling or sorting endosomes (RE/SE). From the EEs they can also be transported to the trans golgi-network (TGN). Proteins destined for degradation are packed and delivered to multi vesicular bodies (MVBs), also called prevacuolar compartments (PVCs), and can move on to the vacuoles or back to the TGN (J Aker).

endosomes pinch off on their way to the PM (Dettmer et al., 2006; Geldner, 2004; Geldner and Jurgens, 2006; Müller et al., 2007) See Figure 4.

Early endosomes are the first station in the endocytic pathway in plants. They accumulate endocytic tracers within 2-5 min and serve as sorting compartments for newly internalized proteins.

The TGN is the station where major sorting events occur, being the only compartment in the cell where endocytic and secretory pathways meet. Hence, this organelle must comprise distinct sorting domains for receiving recycling receptors from the PM as well as recycling proteins from the MVBs. Furthermore specific domains must be involved in receiving newly produced proteins from the Golgi. Recently, Lam et al. (Lam et al., 2007) proposed a model where the TGN, EEs and REs are one continuous organelle serving all the above-mentioned functions.

MVBs are spherical and contain inner luminal vesicles derived from membranous invaginations. In plants, markers for the prevacuolar compartment (PVC) were recently localized to the MVB (Tse et al., 2004), which makes PVCs and MVBs less distinct than in animals and are probably the same compartment in plants. Recently it became apparent that like in mammals, a retromer complex is present in Arabidopsis (Oliviusson et al., 2006). The retromer is a protein complex known to be responsible for retrograde transport of vacuolar cargo receptors from the MVB/PVC to the TGN. Other cargo of the MVB is destined for the degradation pathway and from this station transported to the late endosomes (LE) or the vacuoles. In animal and yeast it was shown that mono-ubiquitination is needed for proteins to

become recognized by ESCRT complexes. These complexes first mediate the internalization of mono-ubiquitinated proteins into luminal vesicles of the MVB before they are delivered to the vacuole or lysosomes (Babst, 2005; Katzmann et al., 2001) All components of the ESCRT complex are also encoded in the Arabidopsis genome (Spitzer et al., 2006).

Several Rab GTPases are specific markers of plant endosomes (Lam et al., 2007). Rab GT-Pases play a role in tethering an incoming vesicle to the correct target organelle. Rab GTPases constitute a large family of small G-proteins that function as molecular switches that oscillate between GTP-and GDP bound conformations. Their regulatory function is restricted to the membrane compartments where they are localized. Each transport step requires the binding of activated Rab proteins to soluble effectors that mediate the process (reviewed by Nielsen et al, 2008). In Arabidopsis 57 members are known. ARA6 (AtRaBF1) and ARA7 (AtRaBF2) that have high homology with the mammalian Rab GTPase, RaB5, are most used as molecular markers. In Arabidopsis ARA6 and ARA7 co-localized with internalized membrane dye FM4-64. ARA6, however, resides only on the early endosomal compartments, while ARA7 localizes to early and late endosomes like the prevacuolar compartment (Samaj et al., 2005; Vermeer et al., 2006). Rha1 is another Rab GTPase localized to early and late endosomes.

After the tethering of membranes through the Rab GTPases, the specific pairing of cognate SNAREs (soluble NSF attachment protein receptor) between the two bilayers ensures precision in the fusion event. SNAREs are enriched in certain organelles, but during vesicle transport spread inevitably throughout many cellular compartments. The Arabidopsis genome encodes 54 t-SNAREs, of which 17 localize to both the PM and to endosomes (Uemura, 2004). Some SNAREs are characterized as specifically involved in fusion events on distinct endosomal compartments and are therefore used as molecular markers. AtSYP41 for example is used as a marker for the TGN, while SYP21 is associated with a late endosomal compartment (Uemura et al., 2004).

Another often-used late endosomal marker is the FYVE-domain. In animal cells, the FYVE domain is a conserved motif that localizes PI(3)P-binding proteins to endosomes (Gillooly et al., 2000). In Arabidopsis protoplasts FYVE localized to endosomes and the nucleus, but also strongly to the vacuole membrane (Vermeer et al., 2006).

Several drugs are used as tools to study endocytosis. The fungal toxin Brefeldin A (BFA) is an inhibitor of several ADP ribosylation factor guanine exchange factor (ARF-GEF) by binding to the ARF and its ARF-GEF. BFA was shown to inhibit Golgi-dependent secretion and also endosomal post-Golgi trafficking. GNOM, the first ARF-GEF discovered in plants is BFA-sensitive and necessary for PIN1 re-localisation (Geldner et al., 2001). BFA treatment led to a rapid and reversible accumulation of PIN1 in "BFA" compartments. PIN1 remained at the PM upon BFA treatment of $GNOM^{M696L}$ root tips, which suggested that the ARF-GEF GNOM is responsible for the recycling of PIN1 from endosomes to the PM (Geldner et al., 2003). BFA not only induced intracellular accumulation of plasma membrane proteins, but also pectins of the cell wall (Baluska et al., 2002), which suggests that BFA induces also uptake of material from the cell wall.

Tyrphostin A23, a generally used inhibitor of the recruitment of endocytic cargo in the clath-

rin-mediated pathway, inhibited PIN2 endocytosis, while other proteins still internalized, as shown by FM4-64 uptake. FM4-64 is a lypohylic membrane dye that stains the PM immediately after application, and internalizes with the membrane. Ten minutes after application, components of the endomembrane system are stained, but after longer incubation time also the Golgi is stained.

Concanamycin A is used as a vacuolar (V) -ATPase inhibitor. This compound blocks H+ V-ATPases and causes alkalinization of the TGN and recycling endosomes and prevents receptor recycling between the Golgi and endosomal compartments (Machen et al., 2003; Robinson et al., 2004).

Conclusions and perspectives

Remobilization by endocytosis and degradation of receptors together regulate the levels and activities of membrane receptor proteins. Two processes lead to degradation of receptors; first poly-ubiquitination of proteins, that targets them to the proteasome. Second, endocytosis after mono-ubiquitination, that leads aside from recycling, to degradation in the lysosomes or vacuoles. An important and yet unresolved question is how and when the decision is made for mono- or poly-ubiquitination of proteins, and hence the direction of trafficking of membrane-receptors. A hypothesis is that a modification like phosphorylation and subsequent conformational changes precedes ubiquitination and endocytosis (Tang et al., 2003). The sub-cellular localization of interacting partners and/or the trafficking of signaling complexes to specific cellular locations could determine the direction of the receptors. The research described in this thesis tries to extend the knowledge on plant receptor endocytosis and trafficking, which processes may start or terminate signaling activity.

Outline of this thesis

One of the major goals of this thesis is to understand the function of CDC48A when present in the SERK1-complex. In addition, the function of SERK1 and SERK3 as the co-receptors of BRI1 was investigated.

In this thesis we have investigated the interaction that was found between SERK1 and CDC48A, in a yeast two hybrid screen and subsequently in a complex immuno-precipitated from Arabidopsis seedlings (Karlova et al., 2006; Rienties et al., 2005). In chapter 2 the location of the co-localizing SERK1 and CDC48A proteins is described and the interaction is measured at these sites of interactions, using Förster Resonance Energy Transfer based Fluorescence Lifetime Imaging Microscopy (FRET-FLIM). SERK1 and CDC48A co-localize and interact at the PM in domains comprising ER-membranes, confirming the possible role of CDC48A in the ER-associated degradation of misfolded proteins. In chapter 3 it is shown that the SERK1 receptor interacts with the hexameric form of the CDC48A protein. FRET-FLIM revealed that SERK1 fused to yellow fluorescent protein (YFP), interacts with the N-terminus as well as the C-terminus of the CDC48 proteins fused to cerulean fluorescent protein (CFP). Also it was shown that SERK1 interacts with the, active, hexameric form of the CDC48A protein

and not with the monomeric form. In the N-domain of CDC48A, responsible for most of the interactions with other proteins (Dreveny et al., 2004; Meyer et al., 2000), Ser-41 was found to be phosphorylated by the SERK1 kinase. The C-terminal peptides could not be recovered by MS-MS, which might contain additional targets for the SERK1 receptor and explain the interaction of SERK1 at the C-terminus of CDC48A. Calculation of the diffusion coefficient of the hexameric full length CDC48A protein fused to an YFP tag, using Fluorescence Correlation Spectroscopy (FCS), showed that the CDC48A protein diffuses very slowly. A deletion mutant lacking the domain which is required for hexamerization, the D2 domain, diffused much faster, confirming that in protoplasts the full length CDC48A-YFP fusion protein is a hexamer. The calculated size of the CDC48A hexamer was much larger than expected, suggesting that in the cell it is predominantly found in a bigger protein complex. Deletion of the N-domain of the CDC48A indeed reduced the diffusion time of the complex.

In chapter 4 the role of the co-receptors SERK1 and SERK3 in endocytosis of the BRI1 receptor is investigated. Over-expression of SERK3 enhanced BRI1 endocytosis in Arabidopsis root tips from double transgenic lines containing BRI1-GFP and SERK3-HA. However BRI1-mediated signaling was not enhanced. Roots of a double mutant line lacking both SERK1 and SERK3, was completely insensitive to BL. BR signaling of BRI1-GFP crossed in this background was very much impaired, while the absence of the co-receptors in root tips did not affect the distribution of fluorescent BRI1 protein on the PM compared to the cytoplasm in cells in which all 3 receptors are normally expressed. However, the total amount of BRI1 protein was decreased, probably due to higher turn-over rate of the BRI1-receptor, which suggested that SERK1 and SERK3 aid in stability of the main receptor BRI1.

In chapter 5 the cellular compartment where interaction between BRI1 and its co-receptors takes place is investigated. Therefore a double line expressing BRI1 fused to GFP as well as SERK3 fused to HA was employed. Using immuno-staining on fixed tissue, endosomal compartments containing both receptors could be distinguished which accumulated after application of BFA in so-called "BFA compartments". BRI1-containing endosomes were fully sensitive to BFA, while only a small part of the SERK3- or SERK1-containing endosomes appeared to be sensitive, suggesting that most of the SERK3 and SERK1 endosomes require another ARF-GEF for recycling than the BFA-sensitive endosomes. However, a small portion of SERK3 co-localized with BRI1 endosomes, which is probably the part that is active in BRI-mediated signaling. In the absence of the co-receptors BR signaling in roots is largely inhibited but the roots are also almost insensitive to BFA, compared to wt roots. BRI1 in roots were the co-receptors are lacking is still sequestered to BFA-bodies, showing that BRI1-mediated signaling predominantly takes place from internalized BRI1/SERK1/SERK3 receptor complexes. Finally, FRET-FLIM confirmed the interaction between the receptors in these BFA-sensitive, accumulated, endosomal compartments.

In chapter 6 the conclusions are summarized.

Chapter 2

The Arabidopsis thaliana AAA protein CDC48A interacts in *vivo* with the Somatic Embryogenesis Receptor-like Kinase 1 receptor at the plasma membrane

José Aker, Jan Willem Borst, Rumyana Karlova, Sacco de Vries

Abstract

Fluorescent Cell Division Cycle (CDC) 48 proteins were studied in living plant protoplasts. CDC48A and SERK1 were found to co-localize in the endoplasmatic reticulum (ER) and at the plasma membrane (PM), but not in endosomal compartments. Fluorescent lifetime imaging microscopy (FLIM) was used to detect Förster resonance energy transfer (FRET) between CrFP/YFP tagged CDC48A and SERK1. FRET is indicative of direct protein-protein interaction. CDC48A was found to interact only with SERK1 in small areas at the PM, but not in endosomes. These findings confirm and extend our previous findings that CDC48A in plants directly interacts with SERK1.

Introduction

The transmembrane Somatic Embryogenesis Receptor like Kinase 1 (SERK1) is a member of a small subset of leucine rich repeat receptor like kinases (LRR RLKs) in Arabidopsis thaliana. In plants the SERK1 protein is found in the plasma membrane (PM) of both male and female gametophytes and in the surrounding sporophytic cell layers such as the tapetum and integument. Later the protein is found in all cells of the embryo and in seedlings it becomes restricted to vascular tissue of roots, shoots and leaves (Albrecht et al., 2005; Hecht et al., 2001; Kwaaitaal et al., 2005). Ectopic expression of the SERK1 gene results in enhanced embryogenic cell formation (Hecht et al., 2001), while a *serk1* knockout mutant does not show a clear phenotype unless it is combined with the *serk2* mutant. The *serk1serk2* double mutant is male sterile due to a failure of tapetum specification (Albrecht et al., 2005).

Previously we have shown that in yeast the SERK1 kinase domain (amino acids 266-625) interacts with the C-terminal part of the Cell Division Cycle (CDC) 48A protein (amino acids 747-806) and co-immunoprecipitates with the protein in Arabidopsis cultured cells (Karlova et al., 2006). In vitro the SERK1 kinase is able to transphosphorylate CDC48A (Rienties et al., 2005) and in vivo CDC48A was identified in a complex with the SERK1 receptor, immuno-precipitated from SERK1-expressing seedlings (Karlova et al., 2006). CDC48A gene expression was shown in floral buds in the developing microspores and in tapetum cells, in the vascular tissue of the anther and in ovules (Feiler et al., 1995). This expression pattern overlaps with the SERK1 expression in plants (Kwaaitaal et al., 2005). At a sub cellular level, the CDC48A protein was found in the nucleoplasm (Feiler et al., 1995), at the phragmoplast, and also in punctate structures distributed in the cytoplasm of both dividing and non-dividing cells (Rancour et al., 2002). CDC48A has 76% identity with the mammalian 97-kDa vasolin-containing protein (p97-VCP).

CDC48A is a member of the ATP-ases Associated with various cellular Activities (AAA-proteins). The central theme in the biochemical function of these ATP- ases is the coupling of ATP hydrolysis to the unwinding, disassembly, or unfolding of protein substrates (Woodman, 2003). The overall structure of one protomer comprises a N-domain important for ubiquitinated substrate and co-factor binding, two highly conserved AAA domains, a D1 domain important for hexamerization, a D2 domain responsible for the major ATPase activity and a C-terminal tail. AAA proteins are only active as a hexamer (Wang et al., 2003a). One activity of p97-VCP or the yeast orthologue CDC48p is to mediate the ubiquitin/proteasome-dependent degradation of proteins. Evidence that mammalian VCP is involved in receptor protein degradation comes from studies using the non tyrosine kinase-type cytokine surface receptors Il-9, Il-2 and the Erythropoietin receptor (Yen et al., 2000). VCP undergoes tyrosine phosphorylation in a cytokine dependent manner and associates with the receptor complex leading to poly-ubiquitination of the receptor. This suggests that VCP targets the receptor to the proteasome for degradation. The p97-VCP complex members Ufd1and NPl4 are co-factors forming heterodimers, binding to the N-domain of p97 and to ubiquitinated substrates (Meyer et al., 2000). The p97-Ufd1-NPI4 complex was shown to be involved in ER associated degradation (ERAD) of inositol 1,4,5-triphosphate (IP3) receptors in the ER membrane, upon

ligand-induced receptor ubiquitination (Alzayady et al., 2005).

Not many functions are described for Arabidopsis CDC48A. (Rancour et al., 2002) showed that the protein can be involved in membrane fusions, as it co-fractionated with the soluble NSF attachment protein receptor (SNARE) proteins SYP21, SYP31 and the cell plate SNARE KNOLLE from Arabidopsis suspension-cultured cells. SNARES are involved in heterotypic fusion of secretory vesicles with their acceptor compartment as well as in homotypic fusion of ER membranes and vacuoles. Arabidopsis CDC48A was also shown to play a role in ERAD-like quality control. A dominant negative CDC48A mutant stabilized a mutant barley (Holdeum vulgare) powdery mildew resistance o receptor (mlo-1) in Arabidopsis protoplasts, showing that CDC48A is necessary for degradation of misfolded proteins (Müller et al., 2005). Substrate ubiquitination is an important feature in this process.

While we have previously shown that SERK1 and CDC48A are part of the same protein complex in Arabidopsis seedlings, it is unknown in which cell compartment this CDC48- and SERK1-containing complex resides. To answer this question, both CDC48 and SERK1 were tagged with the green fluorescent protein (GFP) variants, cerulean and yellow fluorescent protein (CrFP and YFP) and co-expressed in leaf mesophyll protoplasts. Förster Resonance Energy Transfer (FRET) was measured using Fluorescence Lifetime Imaging Microscopy (FLIM), a method increasingly used to measure protein-protein interactions in plant cells (Nougalli Tonaco et al., 2005; Russinova et al., 2004).

Our results show that SERK1 and CDC48A co-localize in the ER and at the plasma membrane but only interact in small ER domains at or close to the plasma membrane. No interaction was observed in endosomal compartments.

Methods

Construction of the CFP/YFP tagged proteins

AtSERK1-CrFP (tagged at the C-terminus), Ara6-YFP and YFP-HDEL-constructs were a gift from E. Russinova. CDC48C was PCR amplified from an EST (RAFL09-46-C07) with primers 5'GGGAGATCTCATATGTGAGGCATGGGGGAGGAGAGGTCGC3' and 5'CG-GGGTACCCTCGAGGGTAAAAGATGGCCC3' and fused to PCR amplified CrFP and YFP after digestion with Kpn1. The full-length tagged cDNA was inserted into pMON999 (Monsanto, St. Louis, MO) using Bgl2 and BamH1.

CDC48A was PCR amplified from an EST (RafL05-04-E20) with primers 5'GTACCCG-GGCATATGTGAGGCATGTCTACCCCAGCTGAA3' and 5'CGGGGTACCATTGTAGAGATCATCATCGTCCCC3'. The full-length cDNA was exchanged with CDC48C into pMON999-CrFP and -YFP using Nde1 and Kpn1, leading to C-terminally fluorescent tagged CDC48A and C. The N-D1 mutant of CDC48A was made by deleting the D1-D2 linker plus the D2 domain from the second Nco1-site which was in frame with the introduced Nco1–site at the start of the YFP. To generate the C-terminally tagged CrFP fusion to CDC48A, CrFP-CDC48C was generated first. Thereby cloning sites Nde1 and

Nhe1 where introduced, by which CDC48A, using PCR, was exchanged. The constructs were verified by sequencing and the size of the fused proteins was verified on Western-blot, using anti-GFP antibodies.

Arabidopsis protoplast isolation and transfection

Arabidopsis mesophyll protoplasts were prepared and transfected according to a protocol described by Sheen (2001) with modifications. The enzyme solution contained 1.5% w/v cellulase R10 (Yakult Hosha Co.) and 0.2% w/v pectinase from Rhizobus sp. (Fluka). Modifications were: 1)The enzyme solution did not contain β-mercapto-ethanol and BSA, and 2)The transfection was done for only 5 minutes in MMG (containing 0.2 M mannitol, 15 mM MgCl, 2 mM Mes pH5.7). Thirty μg DNA per transfection was used. After transfection, protoplasts were kept in W5 medium (154 mM NaCl, 125 mM CaCl2, 5 mM KCl, 2 mM Mes pH 5.7) in the presence of 1 mM glucose in 25 C under light conditions. Transfection efficiencies ranged from 10 to 50 % of the examined protoplasts.

FM4-64 was added in a concentration of 50 μM for 10 minutes on ice and cells were washed twice with W5 medium. Cells were resuspended in W5 plus 1mM of glucose and imaged immediately.

SDS-PAGE, native-PAGE and Western blotting

Sixteen to twenty hours after transfection protoplasts were lysed in RIPA-buffer (50 mM Tris pH 7.5, 150 mM NaCl, 1 mM MgCl2, 1 % NP40, containing a protease inhibitor tablet (Roche)) for 15 minutes on ice. Extracts were centrifuged for 7 minutes at 13.000 rpm at 4 degrees and soluble fractions were supplemented with SDS-PAGE loading buffer, denatured at 95 C for 5 min before loading on an 8% gel, next to a pre-stained marker. Gels were blotted on nitrocellulose. For Native PAGE, the soluble fractions were supplemented with Native-PAGE loading buffer and loaded on a native gel of 4 to 8% acrylamide. Gels were blotted on PVDF membrane. The marker part of the blot was stained with Coomassie immediately after the blotting. Monoclonal antibodies against CDC48A (or the homologue VCP) were obtained from BD Transduction Laboratories. Anti-YFP was generated by Isogen, according to standard procedure. The serum was purified on an YFP-protA column. Intensities of bands on the blots were compared using Gel Pro Analyzer.

Confocal Laser Scanning Microscopy

The CrFP and YFP fluorescence in protoplasts was imaged using a Confocal laser Scanning Microscope 510 (Carl Zeiss, Jena, Germany) excited at 458 and 514 nm with an Argon laser and the fluorescence was detected via a bandpass filter (CrFP: 470-500 nm, YFP: 535-590 nm). Chlorophyll was detected using a 650 long pass filter. FM4-64 was excited with a green He/Ne laser (543 nm) and fluorescence was detected with the bandpass filter 600-650 nm. In

combination with FM4-64, YFP was excited at 488 nm and measured with the bandpass filter 505 and 550 nm.

Fluorescence Lifetime Imaging Microscopy

FLIM was performed using a Biorad Radiance 2100 MP system (Hercules CA) combined with a Nikon TE 300 inverted microscope (Tokyo, Japan) as described by Russinova et al. (2004). For the FLIM experiments, the Hamamatsu R3809U MCP PMT (Hamamatsu city, Japan) was used, which has a time resolution of 50 ps. CrFP emission was selected using a 480DF30 band pass filter. Images with a frame size of 64 x 64 pixels were acquired, and the average count rate was around 104 photons per second for an acquisition time of 90 sec. (Borst et al. 2003). From the fluorescence intensity image the fluorescence lifetime is determined for each pixel. The full fluorescence decay per pixel is calculated for the donor molecule using a double exponential decay model. The fluorescence lifetime (τ values) can then be presented as a false color-coded image superimposed over the visible light image. The fluorescence lifetime of the (CrFP-tagged) donor molecule was fixed to 2450 picoseconds (ps) observed for SERK1-CrFP and to 2650 ps for CDC48A-CrFP.

From each cell expressing CrFP- and YFP- tagged proteins, three possibly interacting domains were chosen to determine mean fluorescence lifetime. Areas of the images in which chloroplasts were observed were not measured, due to high background fluorescence.

Results

SERK1 and CDC48A co-localize at the PM in confined regions

The subcellular localization of SERK1 and CDC48A was investigated in Arabidopsis cells. Both proteins were tagged at the C-terminus with either CrFP or YFP and transiently expressed in Arabidopsis mesophyll protoplasts under control of the 35S Cauliflower mosaic virus promoter. Confocal Laser Scanning Microscopy (CLSM) was used to examine the localization of the fluorescent proteins. CrFP and YFP fluorescence as well as chlorophyll autofluorescence was recorded in separate channels, after which the combination of all three was merged into an overlay image.

In single transfections CDC48A-CrFP was localized at the plasma membrane (PM) and in the cytoplasm (Fig.1A). In putative membrane compartments in an optical cross-section close to the nucleus, fluorescence is observed as well (Fig. 1D) while in about 20% of the positive cells fluorescence was observed primarily in the nucleus. Single transfections of SERK1-YFP demonstrated a localization at the PM (Fig. 1B), and in another optical cross-section of the cell also in vesicle-like compartments in the cytoplasm (Fig. 1C). These vesicle-like compartments were tentatively identified as endosomal compartments (Russinova et al. 2004). The amount of fluorescent SERK1 protein at the PM compared to the amount in vesicles varied from cell to cell and also varied in time after transfection. SERK1 tagged to YFP under control of the SERK1 promoter was shown to complement the male sterility phenotype
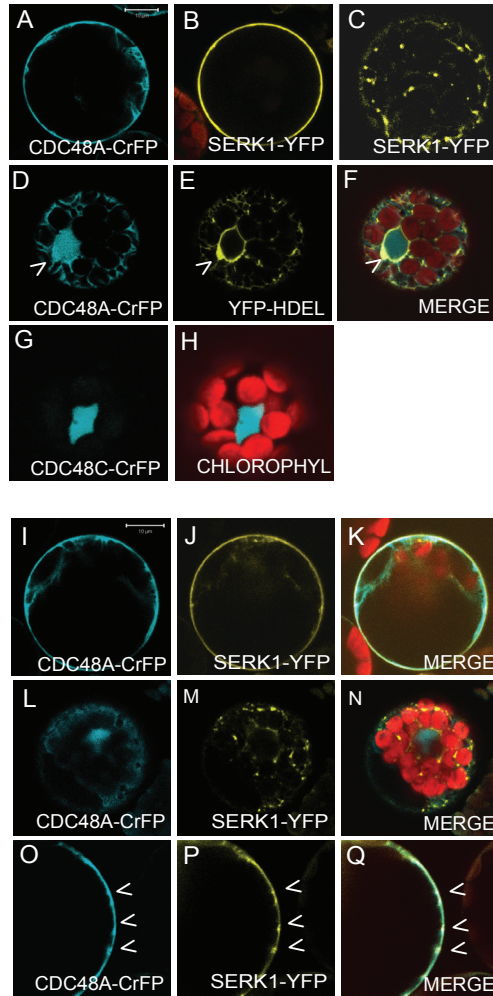
Figure 1. Co-localization of SERK1 and CDC48A in Arabidopsis protoplasts.
Confocal images of single transfections of CDC48A-CrFP at the plasma membrane (PM) (A), SERK1-YFP at the PM (B) and in another optical cross-section in vesicles (C) and CDC48C-CrFP (G), combined with chlorophyll in a merged image (H), recorded 16 h after transfection. CDC48A-CrFP (D) was co-expressed with the ER-marker HDEL-YFP (E) and the combined image is shown in (F). The arrowhead shows co-localization with the perinuclear ER.

The co-transfection of CDC48A-CrFP and SERK1-YFP is shown in image (I) to (Q). (I) to (K) show co-localization of CDC48A-CrFP (I) and SERK1-YFP (J) and the merged image (K) at the PM. (L) to (N) show co-transfection of CDC48A-CrFP (L) and SERK1-YFP (M) in another optical cross-section. CDC48A-CrFP and SERK1-YFP do not co-localize in vesicles in the cytoplasm. (O) to (Q) show a detail of the PM, where CDC48A-CrFP and SERK1-YFP show more co-expression in specific regions. Bars in A and I = 10 µm.

A. SDS-PAGE

B. Native-PAGE

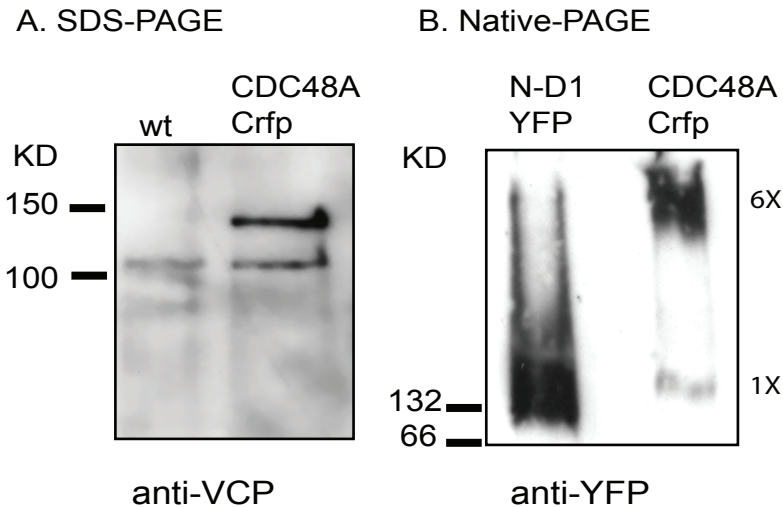**Figure 2. Expression of CDC48A-CrFP and the D2 domain deletion mutant N-D1-YFP in Arabidopsis protoplasts, shown by SDS- and Native-PAGE.**
Panel **A** shows lysates of non-transfected and transfected protoplasts expressing CDC48A-CrFP, submitted to SDS-PAGE and detected with anti-VCP, recognizing the N-domain of both endogenous and tagged CDC48A. The amount of tagged CDC48A protein was 4 times more then the endogenous CDC48, where 50% of the cells were transfected.
Panel **B** shows lysates of protoplasts transfected with the non-hexamerizing mutant N-D1-YFP and wt CDC48A-CrFP submitted to native-PAGE and detected with anti-YFP. Ninety-five % of the wt tagged CDC48A was in the hexameric state, whereas almost all of the N-D1-YFP protein retained the monomeric state. The marker is serum albumin, showing the monomer, 66 KD and the dimer 132 KD.

observed in *sk1sk2* double mutants, resulting in normal siliques and seeds (Albrecht et al. 2005). In addition SERK1-YFP was shown to be localized at the plasma-membrane and in endosomal compartments in plants (Kwaaitaal et al. 2005), suggesting that the SERK1-YFP fusion proteins in protoplasts are functional and the localization is in correspondence with the localization in plants.

The identity of CDC48A-CrFP containing compartments close to the nucleus was investigated by co-expression of CDC48A-CrFP (Fig. 1D) and YFP-HDEL as a marker for the endoplasmic reticulum (Fig. 1E). The latter construct contains the HDEL sequence, which was shown to efficiently retain proteins in the ER of plant cells (Gomord et al., 1997). Co-localization between CDC48A-CrFP and YFP-HDEL was indeed observed in this compartment (Fig. 1F), suggesting that the CDC48A protein is in part located in the ER. The subcellular protein localization of CDC48A-CrFP transiently expressed in protoplasts is similar to the localization of CDC48 as observed "in planta" (Feiler et al., 1995). To exclude that the relatively high amount of protein in the cytoplasm is due to over-expression, another AAA ATPase of Arabi-

dopsis thaliana, CDC48C (At3g01610) having 42% homology at protein level with CDC48A, was also expressed as a fluorescent fusion protein in protoplasts (Fig. 1G,H). The CDC48C-CrFP protein was only found in the nucleus, up to 2 days after transfections and in all of the transfected cells. The observed localization of the CDC48A-CrFP proteins therefore was not due to over-expression of the introduced construct. We conclude that both CDC48A and SERK1 fluorescent proteins faithfully reflect the localization of the endogenous proteins.

When CDC48A-CrFP and SERK1-YFP were co-expressed, co-localization only occurred at the PM (Fig. 1I,J,K). Co-expression of the two different proteins did not change their localization compared to the single transfections (Compare Fig. 1A with 1I, 1B with 1J, and 1C with 1M). No co-localization with CDC48A-CrFP was observed in the vesicle-like compartments that contain SERK1-YFP (Fig. 1L,M,N). Interestingly, in certain confined regions at the PM (arrowheads in Fig. 1O,P,Q), both SERK1 and CDC48A proteins appeared to be more concentrated. These regions resembled some of the SERK1-containing vesicles in the cytoplasm (Fig. 1M).

The amount of fluorescent CDC48A versions with a MW of 130 KD as compared to the endogenous amount of CDC48A in Arabidopsis protoplasts was determined using anti-VCP antibodies that recognize the N-domain of the CDC48 protein (Fig. 2A). Although cross-reaction with other CDC48 family-members cannot be ruled out, CDC48A is the most abundant member of the family and therefore most likely accounts for the majority of the proteins visualized by Western-blotting. In general about 50% of the cells used express the CDC48A-CrFP construct and since the amount of tagged protein is approximately 4 times higher then the endogenous amount, we estimate that there is at most 8 times more fluorescent fusion protein compared to endogenous CDC48. Only cells showing intermediate expression were examined for localization studies and FLIM-measurements.

To investigate whether the fluorescent CDC48A proteins are capable of achieving the biochemically active hexameric state (Wang et al., 2003a) native-PAGE was used to determine the size of the protoplast-expressed fluorescent fusions. For comparison a non-hexamerizing mutant of CDC48A was used containing only the N-domain plus the D1 domain fused to YFP. For VCP it was shown that this so-called N-D1 without the D1-D2 linker sequence is essentially non-hexameric in vitro (Wang et al., 2003b) In Arabidopsis protoplasts the CDC48A-CrFP fusion proteins were primarily found in the hexameric form (Fig. 2B). Only between 0 to 5% of the fusion proteins retained the monomeric state. For comparison, almost all of the non-hexamerizing N-D1-YFP protein was found as monomers (Fig. 2B). This result shows that fluorescently tagged CDC48A protein in protoplasts is hexameric and therefore can be enzymatically active.

SERK1 and CDC48A interact at the PM

Because the SERK1 receptor and the CDC48A proteins only co-localized at the PM and in a number of vesicle-like compartments close to the PM, we next asked whether interaction between both proteins also occurred in this location. The interaction between SERK1 and

CDC48A at the PM was investigated using FRET-FLIM analysis. FRET is the phenomenon that energy transfer from an excited fluorescent donor molecule (CFP) to a fluorescent acceptor molecule (YFP) occurs. After excitation FRET can take place when two proteins of interest that are fused to CFP and YFP are in close proximity, generally between 5 and 10 nm. This distance corresponds to inter-molecular protein-protein interactions (Bastiaens and Pepperkok, 2000; Hink et al., 2002). FLIM is one method to determine FRET by the estimation of the fluorescence lifetime of the CFP-donor molecule. Interaction between CFP and YFP molecules will lead to the reduction of the fluorescence lifetime of CFP which can then be spatially resolved.

FLIM was performed according to the single photon counting methodology as described in methods. The mean fluorescence lifetime ranges from a τ of 2.7 ns (dark-blue, no interaction) to a τ of 1.8 ns (orange-red, interaction) (Fig. 3). The fluorescence lifetime is a given value for each fluorophore and is dependent on the environment or other factors like the refractive index (Borst et al., 2005). It is therefore necessary to independently determine the lifetime for each donor molecule in the abscence of the acceptor molecule.

The mean lifetime of the donor molecule was first determined in cells expressing CDC48A-CrFP alone. Figure 3A shows an example of a fluorescence intensity image of CDC48A-CrFP. From this image the false-color coded image showing the fluorescence decay per pixel was calculated (Fig. 3B). The measurements of the number of cells investigated that were expressing CDC48A-CrFP alone are listed in Table 1 and yielded an average donor lifetime of 2.67 ns. The fluorescence lifetime of the donor molecule alone was homogenous along the whole PM (Fig. 3B). Subsequently CDC48A-CrFP and SERK1-YFP-tagged proteins were co-expressed and an example of a fluorescence intensity image is shown in Fig. 3C. In cells expressing both CDC48A-CrFP and SERK1-YFP a reduction in lifetime was observed at several positions at the PM (arrowheads in Fig. 3C,D). This observation suggests that whereas there is an obvious co-localization of the SERK1 receptor and the CDC48A protein at the PM, their true physical interaction is not evenly distributed. However, it seems that there is both a general reduction from 2.7 ns to about 2.4 ns and a number of "hot spots" where the observed reduction in lifetime was at most 1.8 ns. For every protoplast three of the positions with strongly reduced lifetime were analyzed and an average τ-value of 2.23 ns was calculated (Table 1). In the reciprocal experiment, SERK1-CrFP was used as the donor molecule and CDC48A-YFP as the acceptor. Both proteins showed exactly the same co-localization as their YFP- and CrFP-tagged counterparts. The mean lifetime of the SERK1-CrFP protein alone was 2.5 ns (Fig. 3E and Table 1). In cells expressing both SERK1-CrFP and CDC48A-YFP, we focused on a region at the PM where both proteins (Fig. 3F and Table1) showed a reduction in the fluorescence lifetime from 2.5 ns to 1.9 ns (Table 1). In Fig. 3G, an enlargement of Fig. 3F is shown. Of particular interest is the non-homogenous distribution of the interactions between the SERK1 receptor and the CDC48A protein. For comparison we also used the SERK1-CrFP and SERK1-YFP pair (Fig. 3H, Table 1) confirming the formation of SERK1 homodimers as shown previously (Russinova et al., 2004; Shah et al., 2002).
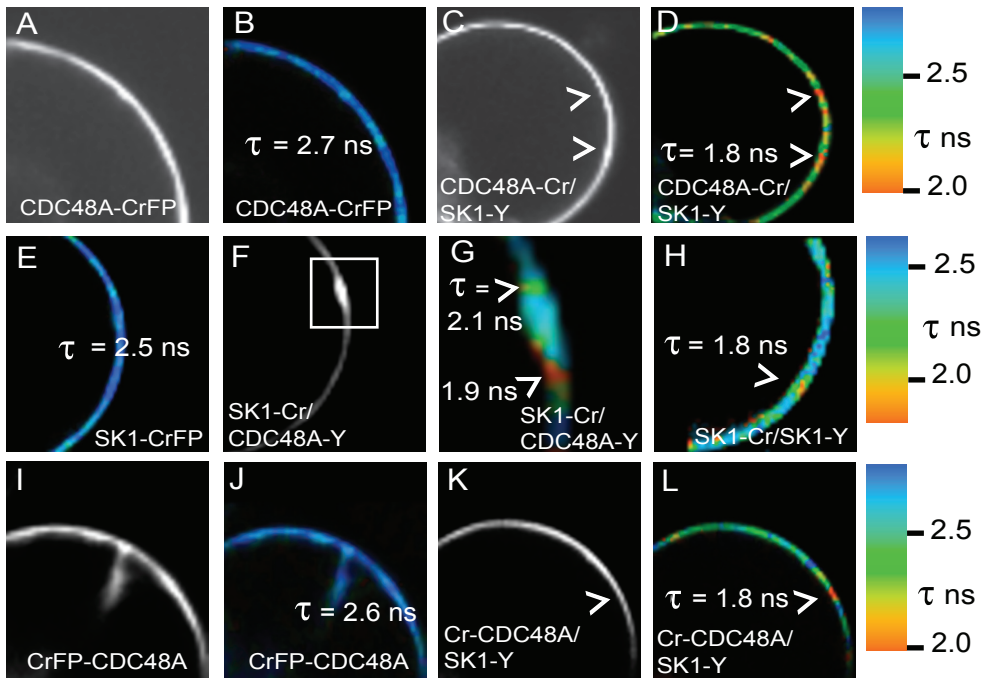
Figure 3. Interaction between SERK1 and CDC48A based on FRET measured by Fluorescence Lifetime Imaging Microscopy.

Examples of Fluorescent intensity images of CDC48A-CrFP alone (A) and CDC48A-CrFP/SERK1-YFP (C) recorded with FLIM, 16 h after transfection. From the fluorescent intensity image a pseudo-color lifetime image, displaying the lifetime per pixel was calculated (see Methods) for the donor CD-C48A-CrFP alone (B) and the co-expressed CDC48A-CrFP and SERK1-YFP (D). The average lifetime of three interacting points at the PM of each cell per expressed protein (-pair) is listed in Table 1. Donor lifetime on average was 2.7 ns (B). In (D) the arrowheads point to areas where a significant reduction in lifetime was measured in an example of a CDC48A-CrFP/SERK1-YFP transfected cell (τ= 1.8 ns).

The fluorescent lifetime image of SERK1-CrFP alone is shown in (E). The lifetime of SERK1-CrFP as the donor was on average 2.5 ns. The fluorescent intensity image of a region at the PM where SERK1-CrFP and CDC48A-YFP co-localize is shown in (F). In the corresponding pseudo-color lifetime image of the selected region, areas are indicated with lifetimes of 1.9 to 2.1 ns (arrowheads in G). In an example of a double transfection of SERK1-CrFP and SERK1-YFP (H) the arrowhead shows a reduction in lifetime to 1.8 ns. The fluorescent intensity image of N-terminally tagged CrFP-CDC48A is shown in Fig. 3I, the fluorescent lifetime image in J. The average lifetime of the donor was 2.6 ns, listed in Table 1. (K) and (L) show an example of the decay in lifetime of the CrFP-CDC48A co-expressed with SERK1. The arrowhead shows a reduction in lifetime to 1.8 ns.

The color bars from red to dark blue, corresponding with the experiments next to them, were set differently for CDC48A-CrFP and CrFP-CDC48A as the donor (2.0 to 2.8 ns) and 1.8 to 2.6 ns for SERK1-CrFP, because of differences in the average lifetimes of the respective donors (τ of CDC48A-CrFP (N or C) = 2.60 -2.67 ns, and τ of SERK1-CrFP = 2.5 ns).

Table 1.   FRET-FLIM analysis of CDC48A and SERK1 proteins in protoplasts.

Proteins	Lifetime τ (ns)	SD	n	N	N neg.
CDC48A-CrFP	2.67	0.05	7	31	
CDC48A-CrFP/SERK1-YFP	2.23	0.10	5	25	5
CrFP-CDC48A	2.60	0.05	2	10	
CrFP-CDC48A/SERK1-YFP	2.10	0.16	2	11	1
SERK1-CrFP	2.53	0.07	4	19	
SERK1-CrFP/CDC48A-YFP	1.90	0.18	2	9	1
SERK1-CrFP/SERK1-YFP	2.00	0.12	2	7	

Lifetime τ(ns) is determined as described in methods. SD is the standard deviation. n is the number of
independent experiments. N is the total amount of protoplasts analyzed.

It is evident that as observed for the interaction between CDC48 and SERK1, receptor ho-
modimerization is also not uniformly distributed along the membrane. A similar observation
was made for BRI1 receptor homodimers (Russinova et al., 2004).

To investigate if SERK1 could also interact with the N-terminal part of CDC48A, CrFP was
tagged to the N-terminus of the CDC48A protein. This protein showed the same localization,
and co-localization with SERK1-YFP, as the C-terminally tagged protein (data not shown).
The CrFP-CDC48 donor alone showed a lifetime of 2.6 ns (Fig. 3I and J). CrFP-CDC48A
co-expressed with SERK1-YFP showed a mean reduction in lifetime to 2.1 ns (Table 1), sug-
gesting an interaction between the SERK1 receptor and the N-terminal part of the CDC48A
protein. An example is shown in Fig. 3L again showing the same in homogenous distribution
as observed in Fig. 3D and 3G.

The C-terminal tail of the CDC48A homoloque VCP is disordered in the crystal structure,
and could in theory either remain at the active D2 domain, or extend back towards the N-do-
main. Therefore it is possible that SERK1-YFP binds to the C-terminus of CDC48A but still
interacts with the N-terminally tagged CrFP. The N-domain and C-domain of the hexamer
however, are located about 85 Å apart (DeLaBarre and Brunger, 2003), a distance too large
to result in FRET between a receptor bound to the C-terminal part of CDC48. Therefore we
conclude that the SERK1 receptor apparently can interact with the N- as well as the C-termi-
nal domain of CDC48A.

Our results show that the SERK1-protein and CDC48A physically interact close to and/or at
the plasma membrane in living cells. Because CDC48 proteins are not integral membrane
proteins, this interaction either occurs when the receptor is at the PM or when the receptors
are localized in the vesicle-like compartments close to the PM (cf. Fig. 1P and 1Q).

SERK1 and CDC48A co-localize in part of the ER and not in endosomes

To investigate the origin of the vesicle-like compartments at the PM where SERK1 and CD-C48A co-localize, we first co-expressed SERK1-CrFP or CDC48A-CrFP with Ara6-YFP. Ara6 is an Arabidopsis small GTP-ase, homologous to mammalian RAB5) which is an established marker for endosomal compartments (Samaj et al., 2005) and co-localizes with the lipophylic membrane dye FM4-64 (Ueda et al., 2001). The SERK1-CrFP containing vesicles all co-localized with Ara6-YFP at the PM (Fig. 4A,B arrowhead 1 and 2) and in the cytoplasmic area (Fig. 4A,B arrowhead 3 and 4). We could also confirm the co-localization of FM4-64 with SERK1-containing vesicles (Fig. 4D,E,F) suggesting that these vesicles derive from the PM and therefore contain internalized receptors, similar to what was shown for the homologous BAK1/SERK3 receptors (Russinova et al., 2004). However, there are many Ara6-YFP containing vesicles that do not contain SERK1-CrFP proteins, suggesting that only a subset of endosomal compartments is used for this particular type of receptors (Russinova et al., 2004). Next we co-transfected cells with CDC48A-CrFP (Fig. 4G) and Ara6-YFP (Fig. 4H). Surprisingly, in contrast to SERK1 none of the Ara6-YFP expressing vesicles contained CDC48A-CrFP (Fig. 4I). Therefore we conclude that the physical interaction between CDC48A and SERK1 is not taking place in an endosomal compartment.

CDC48A-CrFP was shown to co-localize with the ER-marker YFP-HDEL in the cytoplasm as well as at the PM (compare Fig. 1D,E,F with Fig.5A,B,C), suggesting that the observed colocalization of SERK1 and CDC48A at the PM indeed occurs in the ER. We therefore investigated whether SERK1-CrFP and YFP-HDEL also co-localize. Co-expression was observed between SERK1-CrFP and YFP-HDEL at or close to the PM (Fig. 5D and E) in structures that are reminiscent of the compartments where SERK1 and CDC48A co-localize (cf. Fig. 1O and 1P), but not in perinuclear ER structures. For comparison the co-expression of SERK1-CrFP with YFP-HDEL is shown in Fig. 5G and H, in which the arrowheads show the perinuclear ER. However, after treatment with the proteasome inhibitor MG132, that blocks the function of the 26S proteasome frequently associated with the ER (Fig. 5I) (Wojcik and DeMartino, 2003), a huge accumulation of SERK1 protein was visible in the perinuclear ER, apparently resulting from a complete block in the recycling of the protein. Therefore we propose that the failure of co-localization between SERK1 and YFP-HDEL in the perinuclear area is due to removal of the receptor towards its target, the PM. We conclude that CDC48A and SERK1 co-localize and interact only in the peripheral part of the ER membrane system, where it is located close to the PM.
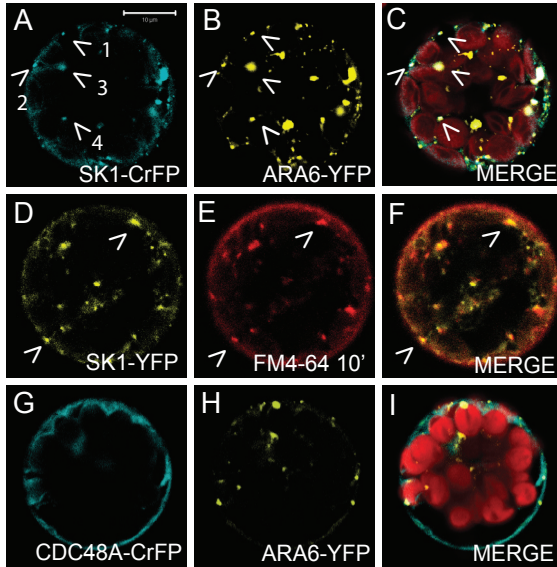
Figure 4. Co-localization of SERK1 vesicles with the endosomal marker Ara6 and the membrane dye FM4-64. Confocal images of Arabidopsis protoplasts (A) to (C) show double transfections with SERK1-CrFP (A) and Ara6-YFP (B). (C) Shows the merged image. Arrowheads indicate co-localization of the proteins; arrowhead 1 and 2 show co-localization at the plasma membrane, arrowhead 3 and 4 show co-localization in the cytoplasm. Images (D) to (F) show a single transfection of SERK1-YFP (D), co-stained with FM4-64 for 10 min (E) (see Methods), and shown in combined image (F). Arrowheads show co-localization between SERK1 and FM4-64. CDC48A-CrFP (G) was co-transfected with Ara6-YFP (H) and showed no co-localization (I). Bar in A = 10 µm.
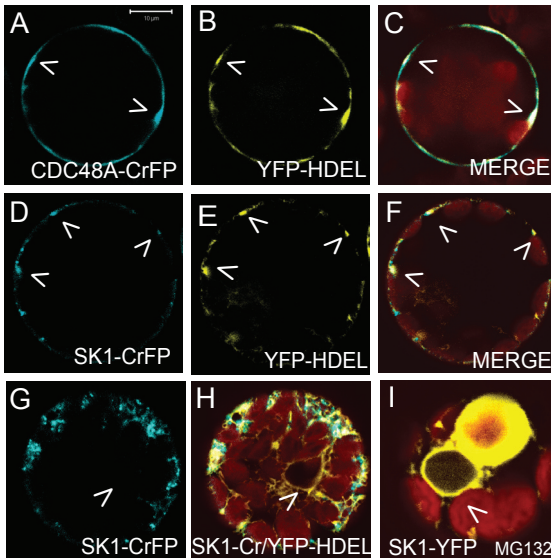
Figure 5. SERK1 and CDC48A plasma membrane compartments do co-localize with the peripheral ER. Confocal images of Arabidopsis protoplasts double transfected with CDC48A-CrFP (A) en YFP-HDEL (B) show co-localization in compartments at the plasma membrane (arrowheads in A,B,C). Protoplasts double transfected with SERK1-CrFP (D, and G) and the ER marker YFP-HDEL (E and H) also showed co-localization in regions at the PM (arrowheads in D,E,F), however, no co-localization could be observed in the perinuclear ER, in another focal plane of the cell (G, H). Accumulation of SERK1-YFP in the perinuclear ER and the 26S proteasome after MG132 treatment (90 minutes, 50 µM) is shown in (I). Bar in A = 10 µm.

Discussion

In this study we observed that the CDC48A protein is localized at the plasma membrane, in the cytoplasm and in the ER. In about one fifth of the cells CDC48A-CrFP was found primarily in the nucleus. The SERK1 receptor was only found at the PM, in endosomal compartments and in ER-derived vesicles. CDC48A and the SERK1 receptor co-localized in specific regions at the PM. Using FRET-FLIM direct interaction between CDC48A and the SERK1 receptor was shown to occur in specific regions at the PM, which coincide with the position of peripheral ER compartments.

There are a number of hypotheses to help explain these findings. The first is that the ER-membrane directly fuses with the PM during endocytosis, and that this process is mediated by CDC48A. Membrane fusion of the ER membrane with the PM in animal cells was shown by (Gagnon et al., 2002) and (Becker et al., 2004). It was shown that membrane fusion occurs during early phagocytosis, a specific form of endocytosis, by macrophages. The authors suggested that when the demand for membrane exceeds the capacity of other sources, the cell reverts to the ER, which harbors more than half of the total cellular membrane. It is possible that CDC48A plays a role in fusion of ER-membranes to the PM, because CDC48A and other homoloques were shown to play a role in the fusion of membranes (Latterich et al., 1995; Rancour et al., 2002). In yeast McNew et al. (2000) found a SNARE complex that was capable of mediating fusion between ER-Golgi and the plasma membrane. However, it does not seem likely that insertion of new membrane derived from the ER is very high in the protoplasts as used here. The role of the SERK1 receptor interaction with CDC48 is also not clear in this model. It could either point to an alternative endocytic mechanism or to a role of SERK1 in activating a membrane fusion event.

A second hypothesis is that AtCDC48A plays a role in the ER-associated degradation of misfolded SERK1 proteins similar to what was shown for a mutant MLO-1 receptor of barley, which was first poly-ubiquitinated (Müller et al., 2005). However, the wild type SERK1 protein did not show strong accumulation in the perinuclear ER close to where probably most of the degradation takes place in the 26S proteasome (Wojcik and DeMartino, 2003). While a role of CDC48A in ERAD of misfolded SERK1 receptors remains plausible, it will require other means such as introduction of mutant SERK1 proteins, to obtain further evidence.

As hinted at above, a third hypothesis is that CDC48A plays a role in internalization of the receptor, following a pathway different from the one visualized by the endosomal marker Ara6 or by FM4-64 staining. The FcεR1 receptor, which undergoes ligand-stimulated ubiquitination moves into detergent-insoluble domains of the plasma membrane after activation (Field et al., 1995; Lafont and Simons, 2001). It is possible that ubiquitination directs the SERK1 receptors to subdomains of the plasma membrane competent for internalization as mediated by CDC48A. For instance VCP, the closest animal CDC48A homologue, was shown to interact at the PM with clathrin (Pleasure et al., 1993), a component of the endocytic machinery. For other eukaryotic receptors like the β2-Adrenergic receptor and the AMPA-receptor GluR2 it was shown that they interact with NSF, which plays a role in the recycling of the receptor (Cong et al., 2001; Osten et al., 1998). NSF however, being a related AAA ATPase but

functioning primarily in SNARE-mediated vesicle fusion (Brunger and DeLaBarre, 2003) is required for transport from early to late endosomes (Robinson et al., 1997), while we did not observe CDC48A in those compartments, assuming that late endosomes are also marked by Ara6.

The C-terminal region of CDC48A was shown to bind to the SERK1 kinase domain and the C-terminal tail of the receptor in yeast interaction experiments (Rienties et al., 2005). Our in vivo FRET-FLIM experiments using C-terminally tagged fluorescent proteins of CDC48A and SERK1 appear to confirm these findings, although we cannot exclude binding to the N-terminus. The substrate binding site of CDC48 homologues is still under debate. In previous studies the N-domains of P97/VCP and CDC48p were shown to bind cofactors which bound to ubiquitinated substrates (Dai and Li, 2001; Meyer et al., 2000). (Zhang et al., 2000) proposed a model in which the central pore of the hexamer undergoes conformational changes due to alternate ATP binding and ADP release at both the D1 and D2 ring. Based on a 'milking' model it was proposed that substrate proteins enter the central pore at the D1 ring, go through to D2 and become processed. However, studies from (Song et al., 2003) and (DeLaBarre and Brunger, 2003), reviewed by (Wang et al., 2004), showed that the D2-ring is responsible for the major ATPase activity of the hexameric protein and induces major conformational changes. Therefore they propose, also because the opening of the hexamer in the D1 ring is extremely narrow, that substrate proteins possibly interact at the exterior and/or the D2 end of the hexamer, rather than through the interior chamber. Our finding that SERK1 and CDC48A can also interact at the C-terminus of the hexamer appears to support this model.

Interaction of the receptor either at the N-terminus or at the C-terminus of CDC48 could reflect different functions in the cell. The ubiquitin-proteasome pathway regulates both the basal turn-over and the ligand-induced degradation of the receptors. Poly-ubiquitinated mis-folded SERK1 receptors could bind to the N-domain of CDC48A to be degraded by the proteasome. In that case SERK1 would be a candidate substrate of CDC48A. In analogy with the VCP/ IL-2, IL-9 or Erythropoeitin receptor complex (Yen et al., 2000), SERK1 could also bind to the C-terminal domain and subsequently trans-phosphorylate CDC48A upon activation of SERK1-mediated signaling. In that scenario, CDC48A would be a substrate of SERK1 that could be involved in the internalization and subsequent degradation of the receptors. The presence of putative 14-3-3 binding sites in AtCDC48A and in the phosphatase KAPP (Rienties et al., 2005), and the composition of the SERK1 complex in seedlings comprising each of these proteins (Karlova et al. 2006), suggests an analogy between the mammalian complex consisting of P97/VCP, the JAK-2 kinase and the PTPH1 phosphatase. Rienties et al. (Rienties et al., 2005) proposed that phoshorylation of CDC48A by SERK1 kinase might mediate cy-tokinesis by re-localization of CDC48A to the cell plate, which would link the role of SERK1 in promoting embryogenic competence to the cell cycle regulation.

Future experiments are required to elucidate whether the sites of interaction between CDC48A and SERK1 at the PM of Arabidopsis protoplasts coincides with the position of lipid rafts, or represent positions where receptor quality control or internalization takes place. We also would like to establish whether ubiquitination of SERK1 occurs in vivo and whether

this is mediated by CDC48A. Furthermore we will attempt to determine whether SERK1 mediated signaling is impaired by CDC48A disfunctioning.

Chapter 3

In *vivo* hexamerization and characterization of the Arabidopsis thaliana AAA ATPase CDC48A-complex using FRET-FLIM and FCS

José Aker, Renske Hesselink, Ruchira Engel, Rumyana Karlova, Jan Willem Borst, Antonie J.W.G., Visser, Sacco C. de Vries

Abstract

The Arabidopsis thaliana AAA ATPase CDC48A was fused to Cerulean Fluorescent Protein (CrFP) and Yellow Fluorescent Protein (YFP). AAA ATPases like CDC48 are only active in hexameric form. Förster resonance energy transfer (FRET) -based Fluorescence Lifetime Imaging Microscopy (FLIM) using CDC48A-CrFP and -YFP showed interaction between two adjacent protomers, demonstrating homo-oligomerization to occur in living plant cells. Interaction between CDC48A and the SERK1 transmembrane receptor occurs in very restricted domains at the plasma membrane. In these domains the predominant form of the fluorescently tagged CDC48A protein is a hexamer, suggesting that SERK1 is associated with the active form of CDC48A in vivo. SERK1 trans-phosphorylates CDC48A on Ser-41. FRET-FLIM was used to show that in vivo the C-terminal domains of CDC48A stay in close proximity. Employing Fluorescence Correlation Spectroscopy (FCS), it was shown that CDC48A hexamers are part of larger complexes.

Introduction

The Arabidopsis thaliana Cell Division Cycle protein CDC48A was previously shown to interact with the Somatic Embryogenesis Receptor-like Kinase 1 (SERK1) (Rienties et al., 2005) and to co-immunoprecipitate with SERK1 in Arabidopsis cultured cells and seedlings (Karlova et al., 2006). In living cells the CDC48A protein co-localizes with SERK1 at peripheral ER based membranes and the plasma membrane (PM). Förster Resonance Energy Transfer-Fluorescence Lifetime Imaging Microscopy (FRET-FLIM) showed that CDC48A interacts with SERK1 at the PM (Aker et al., 2006).

CDC48A is a member of the family of AAA ATPases (ATPases associated with various cellular activities), shown to have various functions in cell division, membrane fusions and in proteasome and ER associated degradation (ERAD) of proteins (Woodman, 2003). The role of AAA ATPases is to generate mechanical force to disrupt or fuse molecular structures by means of ATP binding and hydrolysis. The AtCDC48A protein was shown to play a role in ERAD and in membrane fusions (Müller et al., 2005; Rancour et al., 2002). AAA proteins are present as stacked hexameric rings that are stabilized by the binding of ATP. They are only reported to be active in hexameric form. This study aims to determine the predominant form of the fluorescently tagged CDC48A protein in Arabidopsis protoplasts at the peripheral ER and the PM domains where interactions between CDC48A and the SERK1 receptor take place, and therefore to determine if SERK1 is associated with the active form of CDC48A.

CDC48A is 77 % identical to the mammalian homologue Vasolin Containing Protein (VCP) or p97. Recently, conformational and dynamic changes during the ATP hydrolysis cycle of p97 have been studied by cryo-electron microscopy, crystallography and small-angle X-ray scattering (reviewed in (Pye et al., 2006). The monomeric protein contains an N-terminal domain, two AAA domains and a C-terminal domain (Fig. 1 and 3). The N-domain is important for binding of adaptor proteins and substrates. The two AAA domains D1 and D2 are responsible for binding and hydrolysis of ATP. The D1 and D2 domains form stacked hexameric rings above one another that are connected by a linker. The ATP binding site in the D1 domain and the D1-D2 linker are responsible for hexamerization, while the ATP binding site in the D2 domain possesses the major ATPase activity (Wang et al., 2003a). The N-domain is flexibly attached to the D1 domain, and projects out of the ring, facilitating binding to other proteins. During ATP hydrolysis, large conformational changes are transmitted from the D2 domain via the D1 domain onto the N-domains, due to binding, hydrolysis and release of the nucleotide (DeLaBarre and Brunger, 2003, 2005). In addition the pores within the D1 and D2 rings narrow and widen in different nucleotide states. This causes the rings to rotate relative to each other (Davies et al., 2005). The C-terminal tail was not ordered within the crystal structure and it is therefore unknown whether it stays close to the D2 ring or projects from the core structure towards the N-domain.

For Arabidopsis CDC48A the crystal structure is not known, but in vitro produced proteins form a hexamer, while PUX1 (Plant UBX domain-containing protein) facilitates CDC48A oligomer disassembly (Rancour et al., 2004). Up to now hexamerization of AAA ATPases was only shown in vitro or in total cell lysates, studies that do not reveal any spatial informa-

tion on the oligomerization status of proteins in a living cell. Therefore the protein was fused to the green fluorescent protein variant monomeric cerulean FP (CrFP) or to yellow FP (YFP) and the hexamerization of CDC48A proteins in living cells was monitored by FRET-FLIM. Employing this technique, oligomerization of the CDC48A proteins in living cells was shown to be non-uniform. In addition, inter-subunit distances in the oligomeric CDC48A protein could be calculated revealing that the C-terminal domains stayed in close proximity rather than protruding out of the molecule.

It was also shown that SERK1 interacts with the N-terminus as well as the C-terminus of CDC48A (Aker et al., 2006). After performing a transphosphorylation reaction with the SERK1 kinase domain, only Ser-41, a serine residue found to be in the N-domain of CDC48A was phosphorylated.

To investigate the diffusion of the CDC48A protein in cells, fluorescence correlation spectroscopy (FCS) was employed, in which fluorescence intensity fluctuations caused by diffusion of fluorescent molecules in and out of a femto-liter volume are monitored in time. These fluctuations give information about diffusion times of proteins through the volume and hence about the size of protein complexes.

Our results show that the oligomeric form of CDC48A in living cells is primarily hexameric and that the fluorescently tagged CDC48A is still able to form hexamers. The SERK1 receptor interacts with CDC48A at the same locations where oligomerization of the CDC48A protein is shown. We conclude therefore that SERK1 interacts with the hexameric form of CDC48A. Using FCS the presence of CDC48A in larger protein complexes in vivo was predicted.

Material and methods

Construction of the CrFP/YFP tagged proteins

Plasmid pMON999 is a plant expression vector that contains the enhanced cauliflower mosaic virus (CaMV) 35S promoter, followed by a multiple cloning site and the terminator of the nopaline synthase gene (van Bokhoven et al., 1993). This plasmid, containing the cDNA of cerulean fluorescent protein (CrFP), enhanced yellow fluorescent protein (YFP), or a fusion construct of CDC48A (At3g09840) or –C (At3g01610), C-terminally linked to CrFP or YFP, was used for transfection of protoplasts.

Also a mutant of CDC48A-CrFP and –YFP was constructed, the D2 deletion mutant (CDC48A-N-D1), missing the D2 domain from M448 to the end of the CDC48A sequence, by restriction with NcoI and subsequent ligation of the template.

A second mutant of CDC48A-YFP was constructed, missing the N-domain (AA 1-188). Using the QuikChange® XL Site-Directed Mutagenesis Kit, mutations K254T and K527T were introduced in the Walker A motifs of the D1 and D2 domain, respectively. A combination of the two mutations, in a fusion protein with either CrFP or YFP, resulted in the A1A2 mutant. All constructs were checked by restriction enzyme analysis and the size of the protein was determined by Western-blotting. All constructs were verified by sequencing.

Protoplast isolation and transfection were performed as described before (Aker et al., 2006). FRET-FLIM was measured 16 hours after transfections. For FCS measurements a low amount of fluorescent molecules in the detection volume is essential, therefore cells were measured 6 hours after transfections.

Protein expression analysis

Arabidopsis mesophyll protoplasts were prepared and transfected according to a protocol described by Sheen (Sheen, 2001) with modifications, as described before (Aker et al., 2006). 16 to 20 hours after transfection protoplasts were lysed in RIPA-buffer (50 mM Tris pH 7.5, 150 mM NaCl, 1 mM MgCl2, 1 % NP40, containing a protease inhibitor tablet (Roche)) for 15 minutes on ice. Extracts were centrifuged for 7 minutes at 13.000 rpm at 4 degrees and soluble fractions were supplemented with SDS-PAGE loading buffer, denatured at 95°C for 5 min before loading on an 8% gel, next to a pre-stained marker. Gels were blotted on nitrocellulose. For Native PAGE, the soluble fractions were supplemented with Native-PAGE loading buffer and loaded on a native gel of 4 to 8% acrylamide. Gels were blotted on PVDF membrane. The marker part of the blot was stained with Coomassie immediately after blotting. Anti-YFP was generated by Isogen, according to standard procedure. The serum was purified on a YFP-protA column. As a marker for Native PAGE a mixture of thyroglobuline (669 kD), ferritine (440 kD), and serum albumine (132 and 66 kD) was used.

In vitro transphosphorylation and LC-MS/MS analysis

For the in vitro transphosphorylation 1 μg SK1-KD was added to 1 μg of CDC48A in kinase-buffer (Shah et al., 2001) plus 3 mM cold ATP and 1 μl [γ32-P]ATP in a total reaction of 30 μl. After incubation of 30 minutes at 30°C, sample-buffer was added. The sample was heated for 5 minutes at 95°C, and loaded on SDS-PAGE. After drying the gel, the radioactivity was detected with a Phospho-Imager using the ImageQuant program (Molecular Dynamics).

For MS analysis the in vitro phosphorylation was performed as described, without [γ32-P]ATP. The gel was not dried. The GST-CDC48A 125 kD bands were excised from the gel after staining with the Colloidal Coomassie staining kit (Invitrogen) and cut into 1 mm pieces. In-gel digestion was performed as described by Shevchenko et al. (Shevchenko et al., 1996). After destaining with water, cysteine reduction (with 10 μl of 50 mM DTT (dithiotreitol) in 50 mM NH4HCO3 for 1h at 56oC) and alkylation (with 10 μl of 100 mM iodacetamide in 50 mM NH4HCO3 for 1h. at room temperature in the dark), the gel pieces were washed three times with 100 μL 50 mM NH4HCO3 and dried in a vacuum centrifuge. For proteolytic digestion, the gel was treated over night with 1 μL (in 10 μl 50 mM NH4HCO3) trypsin (sequencing grade, Boehringer Mannheim, Germany). Finally, peptides were extracted from the gel pieces using 15-20 μl 5% TFA (trifluoro-acetic acid) in water followed by sonication for 1 min. A second gel extraction was done using 10-15 μl CH3CN/TFA/H2O (25/1/84 v/v/v) mixture and sonications for 1 min. Extracted peptides were subjected to LC-MS/MS analysis.

Each run with all spectra obtained was analyzed with Bioworks 3.2 (Thermo Electron). For identification of the peptides, the following proteins were added to a database; Arabidopsis thaliana CDC48A (P54609), the GST, Trypsin (bovine, P00760), Trypsin (porcin, P00761), Keratin K2C1 (human, P04264) and Keratin K1CI (human, P35527). The searches were done allowing methionine oxidation and phosphorylation of serine, threonine and tyrosine. The peptide identifications obtained were analyzed with Bioworks 3.2 with the following filter criteria: $\Delta Cn > 0.08$, Xcorr > 2 for charge state 1+ , Xcorr > 1.5 for charge state 2+ and Xcorr > 3.3 for charge state 3+ as described previously (Peng et al., 2003).

FRET-FLIM

FRET takes place when two proteins coupled to appropriate fluorophores are in close distance from each other. FRET measurement is very sensitive since the rate of energy transfer is inversely proportional to the donor-acceptor distance to the power six (Lakowicz, 1999). FRET can reveal distances between fluorophores that are typically in the range of 2-7 nm. FLIM is one method to measure FRET by estimating the reduction of CFP-donor lifetime in case of interaction with a YFP-acceptor molecule. FLIM was performed on a Biorad Radiance 2100 MP system in combination with a Nikon TE 300 inverted microscope, as described by Russinova et al. (Russinova et al., 2004). From the fluorescence intensity image the fluorescence lifetime is determined for each pixel. The full fluorescence decay per pixel was calculated for the donor molecule using a double exponential decay model. The fluorescence lifetime (τ value) can then be presented as a false color image. First the fluorescence lifetime of only the donor molecule was determined by analyzing all the measured pixels in the PM. The resulting average lifetime was subsequently used in the analysis where all decays were fit using two exponentials, with one lifetime fixed to the value for τ of the donor. This two-exponential model assumes two populations of donors: one that does not have an acceptor nearby and therefore has the unquenched lifetime τD, and one that has an acceptor near enough for energy transfer to occur and therefore has a reduced lifetime τDA. Fluorescence lifetime decays were fitted per pixel with a binning factor of 1. A double exponential decay model was used, with the lifetime of one component fixed to the value found for the unquenched lifetime of the donor. Fits were judged by the $\chi r2$ values ($\chi r2 \leq 1.1$). The amount of photon counts in the peak channel was normally around 1000. At least 15 cells were measured for each combination and location in 2 to 5 independent experiments. After measurements the distribution histograms of 5 representative cells were combined and plotted for each combination of proteins. Average lifetime per combination was determined and standard deviations calculated. The distance between donor and acceptor were calculated via

$$E = 1-(\tau DA/ \tau D) \qquad (1)$$
$$E = 1/(1+ (R/R0)6) \qquad (2),$$

where E is the transfer efficiency, R is the actual distance and R0 is the Förster radius, indicating the distance where one observes 50% FRET efficiency. The R0 for the FRET-pair CrFP and YFP was determined to be 4.9 nm, based on the excitation and emission spectra of the in vitro produced proteins (JW Borst, data not shown).

FCS

FCS makes use of a focused laser beam continuously illuminating a sample. Only the fluorescence from particles excited in a small observation volume is detected. The observation volume is defined by the focused laser beam in the x and y direction, and by the pinhole in the z direction, which makes monitoring of a sub-femtoliter volume possible (Rigler et al., 1993). The entrance of a fluorophore into this volume gives rise to a burst of detected photons. The duration of this burst reflects the time the particle needs to diffuse through the observation volume, while the amplitude represents the molecular brightness. The intensity trace is correlated with itself at a later time point to yield the autocorrelation curve G (τ), from which the diffusion coefficient D and the average number of particles in the observation volume N can be obtained.

FCS measurements were performed on a Confocor 2-LSM 510 combination setup (Carl Zeiss, Germany). The 514 nm argon laser line was used to excite YFP (Hink et al., 2002). The system was calibrated with Rhodamine 6 Green (R6G) solution (10 nM) and aligned using a Rhodamine film. The FCS observation volume was positioned in the cytoplasm adjacent to the PM, to avoid measuring in chloroplasts. After a pre-bleach of 1 second with high (70% ~ 0.4 mW) laser power, three measurements of twenty seconds each were performed with low laser power (~ 4 τ W).

FCS data were analyzed using FCS Data Processor 1.4 (Scientific Software technologies Centre, Minsk, Belarus). Since measurements were performed in the cytoplasm we fit the data with a model assuming free diffusion of protein and protein-complexes in three dimensions although interaction with the PM in some cases cannot be ruled out. An additional triplet-state term was used to describe the fast photo-physics of YFP (e.g. conversion to a dark-state, blinking)

$$G(\tau) = 1 + \frac{1}{N}\left(\left(1 + \frac{\tau}{\tau_{dif}}\right)\sqrt{1 + \left(\frac{\omega_{xy}}{\omega_z}\right)^2 \frac{\tau}{\tau_{dif}}}\right)^{-1}\left(1 + \frac{F_{trip}e^{-t/T_{trip}}}{1 - F_{trip}}\right)$$

Eq. (3)

Here, G(τ) is the autocorrelation function, N is the number of molecules in the detection volume, τ dif is the diffusion time of the molecules, Ftrip is the fraction of molecules in the triplet state and Ttrip is the triplet-state relaxation time. ωxy and ωz are the equatorial and axial radius of the Gaussian shaped observation volume, respectively. The ratio ωz/ωxy is also called the structural parameter and was found to be between 5 and 10 in our measurements. The structural parameter was fixed to the value obtained with the R6G solution. The diffusion coefficient (D) were calculated from the τ dif value for each curve and listed in a table for the PM and the nucleus. Standard errors on the D-value were calculated, and a Two-Sample T-test with 95% significance was performed to compare the mean D value of CDC48A with the CDC48A A1A2-, CDC48A Ndel- and CDC48AN-D1-mutants.

The time a molecule on average spends in the observation volume τ dif is linked to the translational diffusion coefficient D by Eq. (4).

$$\tau_{dif} = \frac{\varpi_{xy}^2}{4D}$$

Eq. (4)

The diffusion coefficient of a spherical particle is inversely proportional to the hydrodynamic radius rh according to the Stokes-Einstein relation (Edward, 1970):

$$D = \frac{kT}{6\pi\eta r_h}$$

Eq. (5)

In which k is the Boltzmann constant, T is the absolute temperature and η is the viscosity of the solution. Assuming a globular particle, the molecular weight M is proportional to the hydrodynamic radius to the power three:

$$M = \frac{4\pi r_h^3}{3}\rho N_A$$

Eq. (6)

Where ρ is the mean density of the molecule and NA is Avogadro's number. Combination of equations (4), (5) and (6) yields equation (7), which shows that the diffusion coefficient scales only to the cubic root of the molecular weight, and is independent of the observation volume.

$$D^{-1} \sim \frac{6\pi\eta}{kT}\sqrt[3]{M}$$

Eq. (7)

Hence the larger the molecule is, the lower is the diffusion coefficient. To distinguish particles of different size with FCS, the diffusion times have to differ at least by a factor of 1.6, which corresponds to a four-fold mass difference (Meseth et al., 1999)

Results

Expression and localization of CDC48A wild type and mutant proteins

The CDC48A-protein and various mutants used in this study are depicted in Fig. 1A. CD-C48A consists of the N-domain, the D1 and D2 domain connected by a linker, and the C-terminal tail. The YFP-tag is shown here as a C-terminal fusion and in appropriate constructs it was replaced by CrFP and/or placed at the N-terminus. The CDC48A^{A1A2} mutant contains the K254T and K527T mutations in the Walker A motifs of the D1 and D2 domain, which inhibit ATP-binding and in vitro severely delay hexamerization in the mammalian homologue p97/VCP (Wang et al., 2003a).

A. Constructs
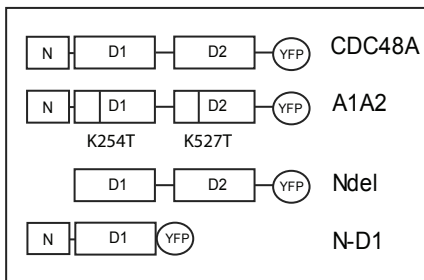
B. SDS PAGE: anti-YFP
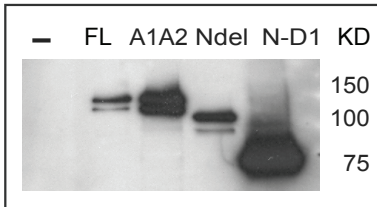
C. Native PAGE: anti-YFP
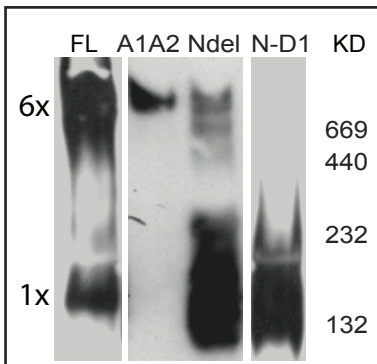
Figure 1. Expression in Arabidopsis protoplasts of CDC48A, CDC48A ^{A1A2}, CDC48A^{Ndel}, and CDC48A^{N-D1} mutants all tagged to YFP. YFP is replaced by CrFP. In panel **A** the various mutants are shown schematically. Lysates of transfected cells were submitted to SDS-PAGE in panel **B**, to Native PAGE in panel **C** and probed with anti-YFP anti-serum. The expected sizes of the denatured proteins are 125 kD for full length (FL) CDC48A- and CDC48A^{A1A2}-YFP, 96 kD for CDC48A^{Ndel}-YFP and 77 kD for CDC48A^{N-D1}-YFP. Non-denatured hexameric CDC48A-YFP is expected to be between 650 and 750 kD depending on the number of YFP tags.

The N-deletion (CDC48A^{Ndel}) mutant lacks the N-domain (AA 1-188), which is in other homologues responsible for binding to co-factors like P47, Ufd1-Npl4 and ubiquitinated substrates (Dreveny et al., 2004; Meyer et al., 2000). The CDC48A^{N-D1} mutant lacks the D2 domain and the linker region between D1 and D2 (from AA 448 to the C-terminus). The D1-D2 linker was shown to be important for hexamerization of VCP (Wang et al., 2003b) in vitro.

To investigate whether the CDC48A-YFP proteins are indeed capable of forming a hexameric complex, the CDC48A-YFP and mutant genes were transiently expressed in Arabidopsis protoplasts and analyzed on denaturing and non-denaturing PAGE. Western-blot analysis (Fig. 1B) shows that in protoplasts the various proteins confirm the expected sizes of around 125 kD for CDC48A and CDC48A^{A1A2}, 96 kD for the CDC48A$^{Ndel\ 1-188}$ and 77 kD for CDC48A^{N-D1}. The estimated size of the full length (FL) CDC48A protein after native PAGE is about 700- 750 kD, in line with the calculated size of 625 and 750 kD, the difference depending on the number of GFP tags present (Fig. 1C). However, about 5 to10 percent of the YFP-tagged protein appears to remain as monomers. Surprisingly, the CDC48A^{A1A2} protein is also predominantly found as a hexamer on native PAGE, despite the mutations delaying hexamerization. In a longer exposure of the Western blot, CDC48A^{A1A2} does show a monomeric protein fraction (data not shown). CDC48A$^{Ndel\ 1-188}$, shows bands of various sizes, but most prominently the monomeric band. In a study of Wang and co-workers, a VCP mutant lacking amino acids (aa) 1-141 of the N-domain is still able to hexamerize in vitro (Wang et al., 2003b). Our data shows that the CDC48A^{Ndel} protein lacking the complete N-domain (AA 1-188) is most likely in the monomeric form. The CDC48A^{N-D1} protein runs as a monomer, in line with the results presented by Wang and co-workers.

To compare the localizations of the different CDC48A mutant proteins, they were co-expressed with CDC48C-CrFP, shown to localize solely to the nucleus (Aker et al., 2006). The localization of the CDC48A protein is at the plasma membrane (PM), in the cytoplasm and ER, but also a small fraction was observed in the nucleus (Aker et al., 2006). In Fig. 2 images of the nucleus of CDC48A are shown in the focal plane. CDC48A co-localizes with CDC48C in the nucleus (Fig. 2A-C) and also localizes to the PM and the cytoplasm. The PM is not in the focal plane and can therefore not be seen. The merge shows an overlay of the cells containing chloroplasts in red, CDC48A in yellow and the nucleus in cyan. The CDC48A^{N-D1} protein (Fig. 2D-F) is found in the cytoplasm but not in the nucleus (arrow head in Fig. 2D). This can be explained by the Tyr808 residue, comparable to Tyr834 in yeast Cdc48p and shown to be required for nuclear translocation (Madeo et al., 1998) and which is present in the deleted part of CDC48A. Apparently, although the two NLS are still present in the mutant these are not sufficient for nuclear targeting. A similar observation was made for the mammalian CDC48 ortholoque VCP (Indig et al., 2003). To our surprise the CDC48A^{Ndel} –protein (Fig. 2G-I), lacking the NLS sequences, still localizes to the nucleus (compare Fig. 2G with H). For VCP, cytoplasmic localization was described when the N-domain of the protein was removed. Indig et al. (Indig et al., 2003) and Wang et al. (Wang et al., 2003b) found that hexamerization of this protein in vitro could still take place. The CDC48A^{A1A2}- protein (Fig. 2J-L) is found in the cytoplasm as well as in the nucleus. We conclude based on the hexamerization status

in vitro and the localization of the mutant proteins in cells that complete hexamerization of CDC48A is not required for nuclear localization.
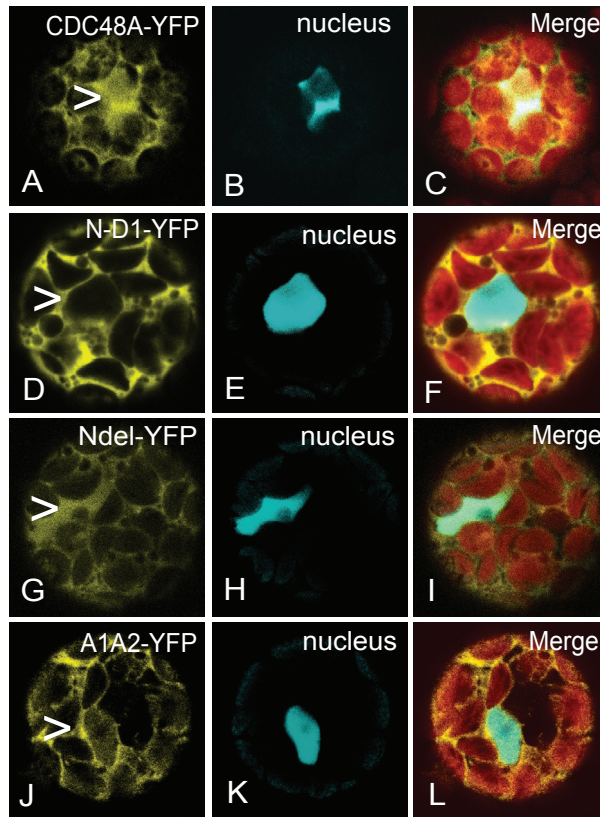
Figure 2. Localizations of CDC48A- or CDC48A^{N-D1}- and CDC48A^{Ndel} –YFP. CDC48C-CrFP was used as a nuclear marker (B,E,H,K). Images are taken at the plane of the nucleus and the merged picture shows the combination of both images together with the chloroplasts in red (C,F,I,L). CDC48A-YFP localizes to the cytoplasm and the nucleus (compare position of arrowhead in A with image B). The localization at the PM is not visible in this focal plane. CDC48A^{N-D1} does localize to the cytoplasm but not to the nucleus (compare the arrowhead in image D with E). CDC48A^{Ndel} does localize to the cytoplasm and to the nucleus (compare the arrowhead in G with H). The localization of CDC48A^{A1A2} (J) is comparable with that of CDC48A (A).

Oligomerization of CDC48A at locations with SERK1-interaction

To investigate if the SERK1 receptor interacts in vivo with the hexameric or the monomeric form of CDC48A, the oligomerization of CrFP and YFP-fused CDC48A protomers in vivo was studied. The CDC48A protein was fused at the C-terminus with CrFP or YFP and expressed in Arabidopsis protoplasts. For the FLIM-measurements CDC48A protomers C-terminally fused to CrFP and YFP (Fig. 3A) were co-expressed, hypothetically leading to a

hexamer as shown in the model in Fig 3B. Only four of the six fluorophores are drawn at adjacent positions at the C-terminus, but in fact these can be randomly positioned at each C-domain. The other combinations used are depicted in Fig. 3C to F. Fig. 3C shows a hexamer with the donor at the C-terminus and the acceptor at the N-terminus, 3D shows a hexamer of CDC48A tagged to CrFP and YFP both at the N-terminus, 3E and F show a monomer of the CDC48A^{N-D1} and CDC48A^{Ndel} with tags only at the C-terminus.
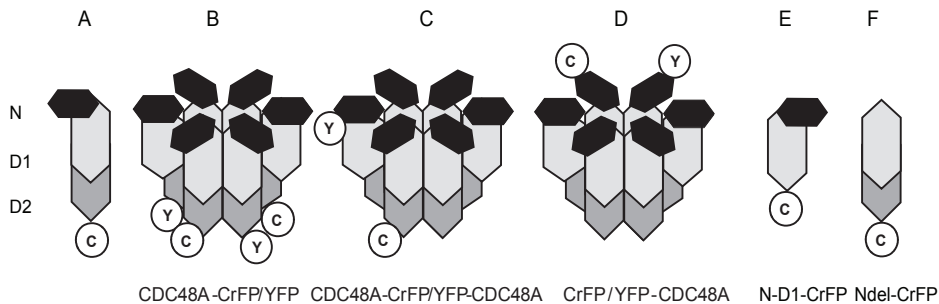

A   B   C   D   E   F

N

D1

D2

CDC48A-CrFP/YFP   CDC48A-CrFP/YFP-CDC48A   CrFP/YFP-CDC48A   N-D1-CrFP Ndel-CrFP

Figure 3. Models of the expected hexamers of CDC48A after co-expression of 2 different protomers. (**A**) Monomeric CDC48A. (**B**) CDC48A fused with CrFP and YFP both at the C-terminus are combined and depicted as a hexamer. For simplicity only 4 fluorophores are drawn at adjacent positions at the C-terminus, but in fact these can be randomly positioned at each C-domain. (**C**) YFP fused to the N-terminus and CrFP to the C-terminus. (**D**) YFP and CrFP fused to the N-terminus. (**E** and **F**) CDC48A^{N-D1} and CDC48A^{Ndel} depicted as a monomer.

A maximum energy transfer efficiency of around 50% can only be achieved when fluorophores are approximately 5 nm apart. The distance between two adjacent C-termini is not known but the inner pore diameter of the hexamer is 5.7 nm, based on the crystal structure of p97/VCP (DeLaBarre and Brunger, 2003; Huyton et al., 2003; Zhang et al., 2000). Not only interaction between two adjacent fluorophores but also between two fluorophores on either side of the pore should therefore theoretically be possible. To measure significant energy transfer, the amount of labeled protein has to be relatively high as compared to the amount of endogenous CDC48A. Based on the previous observation that in transfected protoplasts the fluorescent CDC48A level is around 8 times higher than the endogenous level Aker et al. (Aker et al., 2006) assume that in a hexamer most of the CDC48A protomers contain a fluorescent tag.

First we investigated if at the locations where CDC48A-SERK1 interaction takes place also oligomerization of the CDC48A proteins occurs. In Fig. 4A the intensity image of the donor molecule CDC48A-CrFP is shown. In the false-color image (Fig. 4B) the average lifetime τ at the PM is shown to be around 2.5-2.6 ns. As reported previously co-expression of CDC48A-

CrFP and SERK1-YFP resulted in a reduction of the fluorescence lifetime in a punctuate pattern at the membrane (Fig. 4C,D and inserts). Part of the areas where SERK1 and CDC48A interacted, co-localized with an ER-marker but not with an endocytic marker (Aker et al., 2006). After co-expression of CDC48A-CrFP and CDC48A-YFP, interaction was found in a comparable but more widespread area at the PM (Fig. 4F and insert). We therefore propose that in those membrane areas where interaction between SERK1 and CDC48A occurs, a substantial amount of CDC48A is in oligomeric form. In Table 1 the results of all the measurements are listed. In the upper panel the average lifetimes of the full length CDC48A proteins are listed, in the middle panel the lifetimes of the monomeric mutant CDC48AN-$D1$ and in the lower panel the lifetimes of CDC48C. The left panel refers to the measurements at the PM; the right panel refers to the measurements in the nucleus. The unquenched lifetime of the donor CDC48A-CrFP protein is 2.5 ns in the nucleus as well as at the PM. Fig. 4G shows a false-color image of the nucleus of a protoplast expressing only the donor molecule CDC48A-CrFP. In the left upper corner the corresponding intensity image is shown.

Subsequently CDC48A-CrFP and CDC48A-YFP-tagged proteins were co-expressed. In Fig. 4H an example of a false-color image is shown for the nucleus. This combination shows a significant reduction in lifetime at the PM (Fig. 4F: 2.18± 0.04 ns on average, Table 1) as well as in the nucleus (2.20± 0.07 ns). From the differences in lifetime between donor alone and donor plus acceptor, the distance between the fluorophores can be calculated. The average distance between two fluorophores both at the C-terminus is 6.8 nm, with a FRET-efficiency of 13.5%.

FLIM as a tool to measure distances between subunits in oligomeric complexes

The distances between the N-domains and C-domains in the CDC48A protein as calculated from the crystal structure of the mammalian homologue VCP/P97 (DeLaBarre and Brunger, 2003) are approximately around 8 nm, which is just outside the range at which FRET can be detected between two fluorophores. To determine this distance for the CDC48A protein, a combination of CDC48A-CrFP and YFP-CDC48A was expressed (see model 3C). The mixed protomers showed a minor reduction in the fluorescence lifetime (A-Cr/Y-A, τ = 2.34±0.04 ns; Fig. 4I, Table1) at the PM and 2.44± 0.03 ns in the nucleus (A-Cr/Y-A, Fig. 4J, Table 1). Based on the FRET efficiencies between the CrFP and YFP fluorophores, the estimated distance between the N- and C-terminus using equations (1) and (2) is between 7.6 nm (for the PM) and 8.5 nm (for the nucleus), which is in agreement with the estimated value for p97/VCP of 8 nm. The crystal structure of p97/VCP also showed that at the plane of the N-domains the hexameric protein has a diameter of around 15 nm. Therefore, fluorescent molecules at op posite positions in CDC48 cannot show FRET, so any interaction resulting in a reduction in lifetime would have to originate from adjacent protomers. CrFP- and YFP-CDC48A proteins were co-expressed (Fig. 4L) and the fluorescence lifetimes were compared with the donor (Fig. 4K). No significant reduction in lifetime was measured at the PM (Cr-A/Y-A, τ = 2.47± 0.06 ns. Table 1) or in the nucleus (Cr-A/Y-A, τ = 2.55±0.06 ns. Table1). The distance between
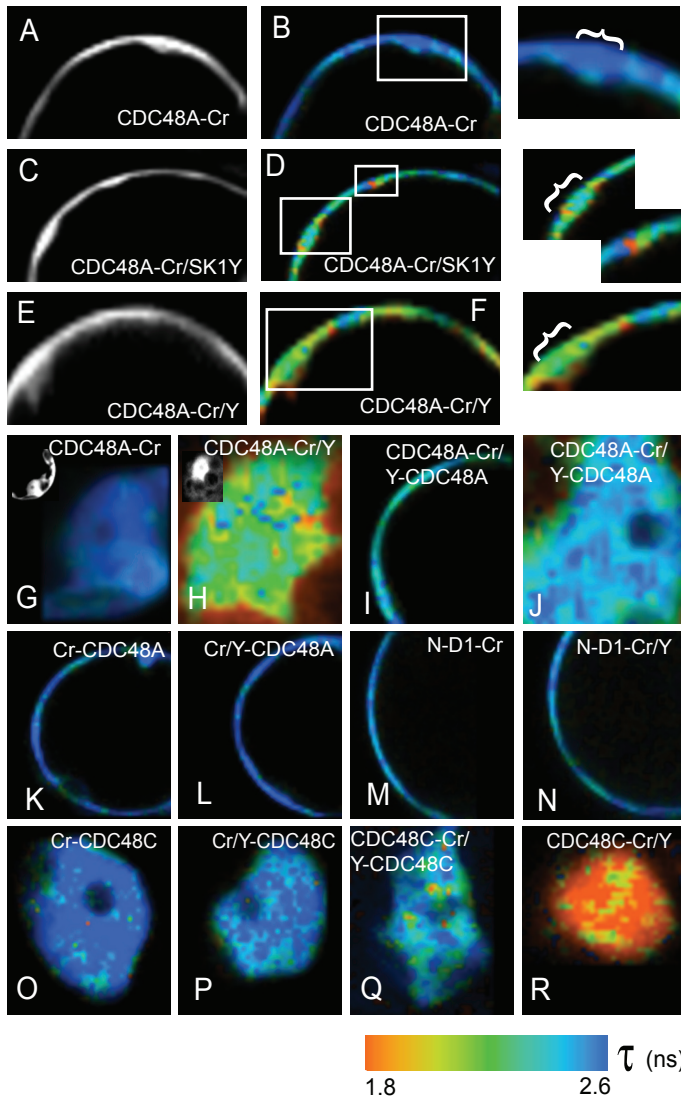
Figure. 4. Interactions between CDC48A tagged protomers based on FRET measured by FLIM.
(A) Intensity images of the PM of part of a protoplast expressing the donor molecule CDC48-CrFP alone and (B) the false-color or lifetime image. A long lifetime, giving a dark blue color, means no interaction; a reduction in donor lifetime generating a shift towards orange, means interaction. The combination of CDC48A-CrFP and SERK1-YFP show a reduction in lifetime at specific regions at the PM (C and D plus inserts). A combination of CDC48A-CrFP and CDC48A-YFP proteins shows a reduction in lifetime at the PM in the same regions were SERK1 and CDC48A interact (F plus insert) and in the nucleus (H). In the left upper corner intensity images are shown. A combination of CDC48A-CrFP and YFP-CDC48A at the PM is shown in (I) and in the nucleus in (J). (K) Image of CrFP-CDC48A alone at the PM and in combination with YFP-CDC48A in (L), showing no reduction in lifetime. (M) Lifetime image of the CDC48A^{N-D1}-CrFP protein as the donor and (N) the combination with a CDC48A^{N-D1}-YFP protein. (O) Lifetime image of the CrFP-CDC48C donor alone and (P) in combination with YFP-CDC48C. Both combinations of CDC48C-CrFP with YFP-CDC48C (Q) or with CDC48C-YFP (R) show a reduction in lifetime.

the N-domains is calculated to be between 9.5 nm (for the PM) and 10.6 nm (for the nucleus), again confirming the structure as determined for p97/VCP. The FRET efficiency is only 1.9 %, meaning that there is no interaction at all.

The CDC48A^{N-D1}-CrFP /-YFP combination did not show a reduction in the fluorescence lifetime (N-D1Cr/Y, τ = 2.40±0.03 ns; Fig. 4N, Table 1) compared to the donor alone (N-D1-Cr, τ= 2.48±0.06 ns; Fig. 4M, Table 1). The FRET efficiency was only 3.2 %, confirming the monomeric nature of this mutant (Fig. 1C) and demonstrating the importance of the D1-D2 linker and/or the D2 domain in the oligomerization.

In general the reduction in lifetime between the donor group CrFP alone and the donor plus the acceptor group YFP was less in the nucleus than in the PM. The reason for differences in lifetimes at the PM or in the nucleus of the same protein could be due to the difference in refractive indices of the environment (Borst et al., 2005).

To confirm the relevance of our protein-protein distance measurements using FRET-FLIM, we next investigated the characteristics of CDC48C, another member of the Arabidopsis ATPase family that in contrast with CDC48A is only present in the nucleus (Aker et al., 2006). Based on the presence of Walker A and B motifs, CDC48C is classified as an AAA ATPase as well and therefore the same hexameric structure is expected. The average donor lifetime

Table 1. FRET - FLIM analysis of CDC48A, ND1 mutant and CDC48C, fused to CrFP or YFP. Lifetime τ is determined as described in methods. The distance d (nm) and the FRET efficiency (Eff.) between the CrFP and YFP fluorophores, is calculated via Eq.1 and 2. The top, middle and lower panels show the average lifetimes of CDC48A, N-D1-mutant and CDC48C proteins, in the left panel for the PM, in the right panel for the nucleus. N-D1 proteins are not localized in the nucleus, CDC48C proteins not at the PM.
A-Cr is CDC48A-CrFP; A-Cr/Y-A is CDC48A-CrFP/YFP-CDC48A; Cr-A/Y-A is CrFP-CDC48A/YFP-CDC48A; A-Cr/A-Y is CDC48A-CrFP/CDC48A-YFP; N-D1-Cr is N-D1-CrFP; N-D1-Cr/Y is N-D1-CrFP/N-D1-YFP; Cr-C is CrFP-CDC48C; C-Cr/Y-C is CDC48C-CrFP/YFP-CDC48C; Cr-C/Y-C is CrFP-CDC48C/YFP-CDC48C; C-Cr/C-Y is CDC48C-CrFP/CDC48C-YFP.

protein	τ PM	d	FRET eff.	τ Nucleus	d	FRET eff.
	ns	*nm*	*%*	*ns*	*nm*	*%*
A-Cr	2.52±0.03			2.53±0.04		
A-Cr/Y-A	2.34±0.04	7.6	7.2	2.44±0.03	8.5	5.6
Cr-A/Y-A	2.47±0.06	9.5	1.9	2.55±0.06	10.6	0
A-Cr/A-Y	2.18±0.05	6.8	13.5	2.20±0.07	6.9	12.7
N-D1-Cr	2.48±0.06					
N-D1-Cr/Y	2.40±0.03	8.7				
Cr-C				2.59±0.03		
C-Cr/Y-C				2.43±0.04	7.8	6.4
Cr-C/Y-C				2.44±0.10	7.9	5.8
C-Cr/C-Y				2.09±0.05	6.4	19.3

of CrFP-CDC48C was 2.59±0.03 (Cr-C, Fig. 4K and Table 1). The combination of CrFP- and YFP-CDC48C showed a lifetime of 2.44±0.1 ns (Cr-C/Y-C, Fig. 4P, Table 1), a significant reduction compared to the donor alone. The FRET efficiency is 5.8%. The combination of CDC48C-CrFP and YFP-CDC48C protomers also showed a minor but significant reduction in lifetime (C-Cr/Y-C, τ = 2.43±0.04 ns; Fig. 4Q, Table 1) comparable with the same combi-

nation for CDC48A. Co-expressed CDC48C-CrFP and -YFP proteins, showed a large reduction in donor lifetime (C-Cr/C-Y, $\tau = 2.09 \pm 0.05$ ns; Fig. 4R, Table 1) comparable to that of the CDC48A proteins. The distance between the fluorophores is 6.4 nm, with a FRET efficiency of 19.3%.

When analyzing FRET-FLIM measurements average lifetimes are calculated from lifetime distributions in order to compare different combinations. However, spatial distributions may be more illustrative for changes in interactions (Nougalli Tonaco et al., 2005). In Fig. 5, examples of lifetime distribution histograms at the PM are shown for CDC48A-CrFP alone (Fig. 5A), in combination with CDC48A-YFP (Fig. 5B) and a combination of CrFP-CDC48A and YFP (Fig. 5C). These histograms are examples recorded from protoplasts displaying fluorescence lifetimes as in images Fig. 4B, F and L respectively. The nucleus in image 4H is surrounded by chlorophyll which has a very short lifetime (normally shorter than 1500 ps) and indicated in a red color. These lifetimes were not taken into account in the histograms shown in Fig. 5 and for the calculations of the average lifetimes. The lifetime distribution histograms clearly show the shift to lower lifetime values when CDC48A-YFP and CDC48A–CrFP were co-expressed (Fig. 5B), while the lack of interaction between the N-terminally placed fluorescent groups is also clearly reflected in the absence of a shift to lower lifetime values (Fig. 5C). For comparison of the various combinations of proteins, combined distribution histograms of 5 representative experiments for each protein-combination were plotted (see Supplementary data).

Taken together, our observations show YFP/CrFP proteins fused at the C-terminus of CDC48A are within the maximal distance for measuring FRET and do interact, which is only possible when the protomers homo-oligomerize and the C-termini stay close together rather than protruding out of the molecule. This oligomerization takes place in the ER-membrane based regions at the PM, where SERK1-CDC48A interaction takes place. A combination of CrFP- and YFP-CDC48A proteins show no reduction in lifetime suggesting that the N-domains of CDC48A, in line with the mushroom-like shape structure of p97/VCP, are not within FRET distance and can not interact. The N-termini of CDC48C, in contrast with CDC48A, are within FRET distance and do interact suggesting that the N-terminal domains of CDC48C are differently organized and probably closer to each other.

SERK1 phosphorylates Ser-41 in the N-domain of CDC48A

In previous work it was shown that SERK1 interacts both with the N-domain, as well as with the C-terminus of CDC48A. To investigate if this interaction involves trans-phosporylation of CDC48A by the SERK1-kinase, an in vitro kinase experiment was performed. The SERK1 kinase domain and full length CDC48A were produced in E. coli as fusions to gluthatione-s-transferase (GST), purified and incubated with [γ32P-ATP]. After incubation, the mixture was, analyzed by SDS-Page and labeled proteins were detected with a Phospho-Imager. The SERK1 kinase domain is heavily auto-phosphorylated (Fig. 6A lane 1, 2 and 3) but also trans-phosphorylates CDC48A (arrowhead lane 1). Next, the experiment was repeated with cold
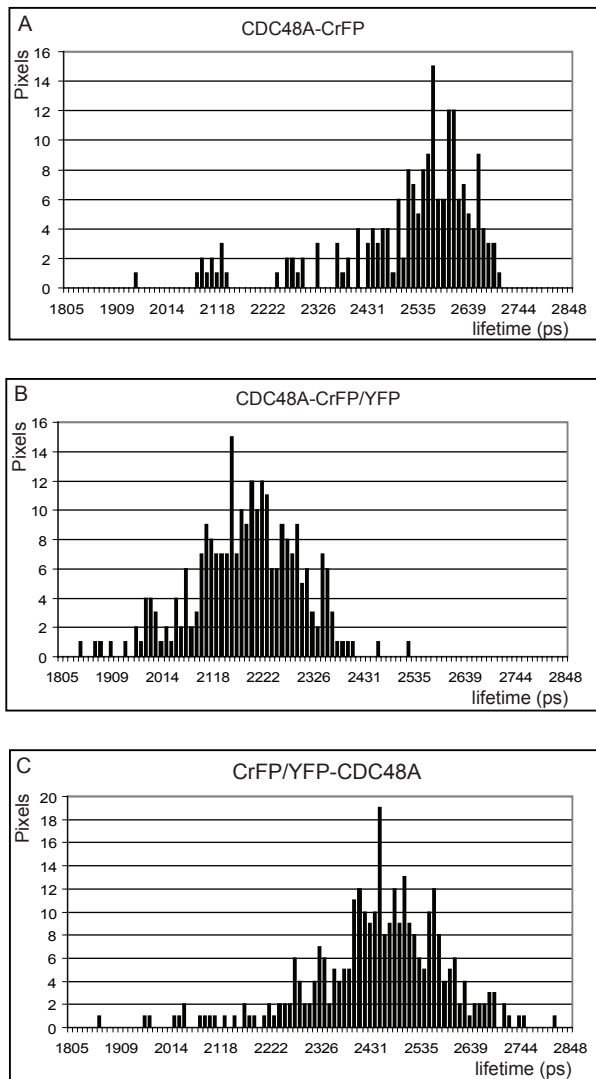
Figure 5. Representative lifetime distribution histograms measured with FLIM at the PM of Arabidopsis protoplasts. (**A**) Histogram of the CDC48A donor alone. (**B**) Histogram of a mixture of CDC48A tagged to CrFP and YFP at the C-terminus, which shifted to lower lifetime values due to interaction. (**C**) Histogram of a mixture of CDC48A tagged to CrFP and YFP at the N-terminus. No significant shift to lower lifetime values is visible.

ATP. The 125 kD CDC48A proteins were isolated from the gel, digested with trypsin, and the resulting peptides analyzed by LC-MS/MS. Only in the sample containing the SERK1 kinase, one phosphorylated serine residue was found at position 41 of CDC48A, which is located in the N-domain. Unfortunately we did not have any peptide coverage in the C-terminal tail (from AA 775 onwards, Fig. 6B), where 3 serines, 3 threonines and 1 tyrosine are present, so there may be additional targets for SERK1 phosphorylation.

The CDC48A complex size in living cells is larger than expected

To investigate the size of CDC48A complexes in living cells, CDC48A-YFP constructs were expressed in Arabidopsis protoplasts. Fluorescence correlation spectroscopy was used to measure the diffusion times (τdif) of CDC48A-YFP proteins (full length, CDC48A^{A1A2},
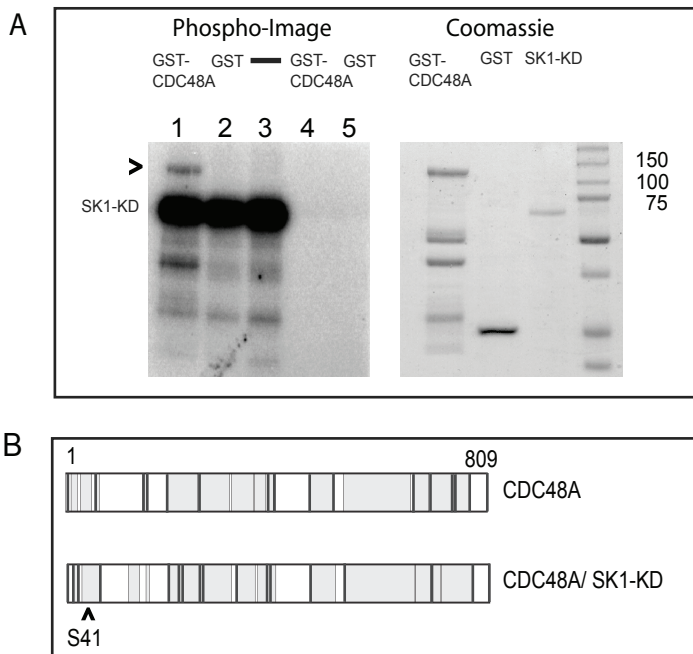
Figure 6. In vitro transphosphorylation of CDC48A, by SERK1 kinase protein.
(**A**, left panel) Phospho-image of CDC48A transphosphorylated by the SERK1 kinase domain. GST-CDC48A, GST alone or water were incubated with the SERK1 kinase domain (SK1-KD) in a buffer containing [γ32-P]ATP (Lane 1, 2 and 3). Two control experiments were performed without SK1-KD. SK1-KD is auto-phosphorylated and transphosphorylates CDC48A (arrowhead lane 1). (**A**, right panel) Equal loading and size control of GST-CDC48A, GST and SK1-KD-protein. (**B**) Peptide coverage of CDC48A in 2 reactions containing CDC48A alone or CDC48A plus SK1-KD, was 66, and 68% respectively (colored in gray). Ser-41 of CDC48A was phosphorylated by SK1-KD.

CDC48A[N-D1] and CDC48ANdel) in the cytoplasm close to the PM and in the nucleus. To estimate cellular viscosities via the Stokes-Einstein equation (Eq. (5)), the diffusion time of free YFP in cells was first measured. Differences in the diffusion times of protein molecules can point to mass differences between them and so, the diffusion time of CDC48 in cells was measured. The results of the FCS measurements are based on 9 independent transfections and summarized in Table 2. In Fig. 7, examples of autocorrelation curves are shown (both the raw data and fitted curves) for CDC48A-YFP, CDC48A[Ndel-] and CDC48A[A1A2] and free YFP in the cytoplasm.

First the diffusion time of free YFP in protoplasts was determined in the cytoplasm close to the PM and in the nucleus. The average values for the diffusion times (τdif) are listed in Table 2A for the cytoplasm and in 2B for the nucleus. From the τdif values of each curve the average diffusion coefficient D (μm^2/s) and the hydrodynamic radius rh (nm) were calculated. The
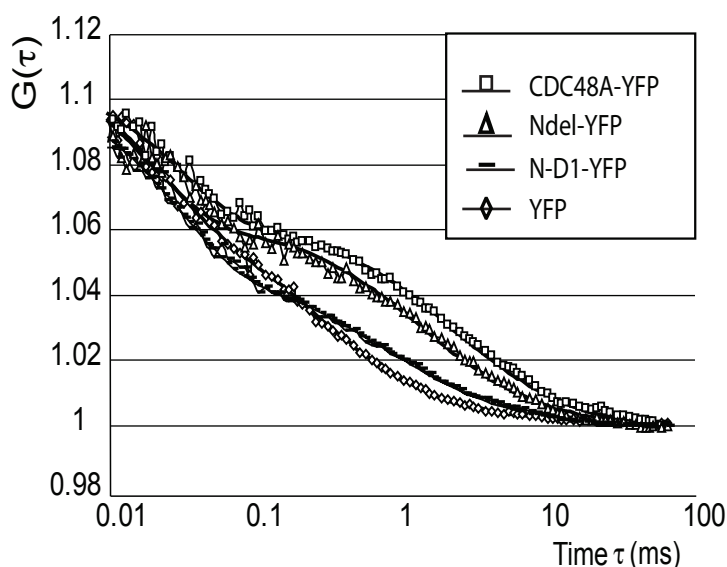
Figure 7. Representative auto-correlation curves from CDC48A- (squares), CDC48ANdel – (triangles) and CDC48AN-D1 –YFP (lines), compared to the curve for free YFP (lowest curve: diamonds) in Arabidopsis protoplasts. The autocorrelation curves were fitted with a one component model. On the Y-axis the autocorrelation function G (τ) is depicted. The correlation time τ (ms) is depicted on the x-axis in log-scale.

diffusion coefficients can be directly compared because in contrast to the diffusion time, the diffusion coefficient is independent of the structural parameter or the shape of the volume. The hydrodynamic radius rh is a measure for the size of the protein (complex). The diffusion coefficient for free YFP in protoplasts was determined to be 37 μm^2/s in the cytoplasm and 30 μm^2/s in the nucleus. The calculated hydrodynamic radii were 1.9 nm and 2.3 nm, close to

the theoretical rh for free YFP of 2.4 nm.

CDC48A-YFP in cells diffuses extremely slowly. A diffusion coefficient (D) of 3.5 μm^2/s was found for CDC48A-YFP in the cytoplasm. To answer whether this is due to the hexameric nature of the CDC48A protein, the monomeric CDC48A^{N-D1}-YFP mutant construct was also introduced into protoplasts. The diffusion coefficient of CDC48A^{N-D1}-YFP was found to be

Table 2   Mean of the diffusion coefficient D ($\mu m2$/s) of various proteins, measured by FCS in the cytoplasm and nucleus of protoplasts.

In the two-sample t-test comparing CDC48A with one of the other proteins, the null hypothesis that the mean of the diffusion constants are the same is rejected when the absolute value of p is lower than the 5% significance level and accepted when p is higher. Values for D and r_h, were calculated via Eq. 4 and 5. N-D1 is not expressed in the nucleus. SD is the standard deviation of the D value, N is the number of curves.

protein	τ_{dif} (ms)	D ($\mu m2$/s)	SD	N	t-test	r_h (nm)
cytoplasm						
CDC48A	1.886	3.5	0.8	20		20.4
YFP	0.214	37.0	16.7	25	$p < 0.05$	1.9
N-D1	0.568	11.7	4.8	74	$p < 0.05$	6.1
Ndel	1.323	6.0	1.7	18	$p < 0.05$	11.9
A1A2	1.223	6.2	0.7	8	$p < 0.05$	11.4
nucleus						
CDC48A	1.420	5.2	2.0	59		13.7
YFP	0.222	30.4	8.0	30	$p < 0.05$	2.3
Ndel	1.243	5.8	2.7	27	$p > 0.05$	12.3
A1A2	1.310	5.9	1.6	41	$p > 0.05$	12.1

11.7 μm^2/s, which is clearly faster then the CDC48A full length protein. However, based on the crystal structure for VCP, CDC48A should have a rh of about 7 nm instead of the calculated 20.4 nm. Therefore we hypothesized that the N-domain, which is considered to be the domain responsible for most of the interactions of CDC48 (p97/VCP) with adaptor proteins like p47 (Dreveny et al., 2004), Ufd-1 and ubiquitinated proteins (Meyer et al., 2000) associated with some of these proteins in the full length CDC48A as well as in the monomeric CDC48A^{N-D1}-YFP. Therefore we deleted the N-domain from CDC48A and measured diffusion times of the mutant CDC48A^{Ndel}-YFP protein. Indeed the diffusion coefficient of CDC48A^{Ndel} -YFP in the cytoplasm (6.0 μm^2/s) is significantly higher than that of CDC48A (3.5 μm^2/s). This could be explained by the lack of the interactive N-domain. Unlike CDC48A, CDC48A^{Ndel} was not predominantly found in the hexameric form on native PAGE (Fig. 1B), which might also explain the faster diffusion of this mutant.

The diffusion coefficient of the CDC48A^{A1A2}-YFP protein (6.2 μm^2/s in the cytoplasm), the mutant which is reported to be severely delayed in hexamerization in vitro for p97/VCP (Wang et al., 2003b), was significantly higher than the diffusion coefficient of the CDC48A protein (3.5 μm^2/s in the cytoplasm). Native PAGE showed that the CDC48A^{A1A2}-YFP protein in

cells is predominantly in the hexameric form, as well as CDC48A. Although the oligomerization of the CDC48A[A1A2]-YFP protein was not tested in the FRET-FLIM experiments, the FCS results suggest that fewer proteins associate with this mutant resulting in faster diffusion of CDC48A A1A2-YFP. This implies that inhibition of ATP-binding also inhibits complex formation with other proteins.

Surprisingly, no significant difference in diffusion coefficient between CDC48A-, CDC48A A1A2- and CDC48A[Ndel]-YFP was measured in the nucleus (Table 2B). In general the diffusion coefficient in the nucleus was the same as in the cytoplasm for all proteins, except for CDC48A-YFP. The diffusion coefficient of CDC48A is much slower in the cytoplasm, suggesting that in contrast with the situation in the nucleus the protein is bound to a larger or different complex.

There is a discrepancy between the complex-size estimated on native PAGE and the size calculated from the FCS analysis. An explanation might be that the CDC48A complex is associated with membranes or large molecules like the proteasome and therefore shows a very slow diffusion. For the native PAGE procedure however, membranes are solubilized and connections of membranes with protein complexes can be lost.

From these data we propose that in vivo membrane-located CDC48A is found in larger protein complexes rather than in hexameric configuration only, while the N-domain could be responsible for the interactions that lead to these large complexes.

Discussion

The CDC48A protein was previously found to be one of the SERK1 interacting proteins (Karlova et al., 2006; Rienties et al., 2005). Because CDC48 proteins are reported to be active only in hexameric form it was deemed essential to determine the oligomerization status in living cells. FRET-FLIM analysis indicated that the CDC48A-CrFP and CDC48A-YFP proteins are oligomerized in living cells. The CDC48A oligomers are predominantly hexameric, and the observed location of putative hexamers coincides with the interaction areas of SERK1 and CDC48A. These results suggest that the CDC48-CrFP/YFP proteins are indeed in their active conformation when expressed in living cells. Based on the prediction of this active configuration in vivo and the crystal structure of the related mammalian p97/VCP hexamer (DeLaBarre and Brunger, 2003) we used FRET-FLIM as a tool to confirm the presence of the hexameric configuration of CDC48A in vivo. Finally, the diffusion rates of the CDC48A proteins in vivo suggest that they are indeed part of a much larger oligomeric complex in vivo.

An unresolved and important question is what the functional relationship is between the CDC48A protein in an intact configuration and the SERK1 receptor. Active ATPases bind and hydrolyse ATP to release the energy for various processes in the cell, among which the protein dislocation from the ER during ERAD (Jarosch et al., 2002). Many adaptor proteins were found to interact with the N-domain of CDC48 or p97/VCP proteins, such as P47 (Dreveny et al., 2004), Shp1 and Ubx2 (Schuberth et al., 2004), Ufd1/Npl4 (Meyer et al., 2000) and Doa1

(Mullaly et al., 2006). These adaptor proteins recognize ubiquitinated substrates thereby facilitating proteasome-dependent degradation. For many studies artifical substrates were used to study the ERAD system (DeLaBarre et al., 2006; Müller et al., 2005). However, to date hardly any physiological substrates of CDC48/VCP proteins are known, thereby limiting the understanding of the function of these proteins in general and in SERK1-mediated signaling in particular. Therefore, it could well be that function of the interaction between CDC48A and SERK1 is to recognize and remove ubiquitinated receptors from the membrane, one of the proposals previously put forward by Aker et al. (Aker et al., 2006). The IP3-receptor in ER-membranes in Rat-1 fibroblasts was ubiquitinated upon ligand binding and coupled via the p97-Ufd1-Npl4 complex to proteasomal degradation (Alzayady et al., 2005).

DeLaBarre et al. (DeLaBarre et al., 2006) found that two Arginines (Arg586 and Arg599) in the D2 domain of P97/VCP were essential for substrate interaction and ERAD, implicating that not every interaction with CDC48 proteins should go via the known adaptor proteins and the N-terminus. This actually supports the idea that SERK1 interaction can occur with the C-terminal part of the CDC48A protein as it has been found that way in yeast two hybrid screens (Rienties et al., 2005). This was later confirmed by the FRET-FLIM evidence of interaction between SERK1-YFP and the C-terminus of CDC48A (Aker et al., 2006). The result of this interaction was hypothesized to be transphosphorylation by the SERK1 kinase (Rienties et al., 2005). Only one phosphorylated residue of CDC48A was found, which is located in the N-domain. Whether transphosphorylation of Ser-41 in the N-domain of CDC48A is necessary for binding to the, possibly, ubiquitinated SERK1-receptor and subsequent degradation of the protein is still unclear. Binding of SERK1 to the C-terminus could be part of the activation mechanism of the CDC48A protein complex. Rienties et al. (Rienties et al., 2005) showed that upon autophosphorylation of the SERK1-kinase domain, there was an increase in interaction with CDC48A. The mechanism of activation has still to be elucidated.

FRET-FLIM was also used to investigate the structure of CDC48A and one of its isomers, CDC48C, by calculating distances between parts of the molecule based on the FRET-efficiencies. Differences in FRET-efficiencies between CrFP and YFP depending on whether they were fused to the N-terminus of CDC48A or of CDC48C, led to the conclusion that the N-domains of CDC48C are differently organized and probably closer together. It is even not clear whether CDC48C has a real N-domain. It could be that CDC48C, being only present in the nucleus, is not involved in ubiquitin/proteasome–dependent proteolysis, but has a function in nuclear envelope reformation during the exit from mitosis. This was also described for p97 (Hetzer et al., 2001). We therefore suggest that the "N-domain" of CDC48C does not serve as a platform for binding ubiquitinated proteins and therefore probably does not protrude from the molecule.

Although FRET-FLIM is commonly used to estimate distances in multimeric complexes (Clayton et al., 2005; Van kuppeveld et al., 2002) a cautionary remark should be made. Due to the hexameric structure and the lack of control over the precise composition of the contributing monomers in our model, the donor group CrFP and the acceptor group YFP are not at a fixed distance from each other. Each donor group could to a certain extent also interact with

a different ensemble of acceptor groups at slightly different distances. It will require much more complex equations to deal with this situation, so the distances as calculated here may suggest a greater accuracy then actually can be measured. The distances calculated between the different subunits in the hexamer are nevertheless in close agreement with the distances as known for the structure of the homologue p97/VCP.

One of the surprising findings in our work was that the complex size of the CDC48A hexamer as derived from the diffusion coefficient determined by FCS was variable depending on the cellular compartment and also much larger then expected. The diffusion rate of CDC48A in the cytoplasm was significantly lower then in the nucleus while the mobility of free YFP and the CDC48A mutants was comparable to that of these proteins in the nucleus. This suggested that the full length hexameric CDC48A protein was the only functional protein and could therefore actively bind to other proteins and in the ER membrane compartments form complexes with adaptors and/or associate directly with the proteasomal complexes. Ubiquitination of the SERK1 receptor mediated by CDC48A might direct the receptor to the proteasome, but this has still to be elucidated. In the nucleus the CDC48A protein may have another function or is in a transit between targets and the proteasomal complexes.

Employing FRET-FLIM, we could provide details of SERK1 and CDC48A interaction and CDC48A oligomerization in vivo that would be difficult to resolve by other techniques. Using FCS it was shown that CDC48A hexamers in vivo are part of much larger complexes. Finally we believe that the use of these microspectroscopic techniques is helpful to validate structural information of protein complexes in an intact cellular environment.

Acknowledgements

Supplementary data

S1, S2 and S3 show histograms of lifetime distributions for different combinations of proteins measured in the nucleus or at the PM. Each histogram shows the combined distributions of 5 representative cells for that combination. Taking 10 in stead of 5 experiments did not change the value for the average lifetime; therefore 5 were taken for the calculations. On the horizontal axis the lifetimes are depicted, on the vertical axis the number of pixels per lifetime. In Figure S1 from top to bottom all the experiments performed with combinations of CDC48A at the PM are listed. The double combinations of CDC48A (2th, 3th and 4th histogram should be compared with the donor alone in the 1th histogram. In the right panel the experiments with CDC48A in the nucleus are depicted. Again the double combinations of CDC48A (2th, 3th and 4th histogram) should be compared with the donor alone in the 1th histogram. In Figure S2 the experiments performed with CDC48C proteins are depicted and these should be compared in the same way. In Figure S3 the CDC48AN-D1 double combination should be compared with the CDC48AN-D1-donor alone.

S1.

S2.

S3.

Horizontal: Lifetime in ps.
Vertical: number of pixels per lifetime.
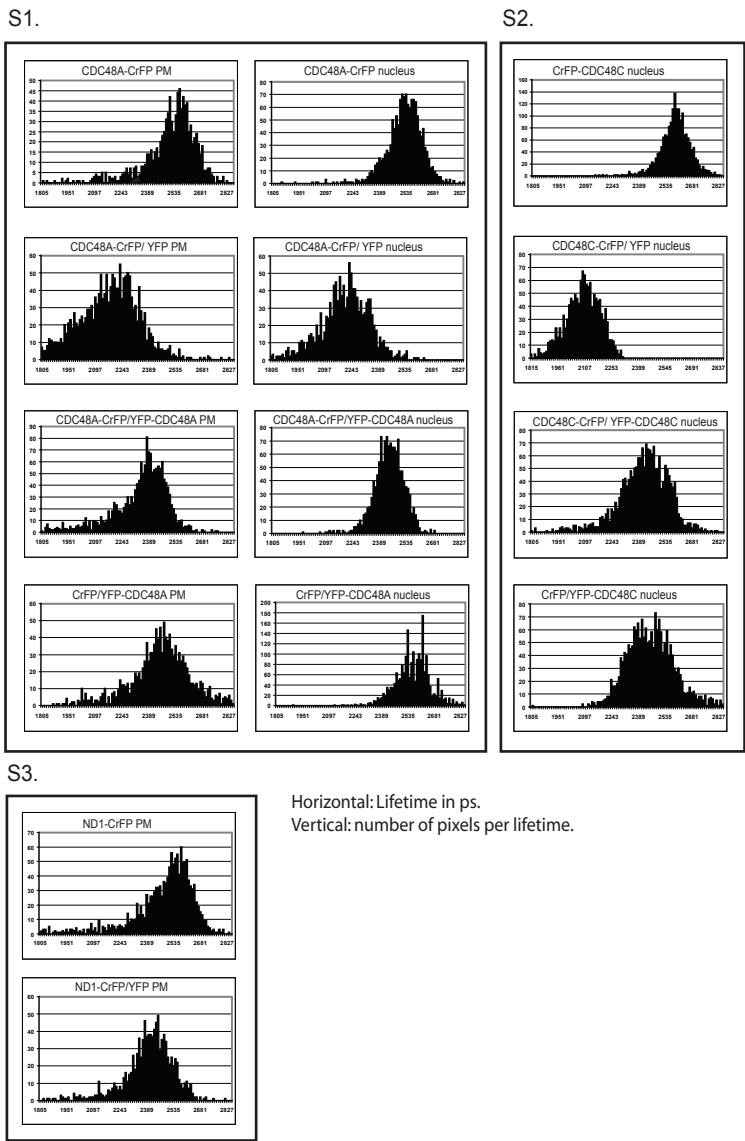
Chapter 4

Internalization of the BRI1-SERK receptor complex

José Aker, Thierry Wessels, Sacco de Vries

Abstract

Brassinosteroids are perceived by a hetero-oligomeric receptor complex consisting of BRI1 and the co-receptors BAK1 (SERK3) and SERK1, members of the small family of somatic embryogenesis receptor-like kinases. BRI1, SERK1 and SERK3/BAK1 undergo endocytosis and form heterodimers in endosomal compartments. The aim of this research was to determine the role of the co-receptors SERK1 or SERK3/BAK1 in the brassinosteroid signaling pathway in roots. Similar to what previously was observed in protoplasts, over-expression of SERK3 resulted in enhanced BRI1 endocytosis. In the absence of the co-receptors SERK1 and SERK3, BRI1 mediated BR signaling is impaired, the BRI1 protein level is reduced, while no reduction was observed in endocytosis. These results suggest that the hetero-oligomeric BRI1/SERK1-SERK3 (BAK1) configuration is involved in maintaining active BRI1-mediated signaling.

Introduction

Receptor mediated endocytosis in plant cells as a mechanism to modulate and diversify cellular sensitivity to external signals is poorly understood. There is evidence for endocytosis of the brassinosteroid-perceiving Brassinosteroid Receptor-like Kinase1 (BRI1) and its co-receptors the Somatic Embryogenesis Receptor-like Kinase1 and 3 (SERK1 and 3) (Russinova et al., 2004), but also other Leucine Rich Repeat–Receptor Like Kinases (LRR-RLK) like Crinkly 4 (Gifford et al., 2005) and the Flagellin Sensitive 2 (FLS2) (Robatzek et al., 2006). The BRI1 receptor was shown to internalize in a ligand-independent fashion, while more recently it was demonstrated that BR signaling can be mediated by internalized BRI1 receptors (Geldner et al, 2007). The FLS2 receptor was the first example of a receptor in plants to become internalized in response to a ligand, flagellin flg22 (Robatzek et al., 2006). Endocytosis of other plant membrane proteins like the plant specific auxin efflux carriers (PIN proteins) is well established (Geldner et al., 2003), and this appears to involve a clathrin-mediated mechanism (Dhonushke et al., 2006).

For the epidermal growth factor receptor (EGFR or ERBB1) it was shown that dimerization, also ligand-independent, rather than receptor kinase activity is important for endocytosis (Wang et al., 2005a). In ERBB signaling, only ERBB1 and ERBB4 are fully functional. ERBB3 has impaired kinase activity, while ERBB2 fails to bind known ERBB ligands, but connects its kinase activity to all possible heterodimers.

BRI1 was proposed to form a tetrameric complex with SERK1 and SERK3 (Karlova et al., 2006). SERK1, closely related to SERK3, was also shown to be internalized in protoplasts, as well as in roots of SERK1-YFP transgenic seedlings (Kwaaitaal et al., 2005). SERK3 and BRI1 undergo endocytosis and co-localize in endosomal compartments (EC). Co-expression of both receptors in protoplasts resulted into accelerated endocytosis, suggesting hetero-oligomerization of RLKs to be important for endocytosis in plant cells as well. ECs either with one or with both receptors were present, suggesting receptor-specific sorting (Russinova et al., 2004).

The aim of this study is to investigate whether BRI1-mediated signaling and endocytosis is affected by the absence of its two co-receptors SERK1 and SERK3. Sensitivity of the roots for BL was used as a measure for BRI1-mediated signaling. The double mutant *serk1-1serk3* (*sk1sk3*) is completely insensitive to brassinolide (BL) in roots, showing that these receptors are required for signaling (Albrecht, 2008). In BRI1-GFP*sk1sk3* roots, Br signaling is very much impaired as compared to in BRI1-GFP wt roots, indicating that the BRI1/SERK-1SERK3 signaling complex is not active in the *sk1sk3* background, while the distribution of the fluorescent BRI1 protein at the PM and in the cytoplasm, is not changed. However the total amount of BRI1 protein was reduced, suggesting that the presence of the SERK1 and SERK3 co-receptors aid in BRI1 stability.

Overexpression of SERK3 together with BRI1 in roots demonstrated enhanced endocytosis, confirming the data of Russinova (2004), while brassinosteroids (BR) signaling was not enhanced compared to the signaling in BRI1-GFP roots alone.

Shah et al (2001) showed that for SERK1 homodimerization the leucine zipper domain is

important. To investigate the effect of mutations in the co-receptor SERK1 on the internalization of BRI1, various SERK1 mutants in combination with BRI1 were transiently expressed in Arabidopsis protoplasts. Even severely truncated SERK1 receptors were sorted together with BRI1 in the same endosomal compartments, except for a SERK1 mutant lacking the external domain, suggesting that this domain is involved in interaction with BRI1.

Methods

Materials and growth conditions
The Arabidopsis thaliana Colombia ecotype was used as a wild-type background.
The following mutants and transgenic plants were described previously: PBAK::BAK1-GFP (J.Li, Chory), PBRI1::BRI1-GFP (N.Geldner), sk1 (C. Albrecht). PSERK::SERK1-YFP (M. Kwaaitaal). PBRI1::BRI1-GFP was crossed into *sk1-1sk-13* double or single mutant background and selected for homozygosity for *sk1, sk3* (verified by PCR) and for BRI1-GFP (verified by selection).
Seedlings were grown for 6 days on plates containing, Murashige and Skooge medium plus vitamins, sucrose and Daishin agar (0.575g, 2.5 and 2 g/500 ml respectively).

Microscopy
Seedlings grown for 6 days were incubated for 20 minutes in MS medium and placed on a microscope slide covered with a slide. Images were taken using a CLSM. 488 nm excitation light for exciting GFP was used, with a laser power of 12 %. Emission light was detected using a band-pass filter of 505-550 nm. After imaging, BRI1-GFP *sk1sk2sk3* seedlings were re-cultivated on soil and genotyped afterwards, to score for *serk2* homo- or hetero-zygosity, as *sk1sk2* homozygous plants are male sterile and therefore don't give any seeds.

Analysis of fluorescence distribution using Image Pro
Images of cells were taken on both sides of each root-tip and analyzed with Image Pro, to investigate the distribution of fluorescence in the PM and the cytoplasm. Using Image Pro it is possible to select for automated analysis of fluorescence intensities in the PM or in the cytoplasm. The program calculates the mean intensities in a section of one image and calculates also the standard deviations. The mean intensities of around 100 cells for each sample were determined.

Constructs
SERK1, SERK3 and BRI1 were fused to CFP or YFP in the pMON999 vector under 35S-promoter as described before (Russinova, 2004). All the SERK1 mutants were cloned without a stop codon subsequently in the Nco1 site created before CFP or YFP. The sequence of the generated constructs were verified by sequencing.

Isolation and transfection of Arabidopsis protoplasts
The transfection procedure was performed as described before (Aker et al., 2006). For analysis times shortly after transfection, protoplasts were kept in W5 on ice o/n after isolation and transfected next morning. Five hours after transfection the protoplasts were incubated with 50 µM Cyclohixamide (CHX) to stop protein production.

Root length assay
Ten to twenty seeds of wt and mutant background were sewn in one line on MS plates containing various concentrations of BL and placed vertically under long daylight conditions at 22 degrees Celsius. After 12 days the length of each individual root was measured. The average root length for each concentration was calculated as percentage of the length on control plates.

Western blotting
One four-week old rosette was frozen in an eppendorf tube in liquid nitrogen together with glass beads. After shaking in a CapMix, 200 µl of lysismix (1 % Triton x-100, 50 mM Tris pH 8, 150 mM NaCL, 10 mM EDTA plus protease-inhibitor mix) was added and mixed again. After 20 minutes incubation on ice, the sample was centrifuged for 7 minutes at 13000 rpm. A protein concentration determination was performed on the supernatant for equal loading. on SDS-Page.

Results

SERK3 enhances endocytosis of BRI1
Russinova et al (Russinova et al., 2004) showed that internalization of BRI1 and SERK3 was more rapid when both the receptors were co-expressed in protoplasts, suggesting that BRI1 endocytosis was promoted by association with the co-receptors. To investigate if this could be confirmed in planta, plants transformed with a pBRI1::BRI1-GFP construct (designated as BRI1-GFP, Geldner et al. 2007) were crossed with plants expressing a pSERK3::SERK3-6xHA construct (designated as SERK3-6xHA). The BRI1-GFP line produced near endogenous levels of BRI1-GFP protein and did not show the typical elongated leaf phenotype of other BRI1-GFP over-expression lines (Geldner et al., 2007). The transformations were performed in a wt background and therefore the generated lines used here contained at most twice the amount of BRI1 receptor. The SERK3-6xHA and the BRI1-GFP/SERK3-6xHA expressing plants do not show a phenotype on stature (Fig. 1A). On Western blots the SERK3-6xHA protein showed the expected size of 72 KD (Fig. 1B). The SERK3-HA protein localized to the PM in the root-tips, as shown using an antibody against the HA tag. In the double transgenic lines antibodies were used against HA and against GFP to visualize both receptors rather then using GFP fluorescence and immunofluorescence simultaneously.
First the specificity of the antibodies in immunofluorescence was determined. As a control
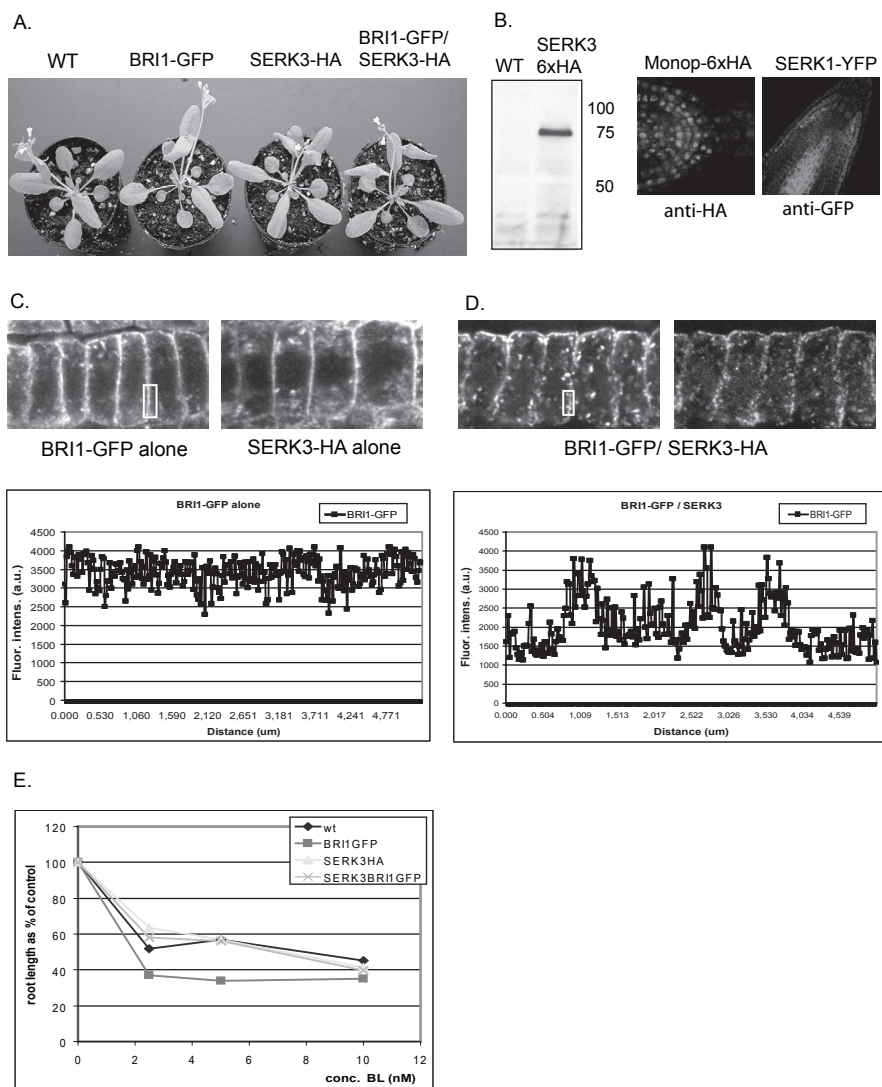
Figure 1. SERK3 enhances BRI1-GFP endocytosis. **A**. Plants of Col wt, BRI1-GFP, SERK3-6xHA and the double line are not phenotypically different. **B**. SERK3-6xHA protein from transgenic seedlings showed the expected protein-size of around 72 KD on a Western-blot. Anti-HA and anti-GFP anti-bodies specifically stained Monopteros-HA in the nucleus and SERK1-YFP in the vasculature and epidermis cells of root tips. **C**. GFP fluorescence at the PM in only BRI1-GFP expressing cells is more evenly distributed and of higher intensity along the PM (Fluorescence intensity in arbitrary units, (a.u.)), compared to in BRI1-GFP and SERK3-HA double-expressing cells, where GFP fluorescence appears more in endosomal compartments, as shown in the graphs (**D**). E. BRI1-GFP roots are hypersensitive to BL, which is restored to wt situation when SERK3 is also over-expressed.

for anti-HA, the monopteros (MP)-6xHA line was used, with the tagged protein residing in the nuclei of root tip cells (Weijers et al., 2006). MP-6xHA seedlings were fixed and immu-

nostained with anti-HA labeled with Alexa 488. As a control for specific anti-GFP staining, transgenic seedlings containing SERK1-YFP were used. SERK1-YFP is expressed in low levels and localizes specifically to the vasculature and to the epidermis cells in the root tip (Kwaaitaal et al., 2005). Indeed anti-HA stained the nuclei of root tip cells, and the anti-GFP signal localized only at places where SERK1-YFP is expressed; in the epidermis cells in the root-tip and in the vascular tissue (Fig. 1B).

To investigate if SERK3 enhances BRI1 endocytosis in plants, BRI1-GFP root tips immunostained with anti-GFP and Alexa-488, or SERK3-6xHA stained with anti-HA and Alexa 546 (Fig 1C images) only, were compared with BRI1-GFP/SERK3-6xHA double transgenic roots (Fig1D, images). In the BRI1-GFP expressing cells, the receptor is evenly distributed along the PM. In a profile of 5 μm taken along the PM, the fluorescence intensities of BRI1-GFP (depicted in a graph, Fig. 1C) hardly fluctuate. In the double transgenic line however, BRI1-GFP is localized in clear vesicles along the PM, and when a profile is taken along the PM, the intensities fluctuate between 1500 and 3500 on a scale of 0 to 4500 (a.u). In the graph in Fig. 1D, ECs at the PM are easily distinguishable, represented by the peaks.

We hypothesize that enhanced endocytosis would also lead to enhanced BRI signaling. Therefore roots of Col wt, BRI1-GFP, SERK3-6xHA and BRI1GFP/SERK3-6xHA seedlings were measured after growth on plates containing different concentrations of BL (Fig. 1E). The BRI1-GFP roots were slightly more sensitive than wt, possibly due to the combination of the endogenous BRI1 protein and the introduced fluorescent version. The SERK3-6xHA roots were as sensitive as wt. In BRI1-GFP/ SERK3-6xHA roots the sensitivity for BL was brought back to the wt situation, thus reduced compared to the BRI1-GFP sensitivity. Altogether, these results suggest that increased endocytosis of the over-expressed BRI1 and SERK3 receptors does not enhance brassinosteroid signaling in roots, but probably only reflects enhanced recycling by endocytosis of an inactive population of receptors.

The co-receptors SERK1 and SERK3 may stabilize the BRI1 protein

To determine the effect of the absence of both the co-receptors SERK1 and SERK3 on the distribution of the BRI1 protein, the pBRI1::BRI1-GFP expressing line (Geldner et al. 2007) was crossed into a homozygous *serk1-1serk3-1* (*sk1sk3*) mutant background. The *sk1-1* allele was previously described by Albrecht (Albrecht et al., 2005), and crossed into a homozygous *sk3-1* background. BRI1-GFP plants in these backgrounds did not show a phenotype (Fig. 2A). Only *sk3* plants are slightly smaller than wt confirming the data of Nam and Li (Nam and Li, 2002) and Li et al. (Li et al., 2002).

As a measure for the functionality of the BRI1-SERK complex, a root length assay was performed to determine BL insensitivity in these lines. Seeds were incubated on various concentrations of BL and root lengths were measured after 12 days (Fig. 2B). The average root length for each line was normalized to 100% using the average length on control plates as a measure. *sk1* and *sk3* roots were less sensitive to BL, compared to wt while *sk1sk3* roots were completely insensitive to BL (Fig. 2C), similar to a weak mutant allele of BRI1 such as *bri1-301*. However, the stature of the *sk1sk3* mutant plants is only mildly reduced compared to that
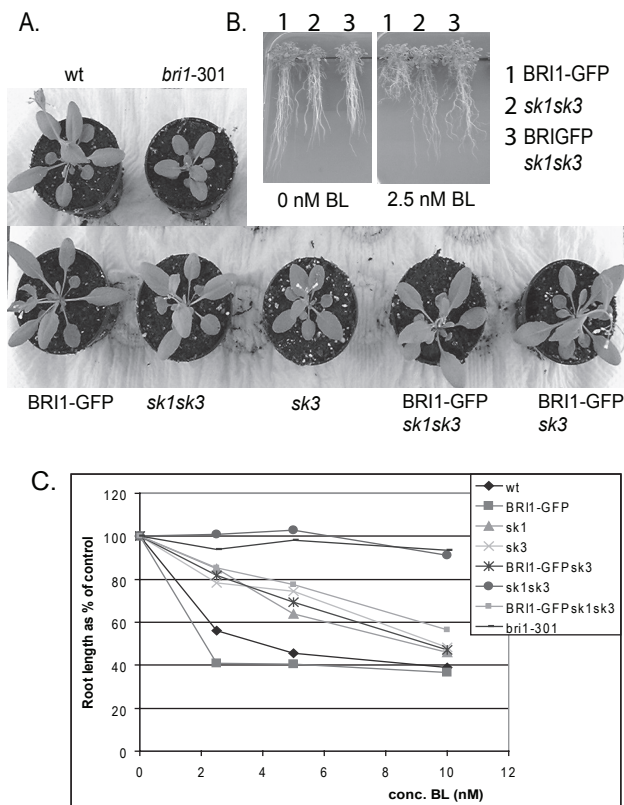
Figure 2. Root length assay using BRI1-GFP in Col wt, *sk1, sk3* **and** *sk1sk3* **mutants**. **A**. Plants of Col wt, pBRI1::BRI1GFP, *sk1sk3*, *sk3* and PBRI1:BRI1GFP in sksk3 or sk3 mutant background, grown under long daylight conditions. *Sk3* plants are slightly smaller, which is rescued by BRI1-GFP. **B**. Root length assay comparing BRI1-GFP, *sk1sk3* and BRI1-GFP in *sk1sk3* mutant background after 12 days on 0 or 2.5 nM BL. **C**. Root length assay using Col wt, *sk1, sk3* and *sk1sk3* mutants, BRI1-GFP in these mutants, and *bri1-301*. 10 to 20 roots were measured per point and normalized to the average root length of each line on 0 nM BL. The graph shows the combined results of 4 to 6 experiments

of the *bri1-301* allele (Fig. 2A), suggesting a more complex organ-specific relation between the three receptors, as pointed out by Albrecht et al, (2008) .

The Kd value reported for the BRI1 receptor is in the order of 15 nM of BL (Kinoshita et al., 2005). Therefore the concentration of 2.5 nM of BL employed here is well within range of the physiological concentrations of BL. The presence of the BRI1-GFP construct in the Col wt background slightly enhanced the root sensitivity for BL (at 2.5 nM a 15% reduction in root length was recorded) confirming the data of Nam and Li, (2002) (Fig. 2C) and see also Fig. 1E). Roots expressing the BRI1-GFP construct in the *sk1sk3* double mutant background were also slightly more sensitive to BL when compared to *sk1sk3* roots. However, although the

presence of additionally introduced active BRI1 receptors can partially restore BR signaling, BRI1-GFP*sk1sk3* roots retained most of the BL insensitivity, suggesting that BR signaling remained largely impaired in the absence of the two co-receptors, especially at lower concentrations of BL (Fig. 2C). Thus, it can be assumed that any visible changes in endocytosis or distribution of the BRI1-GFP receptor in the *sk1sk3* background reflect both impaired BRI1-mediated BR signaling as well as signaling induced by the introduced extra copies of the BRI1 receptor.

To determine whether the BR insensitivity of *sk1sk3* roots was due to a change in BRI1 distribution, root cells were identified in which all three receptors are present. Both BRI1-GFP and SERK3-GFP proteins are localized at the PM and in vesicles in every cell of the root (Nam and Li, 2002) while SERK1-YFP is localized mainly in the vascular tissue and in epidermal cells at the border of the root cap (Kwaaitaal et al., 2005)(Fig. 3A right panel). Therefore these cells were chosen to measure BRI1-GFP fluorescence in the PM and the cytoplasm in wt and in *sk1sk3* roots. (Fig. 3A, left panel). Images of the epidermal cells were obtained from both sides of each root-tip and analyzed with Image Pro (Fig. 3B) to determine the distribution of fluorescence between the PM and the cytoplasm. BRI1-GFP distribution and endocytosis was studied in the *sk1, sk3, sk1sk3* and *sk1sk2sk3* mutant backgrounds. First it was investigated if BRI1 endosomal compartments (ECs) were still formed in the *sk1sk3* background, which was indeed the case (Fig. 3C, right panel). BRI1-GFP ECs co-localized with the endocytic marker dye FM4-64 in wt as well as in *sk1sk3* backgrounds.

Next, the fluorescence intensities in the PM and cytoplasm were determined. The ratio between cytoplasm and PM fluorescence was almost the same for BRI1-GFP in wt, *sk1, sk3, sk1sk3* or *sk1sk2sk3* mutant backgrounds; 0.76, 0.76, 0.70, 0.76 and 0.71 respectively. However, all mutant lines showed a significantly lower BRI1-GFP fluorescence in the PM as well as in the cytoplasm when compared to the control (Fig. 3D). The total fluorescence derived from these measurements is significantly less (around 20 %, $p<0.01$) for *sk1, sk3, sk1sk3* and *sk1sk2sk3* than for wt (Fig. 3E). To verify that the lower expression of BRI1-GFP in the mutant backgrounds is not due to the fact that more generations were necessary to create these lines, a BRI1-GFP revertant line was selected from a BRI1-GFP*sk1sk3* heterozygous line. This line showed a higher BRI1-GFP expression, comparable to the original BRI1-GFP line in wt background (Fig. 3D last bars on the right). These results suggest that the total amount of BRI1- GFP receptors is indeed lower when one or both of the co-receptors are absent.

To summarize, the sensitivity for BL in BRI1-GFP*sk1sk3* roots is strongly reduced compared to BRI1-GFP in the Col wt, while the total amount of BRI1-GFP protein in sk1sk3 background was reduced by about 20%. The ratio between PM- and cytoplasm-localized BRI1-GFP did not change; apparently lacking the co-receptors influenced the total levels of BRI1-GFP protein but not the distribution. When SERK3 was over-expressed, enhanced endocytosis of BRI1-GFP was observed and no increase but rather a mild decrease in BR signaling activity occurred. This is interpreted to suggest that in both situations endocytosis is enhanced, but that in the absence of the co-receptors the balance between recycling and degradation is shifted to the latter while upon over-expression the internalized population of

A.

Figure 3

BRI1-GFP

SERK1-YFP

B.

Image Pro analysis

C.

BRI1-GFP   BRI1-GFP
                sk1sk3

D.

E.

A.

SERK1^{fl}

SERK1^{3T}

SERK1^{S299A}

SERK1$^{\Delta C}$

SERK1$^{\Delta 366}$

SERK1^{ED}

EGF-SERK1^{kd}

B.

C.

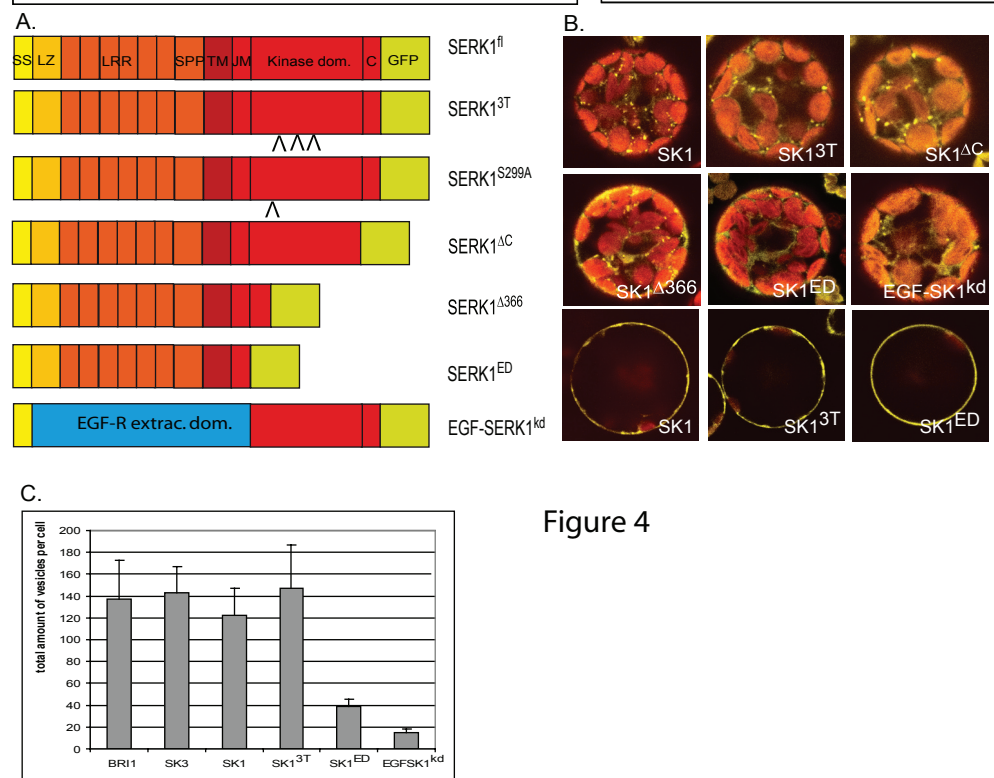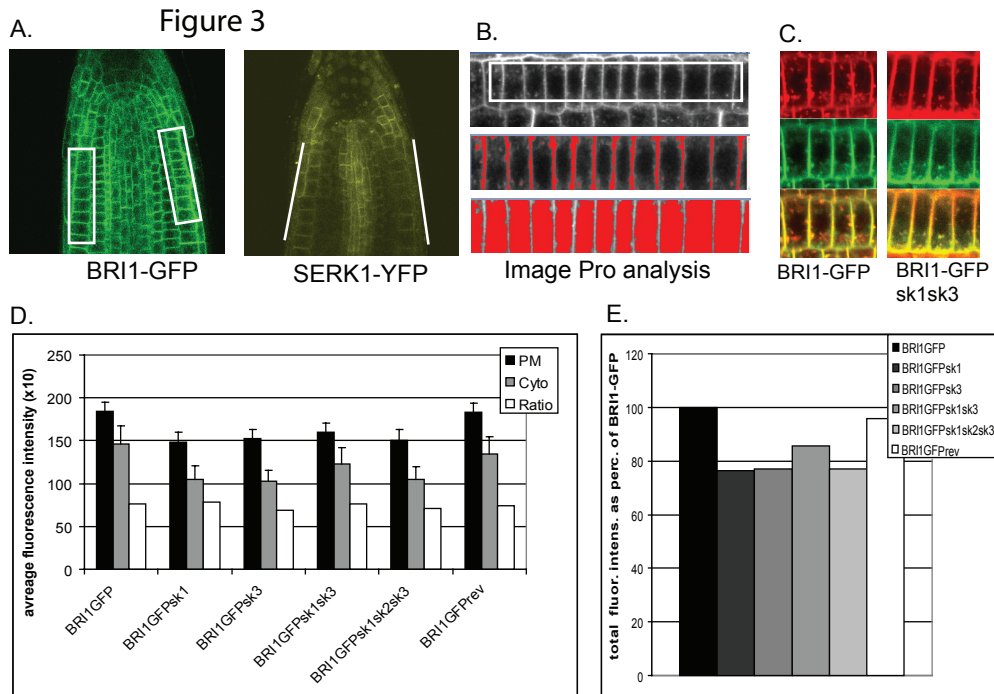## Figure 4

BRI1 receptors is more recycled. Furthermore we conclude that endocytosis of BRI1 does not require the presence of the SERK co-receptors.

SERK1 endocytosis is not dependent on an active kinase domain

The BRI1, SERK1 and SERK3 receptors are involved in brassinosteroid signaling and internalize together. It is however unknown whether the catalytic activity or particular domains of these LRR-RLKs are required for the process of endocytosis. Therefore a series of SERK1 mutant proteins fused to CFP or YFP, were expressed in Arabidopsis protoplasts (Fig. 4A). In cells expressing SERK1 (SK1)^{fl}, SK1^{3T} , SK1$^{\Delta C}$, SK1$^{\Delta 366}$, SK1^{ED} and EGF-SK1^{kd} ECs were visible (Fig. 4B), although SK1^{ED} and EGF-SK1^{kd} contained less. All mutant receptors were still able to localize to the PM, as shown previously for SK1^{3T}, SK1^{ED} but also EGF-SK1^{kd} (Shah et al., 2001a). The images shown in Fig. 4B were taken in one plane of the cell, but also z-stacks were made from cells expressing BRI1, SERK3 (SK3), SK1, SK1^{3T}, SK1^{ED} and EGF-SK1^{kd} and ECs counted for the total cell (Fig. 4C). BRI1, SK3, SK1, SK1^{3T} all contained around 140 ECs per cell, except for the deletion mutants SK1^{ED} and EGF-SK1^{kd}, containing respectively 40 and 20 ECs. The SK1^{3T}, SK1$^{\Delta C}$ mutants lost kinase activity (Albrecht et al., 2005; Shah et al., 2001b)which means that kinase activity is not necessary for internalization. Lack of the total intracellular part of the receptor (in SK1^{ED}) or the extracellular domain (in EGF-SK1^{kd}) impairs internalization strongly, however not

Figure 3.   Distribution of BRI1-GFP fluorescence in PM and cytoplasm of epidermis cells.
A. BRI1-GFP and SERK1-YFP localization in root tips. The white square indicates the cells, which were analyzed for endocytosis levels. **B**. Images show the PM or cytoplasm localized fluorescence, which were separately analyzed by Image Pro. **C**. BRI1-GFP in *sksk3* background (green panel) still localizes to endosomes that co-localize with FM4-64 (red panel). **D**. The average BRI1-GFP fluorescence in the PM, the cytoplasm and the ratio of both for wt, *sk1, sk3* or *sk1sk3*, or *sk1sk2sk3* mutant background. The ratio of fluorescence is the same in all situations: respectively 0.76, 0.76, 0.70, 0.76, and 0.71. **E**. The total (PM plus cytoplasm) BRI1-GFP fluorescence in the mutant backgrounds was significantly lower as compared to the control (respectively 23, 23, 14 and 23 % for *sk1, sk3, sk1sk3* and *sk1sk2sk3*), but not for the revertant BRI1-GFP line 4%).

 Figure 4. Expression and localization of SERK1 full length and mutant proteins in Arabidopsis protoplasts. In panel A the various mutants are shown schematically. SERK1 "fl" is full length; "3T" is the kinase dead, T462, T463, and T468 are changed into Alanines (Shah et al., 2001b).; in "S299A" the serine important for endocytosis in FLS2 is changed; "ΔC" lacks the C-terminal tail; "Δ366" lacks almost the complete kinase domain, apart from 44 amino acids and resembles allele *serk1-3*; "ED" lacks the complete cytoplasmic part of the protein except for 4 Arginines behind the TM domain to keep the protein in the membrane; EGFSERK1^{kd} consists of the external part of the EGF receptor and the kinase domain of the SERK1. B. Expression of various SERK1 mutants in Arabidopsis protoplasts, analyzed after 6 hours. The upper two rows show internalization of SK1^{fl}, and various mutants. All truncated receptors internalize via endocytosis, including receptors without kinase domain or activity, which however, still localize to the PM. C. Total number of ECs per cell, counted in z-stack images of around 10 cells. SK1^{ED} or EGFSK1^{kd} still internalized in ECs, but much less than SK1 and the SK1^{3T}.

totally.

In SERK1, the mutant containing the juxta-membrane domain (JM) but lacking most of the kinase domain, SERK1$^{\Delta366}$, still internalizes the same as SK1^{fl}. In the mutant lacking the kinase domain and the JM (SK1^{ED}), endocytosis is very much impaired. This suggests that a motive in the JM is important for endocytosis. The LRR-receptor kinase FLS2, an interacting partner of BAK1/SERK3, is internalized as a response to flg22. Phosphorylation of a threonine T867 in the JM of FLS2 is responsible for internalization, because mutation of this threonine abolished flg22 response and impaired endocytosis (Robatzek et al., 2006). FLS2^{T867} resembles BRI1^{T880}, which has been identified as in vivo phosphorylation site (Wang et al., 2005). In SERK1, S299A in the juxta-membrane domain resembles FLS2^{T867} and BRI1^{T880} based on sequence homology, and was found to be phosphorylated in vitro (Karlova et al., 2008). It was investigated if S299 in SERK1 was likewise important for endocytosis, by changing this serine to an alanine and co-transfecting the construct fused to YFP with BRI1-CFP into protoplasts. However, the SERK1^{S299A} mutation showed the same number of ECs as compared to SERK1-YFP (Fig. 5B).

From these data we conclude that for internalization, neither the activity of the kinase nor the kinase domain is required. The external domain is important, but also part of the juxta-membrane. However, domain S299A in the JM is not important for endocytosis of SERK1.

The extracellular domain of SERK1 is controlling interaction with BRI1

It was previously shown that BRI1 and SERK3 receptors were sorted in different ECs after internalization (Russinova et al., 2004). To investigate if mutated SERK1 receptors are impaired in internalization together with BRI1, double transfections were performed in Arabidopsis protoplasts with BRI1-CFP and several SERK1-YFP mutants. Confocal images were taken and the number of ECs was counted. The ratio between double and single labeled endosomes was then calculated.

In Figure 5A images of cells co-expressing BRI1-CFP and SERK1-, SERK3-, or SERK1ED-YFP are shown 16 hours after transfection. The number of BRI1-CFP ECs is comparable in every cell analyzed (Fig. 5A.1, 2 and 3), while the number differs with the different SERK-constructs.

To compare endocytosis of the different SERK mutants in combination with BRI1, the number of ECs containing both receptors was calculated as a percentage of BRI1- (grey bars, Fig. 5B) or as percentage of SERK1-ECs (black bars). When only BRI1 fused to CFP and YFP were co-expressed, this resulted in more than 90% of the BRI1-CFP vesicles containing also BRI1-YFP receptors (Fig. 5B, first grey bar). When BRI1-CFP was co-expressed with SERK3-, SERK1-, SERK1^{3T}-, SERK1$^{\Delta366}$-and SERK1$^{\Delta C}$-YFP, between 60 and 80% of the BRI1 ECs contained also SERK receptors (grey bars). BRI1-CFP was also co-expressed with SERK1^{ED}- or EGFSERK1^{kd}-YFP, two mutants lacking either the complete intracellular domain or the complete extracellular domain. In these cells an average amount of BRI1, but only a few SERK1^{ED} or EGFSERK1^{kd} ECs were detected. The number of ECs containing both receptors calculated as percentage of SERK1-YFP vesicles (or BRI1-YFP for the first bar),
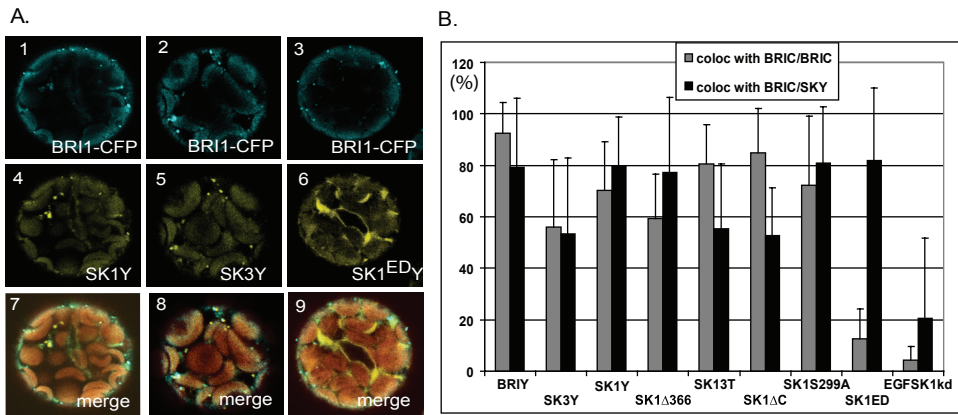
Figure 5. SERK1 mutants co-localize with BRI1. **A.** BRI1-CFP (1,2,3) was co-expressed with SERK1-, SERK3- or SERK1^{ED}-YFP (4,5,6) in protoplasts, and analyzed for the number of ECs. **B**. From images as shown in **A** was investigated how many ECs contained both BRI1 and SERK1 receptors in one plane of a cell (n =15). This was calculated as the number of ECs containing both receptors compared to total BRI1 (grey bars) or SERK1 (black bars). SERK1^{fl} and SERK3^{fl} or most of the truncated SERK1 receptors co-localized for between 60 and 80% with BRI1 or vice versa. Only 10 % of the BRI1 ECs contained also SERK1^{ED} (grey bars). However, 80% of the few SERK1^{ED} ECs contained BRI1 (black bars).
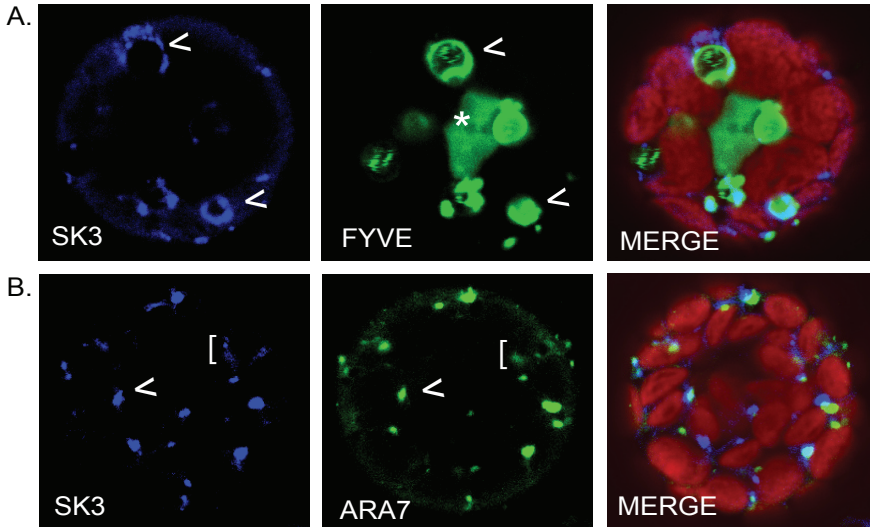
Figure 6. SERK-containing endosomal compartments co-localize in part with prevacuolar membranes. A. Co-localization of SERK3-CFP and DsRED-FYVE in double-transfected Arabidopsis protoplasts. Arrows point to co-localization in prevacuolar membranes. The asterisks points out the nucleus stained by FYVE. B. Co-localization of SERK3-CFP and ARA7-YFP. The arrow points to co-localization in endosomes, the bracket points to a supposed vacuole.

showed that 60 to 80% of the ECs containing SERK1 and SERK3 or SERK1$^{\Delta 366}$ contained also BRI1 (black bars). Only 55 % of SERK1^{3T} and 53% of SERK1$^{\Delta C}$-containing ECs contained also BRI1, as compared to 80 % of SERK1^{fl} vesicles (black bars: in a t-test compared to control p= 0.001 and 0.009e-2 respectively), suggesting that more of these mutant SERK1 receptors internalized without BRI1 than the SERK1^{fl} receptor. However 80 and 85 % of the BRI1-vesicles contained also SERK1^{3T} or SERK1$^{\Delta C}$, showing that the difference is caused by the fact that more ECs are formed when SERK1^{3T} or SERK1$^{\Delta C}$ are expressed, compared to SERK1^{fl}.

Only 10 % of the BRI1 ECs contained also SERK1^{ED} vesicles (grey bar). However, 80% of the few SERK1^{ED} ECs contained also BRI1 (black bar). On the contrary only 20% of the EGFSERK1^{kd} containing ECs contained BRI1. As the external domain of the SERK1 receptor is lacking, this suggests that the external domain of the SERK1 receptor is important for dimerization with the BRI1 receptor. Interestingly, the extracellular domain of SERK1, including the TM was previously noted to be required for homodimerization (Shah et al., 2001a).

Altogether we conclude that between 60-80% of the BRI1 ECs co-localized with SERK3, SERK1, or SERK1- mutants. Thus, truncation of its co-receptors still enables the BRI1-receptor to be internalized into endosomal compartments. Furthermore, mutant SERK1 receptors still end up in the same ECs as BRI1, except for the EGF-SK1^{kd} chimera, which suggests that the external domain is controlling heterodimerization of SERK1 with BRI1.

Receptors in protoplasts follow a normal endocytic pathway

An interesting question still to be answered is whether in protoplasts over-expressed receptors are predominantly recycled to the PM via recycling endosomes, or are also degraded. If they are not degraded, PM localization but also endosomes should accumulate in time. From previous work (Aker et al., 2006; Russinova et al., 2004) it is known that SERK1 and SERK3 containing vesicles co-localize with the early endosomal marker Ara6 and with the membrane dye FM4-64. To investigate if SERK3-containing vesicles are not only recycled to the PM but also degraded via the prevacuolar compartment (PVC) or multi vesicular bodies (MVB) to (lytic) vacuoles, SERK3-CFP was co-expressed with the late endosomal marker DsRED-FYVE. In animal cells, the FYVE domain is a conserved motif that localizes PI(3)P-binding proteins to early endosomes (Gillooly et al., 2000). In plant cells, the FYVE domain was found to co-localize with endosomes but also with the prevacuolar marker AtRabF2b. In Arabidopsis protoplasts FYVE labeled endosomes, the nucleus, but also strongly the vacuolar membrane of prevacuolar compartments (PVC) (Vermeer et al., 2006).

SERK3-CFP indeed localized to small ECs, but in part also co-localized with DsRED-FYVE at circular structures that are probably vacuolar membranes (arrows in Fig. 6. panel A). Inside the vacuoles not many SERK3-CFP ECs are visible, probably due to lysis of the fluorescent proteins. For comparison SERK3-CFP was co-expressed with ARA7-YFP that localizes to early and late endosomal compartments (Samaj et al., 2005; Vermeer et al., 2006). ARA7 has a different localization as compared to FYVE, and co-localizes with SERK-CFP in small

vesicles (arrow in panel B). However also in these images it seems that both proteins meet at membranes of PVCs (See brackets).

These data show that in protoplasts the SERK and BRI1-receptors are localized to early and late endosomes, but also to PVCs, suggesting that BRI1 and SERK-receptors transiently expressed in protoplasts follow a normal endosomal pathway and that protoplasts can be used to study aspects of endocytosis.

Discussion

To determine the role of the SERK1 and SERK3 (BAK1) co-receptors in BRI1-mediated Br signaling a variety of approaches was employed, aimed at modulating the level of the co-receptors. In this study we observed that in epidermal cells of *sk1*, *sk3* or *sk1sk3* mutant roots, the amount of BRI1-GFP protein in the PM and cytoplasm is reduced compared to the control. The same distribution of fluorescence intensity between the PM and the cytoplasm was found. Our results also show that over-expression of tagged BRI1 and SERK3 constructs resulted in enhanced presence of both receptors in endosomal compartments in the root epidermis. This confirmed earlier observations in protoplasts (Russinova et al, 2004) and suggested a role for the co-receptors in promoting endocytosis of the BRI1-receptor. However, no enhanced BR signaling was shown in roots. On the contrary, over-expression of SERK3-6xHA together with BRI1-GFP reduced the mild hypersensitivity for BL of BRI1-GFP alone, suggesting that SERK3 negatively influences the hypersensitivity of BRI1-GFP, maybe due to the formation of more heterodimers. Russinova and co-workers (2004) and Wang and Chory (2006) showed that homodimers also exist, but it is not known if these are part of the active receptor signaling mechanism. The mild hypersensitivity of BRI1-GFP might be the result of BRI1-GFP becoming active as a homodimer, due to the lack of enough co-receptors. Albrecht et al (2008) showed that there is no redundancy with any other SERK-family members in the BRI1 pathway, and that SERK1 and SERK3 are the only co-receptors for BRI1 in BR-signaling. However, this homodimeric BRI1-signaling might only take place when the BRI1/SERK receptor-complex is not in balance. It might be that over-expression of SERK3 together with BRI1 leads to more heterodimers and more endocytosis, but not more signaling due to the lack of SERK1. The enhanced endocytosis visualized in the situation where BRI1-GFP and SERK3-6xHA are over-expressed, while Br signaling is not enhanced, might then only refer to the inactive population of BRI1 or SERK receptors.

In the reverse experiment, we observed that upon removal of either one or both of the functional co-receptors by mutation, an approximately 20% reduction was observed in the amount of BRI1- protein in those cells where all 3 receptors are found in the wt situation. No evidence was obtained for a change in distribution between the PM and the cytoplasm of the same root cells. Surprisingly, only when both co-receptors were absent a clear loss-of-function in BRI1-mediated BR signaling occurred in roots. As BRI1/SERK1SERK3 signaling is less functional in roots lacking the co-receptors while the BRI1-protein is reduced, this might suggest that the co-receptors aid in stabilizing the BRI1-signaling complex and in this way

enhance signaling. The presence of both co-receptors might delay degradation of BRI1 in the heterodimers and extend the signal. If the co-receptors are necessary for stability of the main receptor, lacking these receptors would lead to a pool of less stable BRI1 receptors, and therefore make them more susceptible for degradation.

An explanation for the fact that there is no change in distribution between BRI1-protein levels at the PM and the cytoplasm in *sk1sk3* background, might be that only a small portion of the BRI1-receptors visualized is involved in active BRI-signaling, as was shown before in proto-plasts (Russinova et al., 2004). If lack of the co-receptors results in more overall BRI1-protein degradation, this might not change the distribution over the locations.

Another example of a heterodimeric receptor complex where one receptor influences the stability of the other receptor is Clavata. Clavata1 (CLV1), consisting of an extracellular LRR Receptor like kinase is functional in regulation of meristem development in Arabidopsis. CLV2 is a receptor-like protein functioning in the same pathway but lacks the kinase domain. CLV1 is supposed to form a heterodimer with the CLV2 protein to transduce extracellular signals. CLV1 protein levels in *clv2* mutant background were reduced by more than 90%, suggesting that CLV2 is required for the stability of the CLV1 protein (Jeong et al., 1999).

In protoplasts most of the mutant SERK1 receptors localize to the same ECs as BRI1. Inactive SERK1 proteins and also truncated proteins lacking the whole cytoplasmic domain, although the number of ECs was strongly reduced, still internalize together with BRI. However, the extracellular domain of SERK1 seems to be important for heterodimerization with BRI1. SERK1 protein lacking this domain did not co-localize with BRI1 in ECs. This suggests that the external domain of the SERK1 receptor is important for heterodimerization with the BRI1 receptor, as well as required for homodimerization (Shah et al., 2001a).

From our data it is clear that there is a discrepancy between our cell-biological observations and the phenotypic features of the transgenic plants used in our study. BRI1-GFP*sk1sk3* is impaired in BR signaling in roots, but the plant does not show reduced stature as shown for *bri1*- or *sk3* -mutants. It might be that the roots or the root epidermis we use for our observations, can not explain the functionality of the BRI1-receptor complex in other parts of the plants.

In conclusion, the co-receptors SERK1 and SERK3, although they might influence endocytosis of BRI1, are not absolutely required for endocytosis. However the activity of the BRI1 receptor complex is dependent on both co-receptors. The role of the co-receptors might then be the modulation of the activity of the BRI1-signaling complex, by influencing its stability probably depending on the organ in the plant.

Chapter 5

Endosomal signaling of the brassinosteroid receptor BRI1 requires the SERK1 and SERK3/BAK1 co-receptors

José Aker, Ruud Wijdeven, Jan Willem Borst and Sacco de Vries

Abstract

In Arabidopsis, brassinosteroids are perceived by a receptor complex consisting of the ligand-binding receptor BRI1 and the two co-receptors SERK3/BAK1 and SERK1. BRI1, SERK1 and SERK3 internalize into endosomes. BFA treatment results in internalization of BRI1-GFP in endosomal compartments together with a small subset of SERK3, where the complex remains active in BR signaling. Removal of both SERK co-receptors by mutation results in root insensitivity for both BL and BFA, suggesting that active BR signaling after internalization via endocytosis requires the presence of an intact BRI1-SERK complex.

Introduction

The brassinosteroid (BR) pathway in Arabidopsis regulates various aspects of plant development such as stem elongation, senescence, pollen tube growth, fertility and responses to biotic and abiotic stresses (Clouse et al., 1996; Mandava, 1988). Several BR insensitive mutants have been described; they exhibit a dwarf stature and have long roots when grown on the ligand brassinolide (BL). In the absence of ligands, the main BR receptor BRI1 (Brassinosteroid Insensitive1) is in a homodimeric state and bound to BKI1 (BRI1 Kinase Inhibitor 1). After binding of BL to the extracellular domain of the BRI1 receptor BKI1 is released, which enhances the affinity of BRI1 for BAK1 (BRI1 Associated Kinase 1), identical to SERK3 (Somatic Embryogenesis Receptor-like Kinase 3). Hyperphosphorylation of the BRI1-kinase domains keeps the receptors in an auto-inhibitory conformation by the C-terminal (CT) domain of BRI1. After release of BKI1 a conformational change of the kinase domain occurs and leads to phosphorylation of the CT domain that releases the auto-inhibition and enhances autophosphorylation. The fully activated receptor forms a multimeric complex with its co-receptor SERK3/BAK1 which transduces the BR signal (Wang and Chory, 2006; Wang et al., 2005). Transphosphorylation of the receptors leads to inhibition of BZR1 (Brassinazole resistant 1) phosphorylation by BIN2 (BR insensitive2 kinase). BL also activates the phosphatase BSU1 (BRI1 suppressor protein1) that dephosphorylates nuclear-localized BES1 (BRI1 EMS Suppressor 1). Subsequently, accumulation of dephosphorylated BES1 and BZR1 transcription factors results in transcription of target genes (Vert and Chory, 2006).

Another proposed co-receptor for BRI1 is SERK1 (Karlova et al., 2006). It was suggested that SERK1 and SERK3 can form a tetrameric complex together with BRI1 (Karlova and de Vries, 2006). BRI1, SERK1 and SERK3 are localized at the plasma membrane (PM) and can internalize in protoplasts independent of exogenous ligands (Kwaaitaal et al., 2005; Russinova et al., 2004). However, over-expression of either SERK1 or SERK3 in combination with BRI1 in protoplasts resulted in enhanced endocytosis of both receptors (Russinova et al. 2004). The SERK and BRI1 receptors co-localized in the same endosomal compartments (ECs), but could also be present separately in different ECs (Aker et al., 2006; Russinova et al., 2004). In chapter 4 it was shown that mild over-expression of BRI1 and SERK3 also resulted in enhanced endocytosis of both receptors but did not affect BRI1-mediated BR signaling when compared to wild type. Upon mutation of both SERK1 and SERK3, the roots become almost completely insensitive to BL, suggesting strongly impaired BR signaling (Albrecht et al., 2008). In the *sk1sk3* mutant background the level of BRI1-GFP protein was reduced by approximately 20% (Chapter 4).

The fungal toxin brefeldin A (BFA) was originally discovered as an inhibitor of Golgi-dependent secretion and later as a blocking agent for endosomal post-Golgi trafficking. BFA was shown to inhibit activation of sensitive ADP ribosylation factor (ARF) type small GTPases, by binding to the ARF and its controlling element, the guanidine exchange factors for ADP ribosylation (ARF-GEFs). The first BFA-sensitive ARF-GEF discovered in plants is GNOM (Geldner et al., 2001). BFA treatment led to a rapid and reversible accumulation of the polar auxin transport carrier PIN1 in "BFA" compartments (Geldner et al., 2003). BFA-induced

increased endosomal localization of BRI1 was shown to enhance BRI1-mediated BR signaling, providing evidence that BR signaling can take place after internalization of the receptor (Geldner et al., 2007).

It is unknown whether the SERK1 or SERK3 proteins, although they internalize together with BRI1, employ the same endocytosis or recycling pathway as BRI1. The aim of this study therefore is to investigate the effect of BFA on the co-receptors SERK1 and SERK3 recycling and to determine whether the absence of both co-receptors affects BR signaling from endosomal BFA compartments. The results show that only a small fraction of the SERK1 and SERK3 co-receptors employ a BFA-sensitive pathway together with BRI1. Surprisingly, in the absence of both co-receptors, BR signaling in roots is strongly inhibited and in contrast to wt roots has become largely BFA-insensitive. Because sequestering of BRI1 in BFA compartments is not affected we conclude that BRI1 mediated BR signaling in roots largely occurs from internalized receptors and depends on the presence of the SERK co-receptors.

Material and methods

Growth conditions and immuno-staining
The Arabidopsis thaliana Colombia ecotype was used as a wild-type background.
The following mutants and transgenic plants were described previously: PBAK ::BAK1-GFP (J.Li, Chory), PBRI1::BRI1-GFP (N.Geldner). PSERK1::SERK1-YFP (M. Kwaaitaal). PBRI1::BRI1-GFP was crossed into a SERK3-HA transgenic line (verified by selection for respectively PPT and Hygromycin, and by PCR).
Seedlings were grown for 6 days on plates containing, Murashige and Skooge medium plus vitamins, sucrose and Daishin agar (0.575g, 2.5 and 2 g/500 ml respectively) and PPT/Hygro. After 6 days, seedlings were incubated for 1 hour in MS medium and placed on a microscope slide covered with a slide.

Root length assay
Ten to twenty seeds of wt and mutant background were sewn in one line on MS plates containing various concentrations of BL and/ or BFA and placed vertically under long daylight conditions at 22 degrees Celsius.
After 12 days the length of each individual root was measured. The root length for each concentration was calculated as percentage of the length on control plates.

Confocal Laser Scanning Microscopy
Confocal Images were taken using a Zeiss LSM510. GFP was excited using a laser line of 488 nm, with a laser power of 12 %. Emission light was detected using a band-pass filter of 505-550 nm. The FM4-64 fluorescence was detected using a longpass filter of 650 nm. For double-staining with HA, 488 was used for excitation of GFP or anti-GFP-Alexa 488, 543 was used for antiHA-Alexa-546 and bandpass-filters of 505-530 and 550-615 respectively. Excitation of HA-Alexa 546 with 488 as a control did not catch any signal in the 505-530

region, and excitation of BRI1GFP-Alexa488 using a 546 lser line did not result in a signal in the 550-615 region.

CHX and or BFA (50 μM each) treatments were done for 1 hour, pre-stained or followed by FM4-64 (16 μM) for 5 minutes on ice. Subsequently, seedlings were fixed and immuno-stained according to Jiri Friml et al (2006). Antibodies used, were anti-GFP (generated by Eurogentec), anti-HA, Alexa Fluor 488 and 546 goat-anti-rabbit and anti-mouse (all Invitro-gen) and anti-PIN1 (gift from Dolf Weijers).

FRET-FLIM

FLIM was performed using a Biorad Radiance 2100 MP system (Hercules CA) combined with a Nikon TE 300 inverted microscope (Tokyo, Japan) as described by Russinova et al. (2004). For the FLIM experiments, the Hamamatsu R3809U MCP PMT (Hamamatsu city, Japan) was used, which has a time resolution of 50 ps. FRET between Alexa-488 and Alexa-546, coupled as secondary anti-bodies to respectively anti-GFP(or anti-PIN1) and anti-HA on BRI1-GFP (or PIN1) and SERK3-6xHA, was used. Alexa-488 emission was selected using a 515(DF30) band pass filter. Images with a frame size of 64 x 64 pixels were acquired, and the average count rate was around 104 photons per second for an acquisition time of 120 sec. (Borst et al. 2003).

From the fluorescent intensity images, fluorescent lifetimes were calculated per pixel using a two-exponential decay model. The fluorescence lifetime of the donor molecule BRI1-GFP (aGFPAlexa488) was fixed to 2450 picoseconds (ps).

Results

BR signaling occurs from BFA compartments containing BRI1 and SERK receptors
To investigate the function of the co-receptors in endosomal signaling, a BRI1-GFP*sk1sk3* line was used, as described in chapter 4. Geldner et al. (Geldner et al., 2007) showed that signaling takes place from BFA compartments. As a read-out of BR-signaling, Geldner et al. used dephosphorylation of the transcriptional regulator BES1 as a BL response. First, this experiment was repeated using root sensitivity as a read-out for BR-signaling. As can be seen in Figure 1A, wt roots are sensitive to both BL and BFA confirming that BFA induces BR-signaling similar to BL. When BFA was added together with BL, signaling was not enhanced further suggesting that BRI1 receptors blocked from reinsertion into the PM lost the capacity to respond to exogenous BL. However, when the BFA concentration was increased to 5 μM, there was a significant enhancement of BR signaling, again confirming the observations of Geldner et al. (2007). Roots from BRI1-GFP expressing seedlings were slightly more sensi-tive to BL than wt roots, similar to what was shown previously and due to approximately two-fold over-expression of the BRI1 receptor (chapter 4). BFA treatment on BRI1-GFP ex-pressing seedling roots had the same effect as on wt roots, suggesting that internalization of the fluorescently tagged receptors does not affect the signaling properties of the endogenous

A.

B.
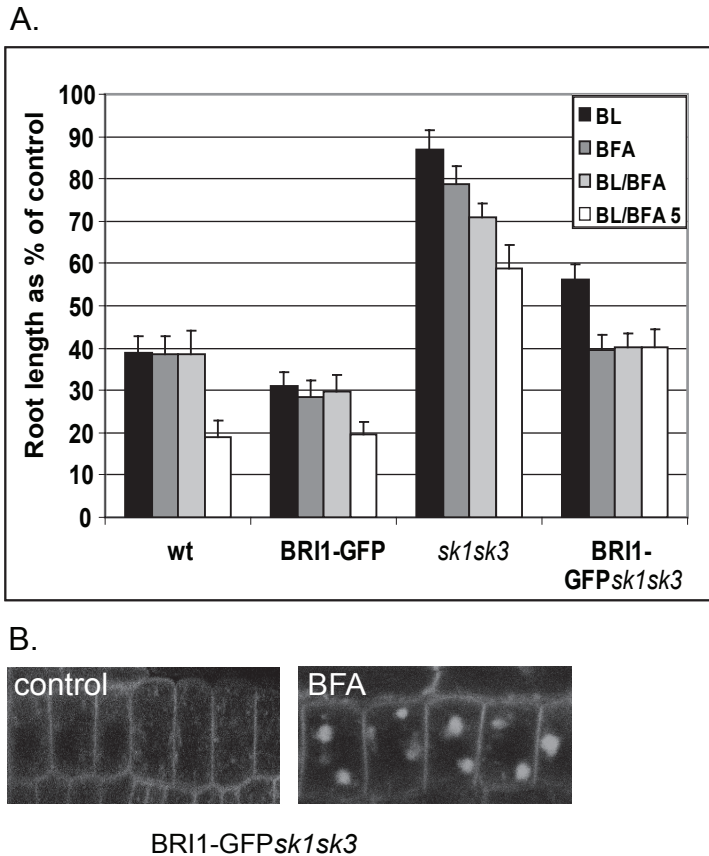
BRI1-GFP*sk1sk3*

Figure 1. BFA has the same effect on root length growth as BL. **A.** Wt and BRI1-GFP seedlings are inhibited in root length growth on plates containing BL or BFA, while *sk1sk3* roots are insensitive to both of them. BFA together with BL (with 2.5 or 5 µM BFA) enhances the inhibition even more. **B**. BRI1-GFP in *sk1sk3* roots is still able to translocate to BFA compartments.

BRI1 receptors.

Sk1sk3 seedling roots are almost completely insensitive to BL (Fig. 1A) and were also insensitive to BFA when compared to BRI1-GFP expressing and wt roots. This result suggests that SERK1 and SERK3 are essential for BR signaling when initiated from internalized BRI1 receptors in the BFA compartments. BRI1-GFP partially rescues the *sk1sk3* insensitivity for BL, which can be explained by active homodimers in an over-expression situation (see chapter 4), and can completely restore the insensitivity for BFA like simultaneous treatment with BL and BFA. Apparently, mild over-expression of BRI1-GFP can override co-receptor mediated impaired BR signaling from BFA compartments. It is not clear whether this effect can be attributed to PM-based BRI1 mediated signaling or due to the higher amount of BRI1 receptors in BFA compartments. BRI1-GFP still accumulates in BFA compartments in *sk1sk3* roots (Fig.1B) so apparently the presence of the BRI1 receptors in the endosomal compart-

ments does not require the co-receptors. Geldner et al (Geldner et al., 2007) showed that BFA blocks the degradation pathway of BRI1-GFP from the endosomal compartments to the lytic vacuoles, which might explain the enhanced signal derived from the BRI1-homodimers upon BFA-treatment.

The next question to be asked was how many of the ECs at the PM contain both BRI1 and SERK3. From the work of Russinova in protoplasts (Russinova et al., 2004) it became apparent that BRI1-SERK3 heterodimerization is non-uniformly distributed over the PM and appears to coincide with developing ECs that contain both receptors. To visualize both BRI1 and SERK3 proteins, a transgenic line was used expressing both BRI1-GFP and SERK3-6xHA constructs (chapter 4). Root tips of this line were fixed and immuno-labeled with anti-GFP and anti-HA (Fig. 2A). BRI1 and SERK3 co-localize in ECs at the PM and in the cytoplasm, but also alone in separate ECs (Russinova et al. 2004 and Chapter 4). This suggests that only a subset of BRI1 and SERK3 receptors internalize together. Merged images of cells in which BRI1 and SERK3 were immuno-labeled with and without treatment with BFA (Fig. 2A), were analyzed by counting the amount of vesicles containing the different receptor populations in regions of the PM and the cytoplasm. Green represents BRI1, red is SERK3 and yellow represents ECs that contain both receptors. The graph shows an example of a selected region on the PM where the different populations were counted (Fig. 2B). A region in the cytoplasm where no ECs were visible was used to determine the background fluorescence, pointed out as the blue line in the graph.

The average number of differently colored ECs in the PM or the cytoplasm was calculated (Fig.2C). In the BFA compartments it was not possible to count separate ECs. In control cells, only 20% of the total amount of ECs counted in the PM were yellow, so contained both BRI1 and SERK3. This amount did not change after BFA treatment. In the cytoplasm, only 14% of the ECs in the control cells contained both BRI1 and SERK3, and this was reduced to 8% after BFA treatment, apparently due to preferential accumulation of the BRI1/SERK3 containing ECs into the BFA bodies. Therefore we propose that the BRI1/SERK3 containing ECs that became trapped in the BFA compartments represent the receptors active in BR signaling in wt conditions.

SERK3 recycling is in part BFA sensitive

To investigate the recycling of the receptors to the PM in roots, BRI1-GFP or SERK3-GFP seedlings were treated with BFA and cycloheximide (CHX). BFA compartments were formed in epidermis cells of BRI1-GFP roots, but hardly in SERK3-GFP or SERK1-YFP expressing cells (Fig. 3A). In contrast, clearly defined SERK2 containing BFA compartments were observed suggesting a highly specific sorting mechanism capable of distinguishing between closely related receptors. Accumulation of BRI1-GFP in BFA compartments was reversible confirming previous observations (Geldner et al. 2007) (Fig. 3B).

To compare the different effects of BFA on BRI1 and SERK3 more in detail, BRI1-GFP and SERK3-GFP root cells treated with BFA and CHX were stained with FM4-64 prior to treat-
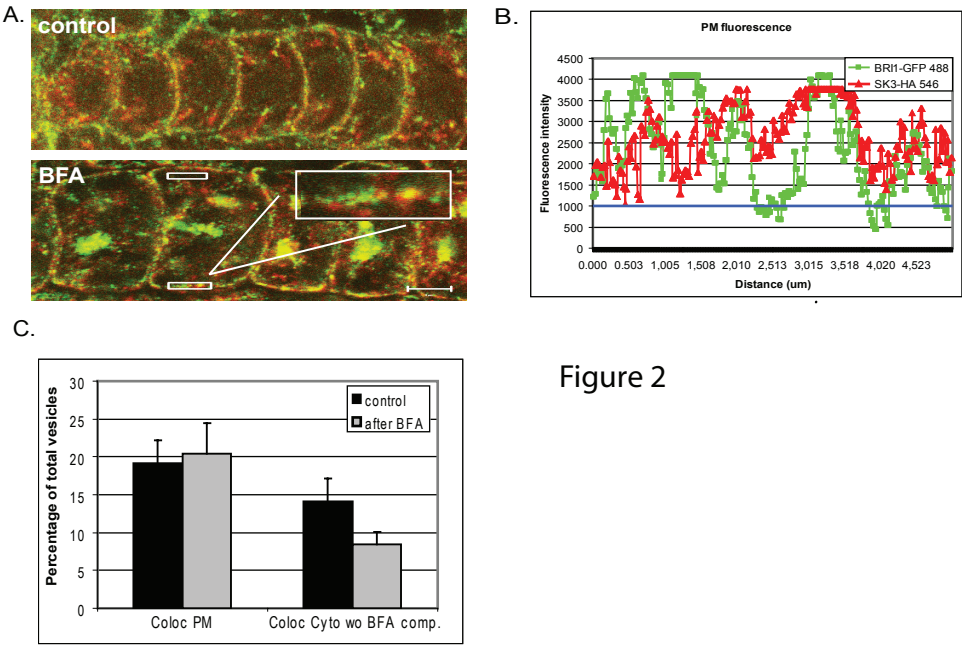
A. control

BFA

B. PM fluorescence

C.

Figure 2

A. BFA/CHX

BRI1-GFP   SERK3-GFP   SERK1-YFP   SERK2-YFP

B.

BRI1-GFP + BFA   BFA + wash

Figure 3

C. control   BFA/CHX   ConcA
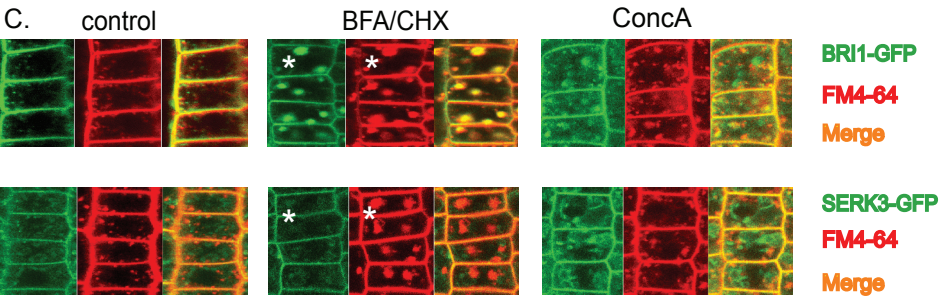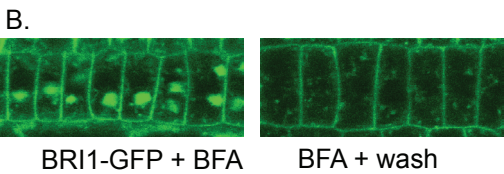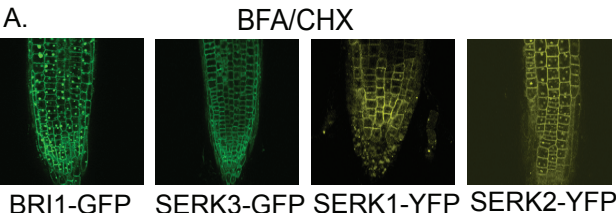
BRI1-GFP
FM4-64
Merge

SERK3-GFP
FM4-64
Merge

ment. FM4-64 stains the PM and after prolonged incubation also internalized membrane-derived compartments. After treatment with BFA, most of the BRI1-GFP protein in root BFA compartments co-localized with FM4-64, while most of the SERK3-GFP protein did not co-localize.

To verify that inhibitors of another part of the endocytic route show an effect on trafficking of the BRI1- GFP and SERK3-GFP proteins, seedlings were treated with Concanamycin A (Conc A). This compound blocks H+ V-ATPases and causes alkalinization of the TGN and recycling endosomes, and prevents receptor (Machen et al., 2003; Robinson et al., 2004). Dettmer et al (2006) (Dettmer et al., 2006) showed that ConcA interferes with transport from early ECs to the vacuole. Accumulation of BRI1- as well as SERK3-GFP was clearly visible (Fig. 3C), suggesting that both receptors can follow the same route when in transit from ECs onwards.

Taken together, these results show that the BRI1, SERK1 and SERK3 proteins, elements of the same receptor-complex, undergo similar but also different recycling pathways.

The BFA-sensitive subset of SERK3-HA co-localizes and interacts with BRI1-GFP

Although SERK3 recycling is mostly insensitive to BFA, a small subset of SERK3-GFP accumulates in BFA compartments. To investigate if SERK3 indeed co-localizes with BRI1-GFP in BFA compartments, roots of BRI1-GFP, SERK3-6xHA and BRI1-GFP/SERK3-6xHA expressing lines were treated with BFA and CHX, fixed and prepared for immuno-labeling with anti-HA and anti-GFP antibodies. Confirming the results shown in Fig. 2 and 3, BRI1 localizes to the PM and in BFA-bodies (asterisks in green panels, Fig.4A). The cytoplasm seems to be almost devoid of ECs, compared to the control roots. SERK3-6xHA also localizes to the PM, but in addition, in part in BFA compartments, although no distinct pattern as was seen

Figure 2. BFA leaves the population of ECs containing both BRI1 and SERK3 at the PM intact. **A**. Images of BRI1-GFP/SERK3-HA expressing cells treated with BFA and control cells. **B.** Profiles of PM-regions were taken and analyzed for the different populations of colored endosomal compartments (ECs), where green contains BRI1-GFP), red contains SERK3-HA and yellow contain both. Part of the cytoplasm with low fluorescence was taken as the background fluorescence (blue line in the graph). **C**. Percentage of ECs where BRI1-GFP and SERK3-HA co-localize does not change after BFA treatment (20% in control and after treatment), but in the cytoplasm they moved to BFA compartments, as a significant reduction from 14% to 8% was found in the rest of the cytoplasm.

Figure 3. BFA enhances accumulation of endosomal compartments in epidermis cells of Arabidopsis roots. **A**. BRI1-GFP and SERK2-YFP, but not SERK3-GFP and SERK1-YFP are sensitive for BFA. **B**. Wash-out of BFA-bodies containing BRI1-GFP, showing that these bodies were formed due to treatment with BFA. **C**. BRI1- and SERK3-GFP seedlings treated or not with BFA, stained with FM4-64 prior to treatment. BRI1 is sensitive to BFA and BFA-bodies are formed due to blocking of the recycling (asterisks). SERK3 is less sensitive to BFA, while BFA treatment still induced body formation of other membrane proteins as shown with FM4-64. Concanamycin A induced accumulation of BRI1-GFP as well as SERK3-GFP showing that other parts of the endocytic route were impaired in SERK3-GFP seedlings.

for BRI1 (asterisks in red panels, Fig. 4A).

Next the roots of BRI1-GFP/SERK3-6xHA double transgenic lines were analyzed after im-muno-labeling, visualizing BRI1 in green and SERK3 in red. In control roots, BRI1-GFP and SERK3-6xHA are equally distributed over the PM (Fig. 4B). To accumulate the ECs in which both receptors are present by means of blocking the recycling process, BRI1-GFP/SERK3-6xHA seedlings were treated with BFA and CHX. BRI1 is clearly accumulated in BFA com-partments, compared to the control. In the red panel, BFA compartments are visible con-taining SERK3-6xHA receptors that co-localize with BRI1-GFP receptors (Fig. 4C, merged image). Figure 4D shows the glow-scale images of Figure 4B and C, where the fluorescence is depicted in blue, green and red, for respectively low, medium and high fluorescence intensi-ties. The images of these cells show that although there is more SERK3-6xHA protein at the PM and in the cytoplasm when compared to BRI1-GFP, there is less SERK3-6xHA protein in BFA compartments. This suggests that only a minority of the SERK3-6xHA proteins ac-cumulate in BFA compartments, while most are not sensitive to the toxin. The pattern of SERK3-6xHA aggregates resembles the pattern of BFA-resistant ARF-GEF GNOM-LIKE 1, co-localizing only in part within BFA-bodies and accumulating mostly around them (Geld-ner et al., 2007). In control cells 60 % of the total amount of BRI1-GFP and SERK3-6xHA proteins were localized at the PM, as measured by the fluorescent intensities of BRI1-GFP/Al-exa-488 and SERK3-6xHA/Alexa 546 (Fig. 4E), while 40% was in the cytoplasm. After BFA treatment the amount of BRI1-GFP at the PM was reduced to 50% while a substantial part of the cytoplasmic BRI1-GFP proteins were found in BFA compartments. The SERK3-6xHA protein distribution between the PM and cytoplasm after BFA treatment was unchanged com-pared to control, and in the cytoplasm only half of the SERK3-6xHA proteins were found inside BFA compartments. Based on the observed BFA insensitivity of BRI1 mediated sig-naling in *sk1sk3* mutant roots, we conclude that the BRI1- SERK3 receptor complex in BFA compartments is the active form.

To investigate if SERK3-6xHA and BRI1-GFP receptors co-localizing in BFA compartments directly interact, we measured Förster Resonance Energy Transfer by Fluorescence Lifetime Imaging (FLIM) between the two Alexa-dyes (A488 and A546) used as secondary antibod-ies to recognize BRI1-GFP and SERK3-6xHA, as a measure for interaction between the two proteins. First, the average fluorescence lifetime of BRI1-GFP-A488 was determined in BFA compartments (Fig. 5A) and a τ of 2450 ps was found (Table 1).

The lifetime of BRI1-GFP-A488 in the presence of SERK3HA-A546 in BFA bodies was 2180 ps. This represents a significant reduction according to Students T-test ($p < 0.001$). As a control the fluorescence lifetime of PIN1-A488 in the presence of SERK3HA-A546 was measured (Fig. 5C) and no changeof the donor lifetime was found.

Taken together, these cytological data support our hypothesis that cytoplasmic endosomal compartments contain hetero-oligomeric and active SERK3 and BRI1 receptor signaling complexes.
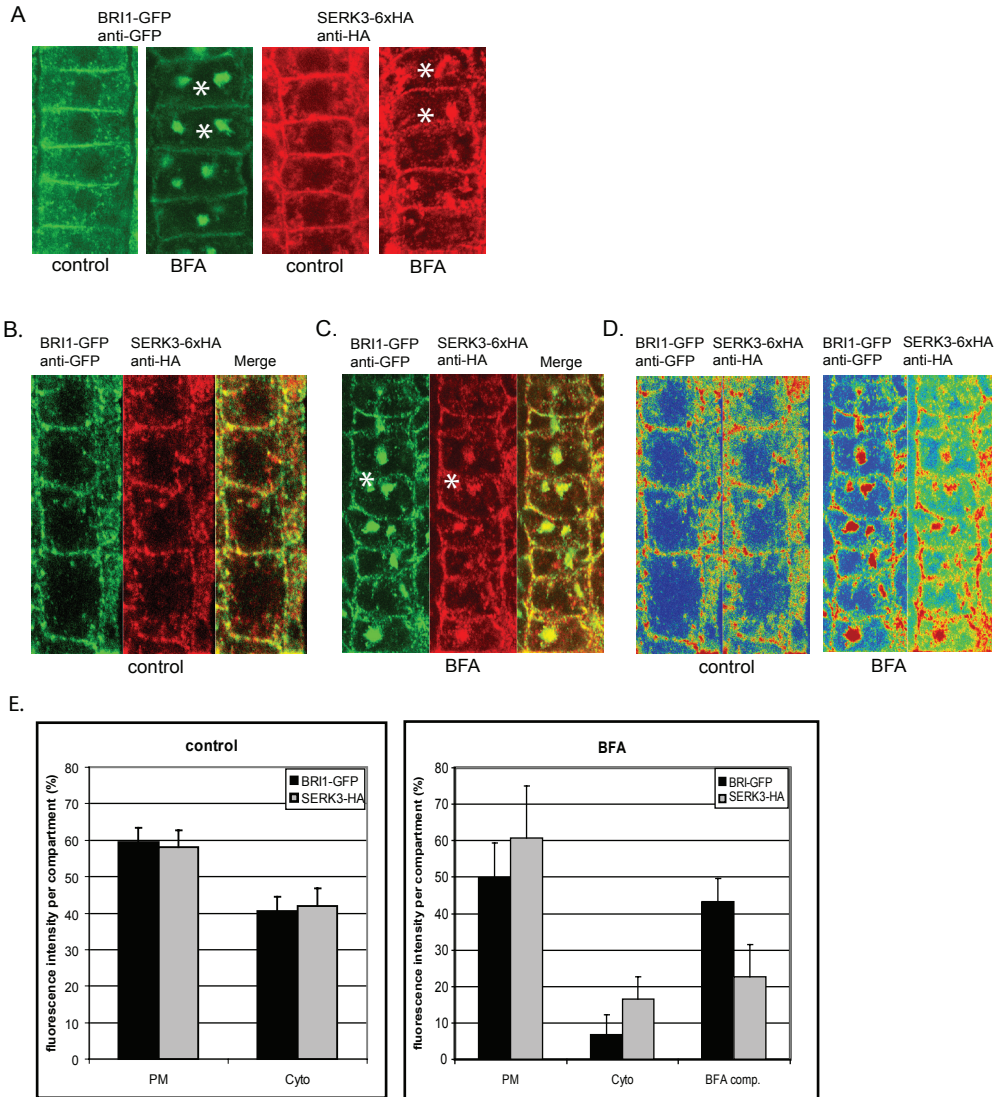
Figure 4. SERK3 is in part insensitive to BFA. **A.** Localization of BRI1-GFP or SERK3-HA express-ing lines using GFP and HA antibodies localization was the same as in freshly prepared seedlings. **B**. and **C.** BRI1-GFP and SERK3-HA double expressing lines were treated or not with BFA, fixed and pre-pared for immuno-labeling. Much of the BRI1-GFP protein accumulated in BFA compartments, while only a small portion of SERK3-HA did. **D**. Glow scale-images of the images in A and B, where a blue color means low fluorescence intensity, green is medium intensity and red is high intensity. Although there is more SERK3 fluorescence at the PM and in the cytoplasm, compared to BRI1 fluorescence, there is less SERK3 in BFA-compartments, showing that SERK3 is less sensitive to BFA. **E**. Using Im-age-Pro, the amount of fluorescence was determined in the PM and the total cytoplasm, for BRI1-GFP or SERK3-HA in the double-line, before and after treatment with BFA in around 50 cells. In the images of BFA-treated cells, the fluorescence was also measured for the BFA compartments and the rest of the cytoplasm. BFA accumulated more BRI1 in BFA compartments than SERK3 proteins.

BRI1-GFP-A488   BRI1-GFP-A488/   aPIN1-A488/
                 SERK3-HA-A546   SERK3-HA-A546
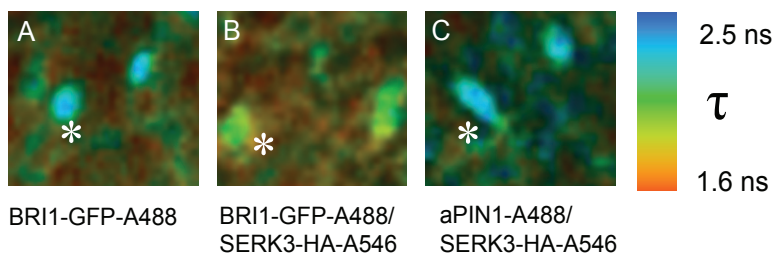
Table 1.

Average lifetime (τ) of BRI1-GFP alone or in combination with SERK3-HA in BFA compartments. The combination of PIN1 and SERK3-HA was taken as a control. n is the number of compartments measured.

Protein	τ (ns)	+/-sd	n
BRI1-GFP donor	2412	108	19
BRI1-GFP/SERK3-HA	2187	91	33
PIN1 /SERK3HA	2495	103	22

Figure 5. BRI1 interacts with SERK3 in BFA compartments. FRET-FLIM data shows that in BRI1-GFP containing BFA compartments (anti-GFP/A-488) where also SERK3-HA (anti-HA A-546) was present (asterisk in **B**.), compared to BRI1-GFP alone (**A**.), a significant reduction in lifetime of A488 was measured from 2.41 to 2.19 ns, suggesting an interaction between BRI1 and SERK3. In BFA compartments stained with anti-PIN1-A488 and A546 for SERK3-HA (**C**.), as a negative control, no reduction in donor-lifetime was measured.

Discussion

In this report we present evidence that the SERK3 and SERK1 co-receptors are required for endosomal signaling of BRI1. Previously we have proposed that the role of the co-receptors SERK1 and SERK3 was related to stabilization of the main receptor BRI1 (chapter 4). Together with the data presented by Geldner et al. (Geldner et al., 2007) who showed, that BFA treatment resulted in internalized BRI1 receptors that were still able to signal, a picture emerges where upon BRI1 activation and interaction with its co-receptors an active hetero-oligomeric complex is formed that needs to be maintained in order to engage in endosomal BR signaling. However, we also provide evidence that while BL insensitivity of roots was observed only in *serk1serk3* seedlings (Albrecht et al., 2008), the BRI1 receptors can also signal in the complete absence of the co-receptors when over-expressed. This is in line with the observed much weaker phenotypes of *bak1/serk3 serk1* mutants when compared to strong *bri1* alleles (Nam and Li, 2002, Li et al. 2002, He et al. 2007, Albrecht et al. 2008). Endosomal signaling of BRI1 homodimers in the absence of the co-receptors, taking place only in an

over-expression situation, was enhanced after blocking of the recycling to the PM, but might also be caused by the blocking of the degradation pathway (Geldner et al., 2007).

In this work we also show that BRI1, and a small portion of SERK3 is recycled back to the PM via a BFA-sensitive compartment, in which both receptors remain active. However, most of the SERK3 receptors are not sensitive to BFA, suggesting that they employ a trafficking route not involving BFA-sensitive ARF-GEFs. This is the first evidence of a receptor protein apparently following two different pathways for recycling. It was shown that SERK3 also has a function in innate immunity alone (Kemmerling et al. 2007) as well as in cell death together with SERK4 (He et al., 2007; Kemmerling et al., 2007), and is the co-receptor of the flagellin receptor Flagellin sensitive 2 (FLS2) (Chinchilla et al., 2007). So those SERK3 receptors that function with other partners could use different BFA insensitive ARF-GEFs for trafficking. In analogy to the EGFR family, receptor routing could be determined by the precise combination of receptors used. Only ErbB1 (EGFR) and ErbB4 are fully active in terms of ligand binding and kinase activity. ErbB3 has impaired kinase activity, while ErbB2 receptor without its extracellular domain (ECD) is constitutively active, but cannot bind the ligand and needs heterodimerization with one of the other receptors. The activated EGFR and ErbB2 are directed towards degradation, while ErbB3 is recycled. However, when the C-terminal tail of ErbB3 is fused to EGFR, this redirects EGFR to the recycling route and enhances the signal. This suggests that pools of ErbB3 receptors combined with different partners follow different routes (Warren and Landgraf, 2006). A mechanism reminiscent of that of ErbB3, exists in Arabidopsis where the RLK AtCRR2, has a deletion in the kinase domain but displays attenuated kinase activity. It has been shown that AtCRR2 is phosphorylated by the Arabidopsis CRINKLY4 homologue ACR4, suggesting that these receptors could signal after heterodimerization upon AtCRR2 activation (Cao et al., 2005). It is however unknown which recycling or degradation pathways these receptors follow after signaling.

The number of BRI1/SERK3 containing ECs at the PM did not change after BFA-treatment suggesting that these ECs are not the signaling compartments. This raises the question which function these BRI1/SERK3 receptor containing ECs have. One explanation can be that the PM localized BRI1-SERK3- containing ECs contain preformed hetero-dimerized receptor-pairs. Although (Wang and Chory, 2006) proposed that SERK3 dimerizes with BRI1 after ligand binding, it could be that dimerization takes place before, whereas activation takes place after ligand-binding, analogous to the erythropoietin receptors (EPORs) that in erythroid cells regulate proliferation, differentiation and maturation. The EPORs were shown by crystallography to be present as preformed dimers before ligand activation. Upon ligand-binding a conformational change takes place that activates the receptor pair (Livnah et al., 1999). Analogous to the EPORs, BRI1 and SERK3 could appear shortly after biosynthesis as preformed dimers, stay close to the PM and be inserted into the PM when required.

The function of signaling from endosomes is not well understood. Geldner et al. (Geldner et al., 2007) suggested that endosomes increase the effective surface area available for signaling, and that longer-lasting downstream signaling events from endosomes would shorten the dwelling time of the receptors on the PM, in this way making space for other receptors.

It was also shown that due to prolonged residence of activated EGFR on the PM, by using a mutant Dynamin that led to impaired endocytosis, activity of some downstream signaling components was blocked (Miaczynska et al., 2004). This suggests that signaling from ECs is absolutely required for signal transduction. Spatial and temporal compartmentalization in various endosomal compartments might also add additional layers to specificity and regulation, as put forward by (McPherson et al., 2001).

From our data, we confirm that BRI1-mediated Br signaling can commence from endosomal (BFA) compartments. Endosomal signaling requires the presence of the heteromeric receptor-complex, including BRI1 and the co-receptors SERK1 and SERK3. In the future it needs to be determined whether BRI1 endocytosis is a method to spatially separate different signaling activities and/or is a means to change the residence time of active signaling complexes at the PM.

Chapter 6

Summarizing discussion

José Aker and Sacco de Vries

Plants perceive signals from the environment and thereby respond to changing conditions. For that purpose cells express receptor proteins on their surface to receive signals and transduce them intracellularly. Receptor proteins are composed of an extracellular domain exposed to the outside of the plant cell, a transmembrane domain and an intracellular domain harboring the kinase domain, which transduces signals via interactions with other proteins. The receptors described in this thesis belong to the large family of leucine rich repeat receptor like kinases (LRR-RLKs) in Arabidopsis and function in the brassinosteroid signaling pathway. This pathway is triggered by binding of plant hormones like brassinosteroids (BR) to the extracellular domain of the receptor BRI1 (Brassinosteroid Insensitive 1) and controls many processes like cell growth and division as well as developmental processes.

BRI1 is the main receptor for the BR signaling, but also other receptors are required. These receptors, SERK1 and SERK3 (Somatic Embryogenesis Receptor Like Kinases) can dimerize with BRI1 upon ligand binding, activate downstream proteins by transphosphorylation and transduce the signal via yet an unknown mechanism to the nucleus where gene-transcription takes place (Li et al., 2002; Nam and Li, 2002).

After activation of the pathway, this signal has to be blocked to prevent over-stimulation. There are different ways to accomplish this, but the receptors need first to be internalized. After internalization the receptors can be directed for degradation to the proteasome, or directed via the endosomal pathway for either a recycling or degradation process. The proteasome consists of a protein complex that recognize the small molecule ubiquitin on proteins which are prone for degradation (Kurepa and Smalle, 2008). In the endosomal pathway, early endosomes containing the internalized receptors fuse with other endosomes to form multivesicular bodies (MVBs). These MVBs also contain lysosomes that upon release of their content can degrade the proteins. From the early endosomes as well as from MVBs, proteins can escape and recycle back to the PM (Dettmer et al., 2006; Geldner, 2004; Geldner and Jurgens, 2006; Müller et al., 2007).

The choice for the trafficking route to either the proteasomal or the endosomal pathway depends in both cases on ubiquitin that is attached to proteins early after signaling. Actually, the length of the ubiquitin chain determines which route is followed. One ubiquitin molecule directs to the endosomal pathway, while a poly-ubiquitin chain directs to the proteasome. The CDC48A protein, of which mammalian and yeast homologues are involved in directing ubiquitinated proteins to the proteasome, was found as an interacting partner of SERK1. The interaction between these two proteins was found in earlier research in a yeast-two hybrid screen in yeast (Rienties et al., 2005) and in an immuno-precipitation of the SERK1 complex in Arabidopsis seedlings together with the phosphatase KAPP and a 14-3-3 protein (Karlova et al., 2006). It was also described that CDC48A plays a role in ER-associated degradation (ERAD) of mutant powdery mildew (mlo-1) receptors in Arabidopsis (Müller et al., 2005).
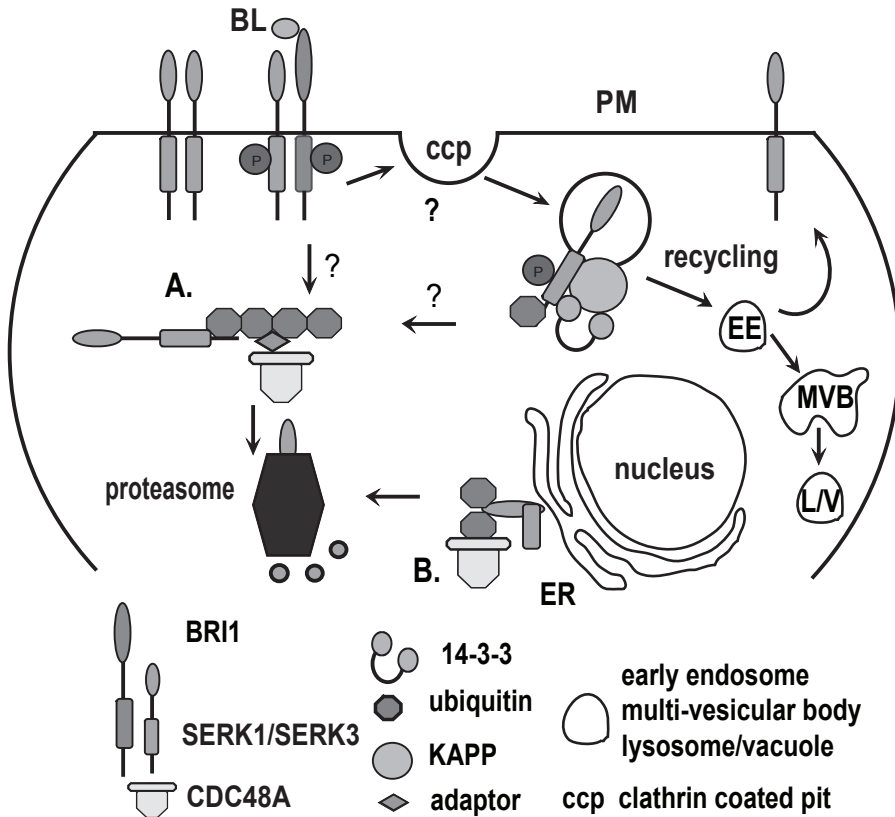
Figure 1. Hypothetical degradation pathways of the SERK1 receptor after activation. Upon binding of the brassinosteroid BL, BRI1 and SERK1 (and/or SERK3) receptors dimerize and trans-phosphorylate. After activation, mono-ubiquitination can be a signal for internalization (via clathrin coated pits?) acquiring the phosphatase KAPP to give rise to early endosomes. From these endosomes, the receptors can recycle to the PM or are targeted to MVBs and subsequently to lysosomes or vacuoles to be degraded. (**A**) Poly-ubiquitination after activation of the receptors is a signal for degradation in the proteasome, acquiring adaptor proteins and CDC48A. It is not clear if this pathway also involves endosomal compartments. (**B**) Misfolded SERK1 receptors are pulled out of the ER-lumen, poly-ubiquitinated and targeted to the proteasome acquiring CDC48A again (Aker and de Vries, Plant Physiol. 2008).

In chapter **2** the physical interaction between SERK1 and CDC48A was investigated in plant protoplasts. Using FRET-FLIM it could be determined that SERK1 and CDC48A interact in domains at the PM that co-localize with ER-markers. We assumed therefore that CDC48A plays a role in retracting and directing misfolded SERK1 proteins from the ER to the protea-some and therefore in the quality control of newly synthesized SERK1 receptors. SERK1 is able to interact with the N-domain of CDC48A which is responsible for most of the interac-

tions with substrates in mammalian homologues (Dreveny et al., 2004; Meyer et al., 2000), as well as with the C-terminus. This finding could reflect different functions in the cell.

First, proteasome dependent turnover of SERK1 receptors might be a way to regulate its activity. In analogy with the mammalian IL-2/IL3 or the erythropoietin receptors and the CDC48 homologue VCP, SERK1 could bind to the C-terminus of CDC48A upon activation of SERK1-mediated signaling (Yen et al., 2000), which then targets SERK1 to the proteasome. It is not clear if this pathway also involves endosomal compartments. Another hypothesis is, as mentioned before, that the CDC48A protein mediates ERAD-like quality control of SERK1 receptors. As much as thirty percent of newly synthesized proteins contain peptides arising from degraded misfolded proteins, which are in part ubiquitinated (Schubert et al., 2000). In the ER a strict quality control must therefore ensure that aberrant proteins are not exported. The conformational change of CDC48A during ATP-binding and subsequent release supplies the mechanical force to pull ERAD substrates from the ER-membrane and translocate them to the proteasome-machinery in the cytoplasm.

Mutant MLO-1 receptors became highly poly-ubiquitinated and accumulated upon treatment with the proteasomal inhibitor MG132 (Müller et al., 2005). SERK1 expressed in protoplasts was also accumulating in the perinuclear ER upon MG132 treatment, suggesting that in protoplasts newly synthesized SERK1 proteins are in part misfolded and must be degraded. The hypothetical degradation pathways of SERK1 involving CDC48A are depicted in Figure 1(A. and B.)

An attempt was undertaken to investigate if the interaction between SERK1 and CDC48A was ubiquitin-dependent, by co-expressing the non-active CDC48A mutant A1A2 with SERK1 in protoplasts to accumulate poly-ubiquitinated SERK1, that was analyzed after immunoprecipitation. Unfortunately, due to technical problems this was not successful. Also identification of ubiquitinated residues on SERK1 protein immuno-precipitated from seedlings was performed. Ubiquitin molecules leave a hallmark on its lysine residue that shifts the mass with 114 Da (Peng et al., 2003) which can be determined by mass spectrometry. On the peptides analyzed that covered 60% of the SERK1 protein, no ubiquitinated modification was observed. However, since only one residue is necessary for ubiquitination, it might reside in the part of the protein that was not covered.

In chapter **3** we investigated the molecular interaction between SERK1-CDC48A in more detail. CDC48A proteins consist of six monomers that together form an active ATPase, but in plant cells the monomeric, inactive form has also been found (Rancour et al., 2004). Therefore, it was investigated if CDC48A proteins fused to a GFP-tag were able to hexamerize. Furthermore it was determined which form was interacting with SERK1. Using CDC48A monomers fused to cerulean or yellow fluorescent proteins (FP) the formation of an oligomer or hexamer could be measured via the interaction between the fluorescent proteins. Therefore presumably the hexameric CDC48A protein interacts with SERK1. The size of the oligomeric CDC48A protein was determined to be a hexamer using Native-gel-electroforesis. By using fluorescence correlation spectroscopy (FCS) the apparent diffusion coefficient of the CDC48A protein was determined to be 3.5 μm^2/s in the cytoplasm, correlating with a

hydrodynamic radius (Rh) of the molecule of 20.4 nm. The expected Rh for only a hexamer would approximately be 7 nm. Hence, the CDC48A protein complex appeared much larger than expected showing that CDC48A exists in a protein-complex comprising of e.g. SERK1 or other proteins that need to be degraded. Deletion of the N-domain known to bind ubiquitinated target proteins, led to a higher diffusion coefficient (6.2 $\mu m^2/s$), suggesting a reduced complex-size. The CDC48A A1A2 mutant in which ATPase activity was inhibited also displayed a higher diffusion-coefficient (6.0 $\mu m^2/s$), suggesting that these mutations influence the complex-formation. In the nucleus CDC48A diffused much faster than in the cytoplasm and the difference with the mutants disappeared; suggesting that in the cytoplasm the protein is bound to a larger or different complex.

To investigate if the interaction between SERK1 and CDC48A is phosphorylation-dependent an in vitro kinase assay was performed. SERK1 indeed was able to transphosphorylate CDC48A proteins. Interestingly, the Ser-41 amino acid was phosphorylated residing in the N-domain. Unfortunately no peptide coverage of the C-terminal tail was found, but it comprises 3 serines, 3 threonines and 1 tyrosine. Hence SERK1 might have additional targets in the C-terminus.

In chapter **4** endocytosis of the BRI1-SERK complex was investigated in Arabidopsis epidermis cells in root tips, in which the receptors BRI1, SERK1 and SERK3 all localized to the PM. Roots of a transgenic line containing BRI1 fused to green fluorescent protein (GFP) and SERK3 fused to a HA-tag were fixed and stained with antibodies to visualize these proteins. SERK3 over-expression enhanced BRI1 endocytosis; however this did not result in enhanced signaling. BRI1-GFP alone is mildly hypersensitive to BL as compared to wildtype Arabidopsis in a root length assay. However SERK3 over-expression in the BRI1-GFP line reduced this effect, suggesting that SERK3 negatively influences the hypersensitivity of BRI1-GFP. The mild hypersensitivity of BRI1-GFP might be the result of BRI1-GFP becoming active as a homodimer, due to the lack of enough co-receptors. However, this homodimeric BRI1-signaling might only take place when the BRI1/SERK receptor-complex is not in balance. Over-expression of SERK3 together with BRI1 might lead to the formation of more heterodimers and enhanced endocytosis, but not to stronger signaling due to lack of SERK1. The enhanced endocytosis visualized in the situation where BRI1-GFP and SERK3-6xHA are over-expressed but where BR signaling is not changed might be the result of an inactive population of BRI1 or SERK receptors.

Subsequently, BRI1-GFP was crossed in different lines where each one or both of the co-receptors SERK1 and SERK3 were deleted by mutation, to investigate if this would change the distribution of BRI1-GFP protein in the PM or the cytoplasm. The *sk1sk3* mutant roots were completely insensitive to BL, which was only slightly restored when BRI1-GFP was crossed in, showing that BRI1 needs the co-receptors for signaling. The distribution of BRI1-GFP fluorescence between PM and cytoplasm was not changed, but the total amount of BRI1 protein was reduced in *sk1sk3* roots, as compared to the control BRI1-GFP. The presence of both co-receptors might delay degradation of the heterodimers and extend the signal. Lacking the co-receptors receptors might lead to a pool of less stable BRI1 receptors that makes them

more susceptible for degradation. The role of the SERK receptors might be the modulation of the stability and activity of BRI receptor-complexes.

In chapter **5** the role of the co-receptors SERK1 and SERK3 was studied in more detail. The recycling of BRI1 and the SERK receptors was investigated using the toxin brefeldin A (BFA) that inhibits most of the ARF-GEFs (ADP ribosylation factor-guanine exchange factor) responsible for membrane fusions and recycling of internalized membrane proteins to the PM. SERK3 and also SERK1 are only in part sensitive to the drug as compared to BRI1. The BFA-sensitive portion of SERK3 resides in endosomal compartments containing both SERK3 and BRI1 internalized receptors, but most of the SERK3-recycling follows a different route via a BFA-insensitive ARF-GEF. One explanation could be that the insensitive portion of SERK3 receptors functions together with the other known partners of SERK3, like SERK4 in cell-death control (He et al., 2007), or with FLS2 in pathogen-associated molecular pattern (PAMP) triggered immunity (Chinchilla et al., 2007). In these pathways other ARF-GEFs could be involved in recycling of the receptors.

BFA accumulates endosomal compartments resulting in enhanced BRI1 signaling in over-expression lines shown by Geldner and co-workers (Geldner et al., 2007). Surprisingly, the *sk1sk3* roots were insensitive to BFA, as they were to BL, showing not only that SERK1 and SERK3 are required for BR signaling, but moreover that they are required for signaling from these endosomal compartments. Because sequestering of BRI1 receptors in BFA compartments is not affected in *sk1sk3* roots we conclude that BRI1 mediated BR signaling in roots largely occurs from internalized receptors and depends on the presence of the SERK co-receptors.

Outlook

The research described in this thesis adds to the knowledge of the pathways membrane-receptors undertake after signaling. CDC48A might play a role in targeting SERK1 proteins to the proteasome to regulate its activity, or to control the quality of the newly synthesized SERK1 proteins. SERK1 and SERK3 are important for BRI1-mediated signaling, that takes place from internalized receptors but not for the process of endocytosis itself. The presence of the co-receptors influences the stability and activity of the main receptor and might be important for the trafficking of the BRI1-receptor after signaling. We hypothesized that the quantities of the different receptors in the BRI1-complex are important for stabilization of the complex, subsequent signaling and recycling and might be different in various cell-types and organs of the plant. Future research should provide an answer to that.

References

Abas, L., Benjamins, R., Malenica, N., Paciorek, T., Wisniewska, J., Moulinier-Azola, J., Sieberer, T., Friml, J., and Luschnig, C. (2006). Intracellular trafficking and proteolysis of the Arabidopsis auxin-efflux facilitator PIN2 are involved in root gravitropism. Nat Cell Biol 8, 249-256.

Aker, J and de Vries SC. (2008). Plasma Membrane receptor Complexes.Plant Physiol 147(4) 1560-1564.

Aker, J., Borst, J.W., Karlova, R., and de Vries, S.C. (2006). The Arabidopsis thaliana AAA protein CDC48A interacts in vivo with the Somatic Embryogenesis Receptor-like Kinase 1 receptor at the plasma membrane. Journal of Structural Biology 156(1) 62-71.

Altmann, T. (1999). Molecular physiology of brassinosteroids revealed by the analysis of mutants. Planta 208, 1-11.

Albrecht, C., Russinova, E., Hecht, V., Baaijens, E., and de Vries, S. (2005). The Arabidopsis thaliana SOMATIC EMBRYOGENESIS RECEPTOR-LIKE KINASES1 and 2 control male sporogenesis. Plant Cell 17, 3337-3349.

Alzayady, K.J., Panning, M.M., Kelley, G.G., and Wojcikiewicz, R.J.J. (2005). Involvement of the p97-Ufd1-NPl4 complex in the regulated endoplasmatic reticulum-associated degradation of inositol 1,4,5-triphosphate receptors. JBC 280, 34530-34537.

Babst, M. (2005). A protein's final ESCRT. Traffic 6, 2-9.

Baluska, F., Hlavacka, A., Samaj, J., Palme, K., Robinson, D., Matoh, T., DW, M., Menzel, D., and D, V. (2002). F-actin-dependent endocytosis of cell wall pectins in meristematic root cells. Insights from brefeldin A-induced compartments. Plant Physiol 130, 422-431.

Barth, M., and Holstein, S. (2004). Identification and functional characterization of Arabidopsis AP180, a binding partner of plant alphaC-adaptin. J Cell Sci 117, 2051-2062.

Bastiaens, P.I.H., and Pepperkok, R. (2000). Observing proteins in their natural habitat: The living cell. Trends Biochem Sci 25, 631-637.

Becker, T., Volchuck, V., and Rothman, J.E. (2004). Differential use of endoplasmic reticulum membrane for phagocytosis in J774 macrophages. PNAS 102, 4022-4026.

Bernhardt, A., Lechner, E., Hano, P., Schade, V., Dieterle, M., Anders, M., Dubin, M., Benvenuto, G., Bowler, C., Genschik, P., et al. (2006). CUL4 associates with DDB1 and DET1 and its downregulation affects diverse aspects of development in Arabidopsis thaliana. Plant Journal 47, 591-603.

Blackbourn, H., and Jackson, A. (1996). Plant clathrin heavy chain: sequence analysis and restricted localisation in growing pollen tubes. J Cell Sci 109, 777-786.

Borst, J.W., Hink, M.A., van Hoek, A., and Visser, A.J.W.G. (2005). Effects of refractive index and viscosity on fluorescence and anisotropy decays of enhanced cyan and yellow fluorescent proteins. J Fluoresc 15, 153-160.

Brunger, A.T., and DeLaBarre, B. (2003). Minireview. NSF and p97/VCP: similar at first, different at last. FEBS Lett 555, 126-133.

Cao, X., Li, K., Suh, S., Guo, T., and Becraft, P. (2005). Molecular analysis of the CRINKLY4 gene family in Arabidopsis thaliana. Planta 220, 645-657.

Chinchilla, D., Zipfel, C., Robazek, S., Kemmerling, B., Nurnberger, T., Jones, J., Felix, G., and Boller, T. (2007). A flagellin-induced complex of the receptor FLS2 and BAK1 initiates plant defence. Nature 448, 497-500.

Clayton, A.H., Walker, F., Orchard, S.G., Henderson, D.F., Rothacker, J., Nice, E.C., and Burgess, A.W. (2005). Ligand-induced dimer-tetramer transition during the activation of the cell surface epidermal growth factor receptor-A multidimensional microscopy analysis. JBC 280, 30392-30399.

Clouse, S., Langford, M., and McMorris, T. (1996). A Brassinosteroid-lnsensitive Mutant in Arabidopsis thaliana Exhibits Multiple Defects in Growth and Development'. Plant Physiol 111, 671-678.

Cong, M., Perry, S.J., Hu, L.A., Hanson, P.I., Claing, A., and Lefkowitz, R.J. (2001). Binding of B2 Adrenergic Receptor to N-Ethylmaleimide-sensitive Factor regulates Receptor Recycling. The Journal of Biological Chemistry 276, 45145-45152.

Coscoy, L., Sanchez, D., and Ganem, D. (2001). A novel class of herpesvirus-encoded membrane-bound E3 ubiquitin ligases regulates endocytosis of proteins involved in immune recognition. J Cell Biol 155, 1265-1273.

Dai, R.M., Chen, E.Y., Longo, D.L., Gorbea, C.M., and Li, C.C.H. (1998). Involvement of valosin-containing protein, an ATPase co-purified with I kappa B alpha and 26 S proteasome, in ubiquitin-proteasome-mediated degradation of I kappa B alpha. J Biol Chem 273, 3562-3573.

Davies, J.M., Tsuruta, H., May, A.P., and Weis, W.I. (2005). Conformational changes of p97 during nucleotide hydrolysis determined by small-angle X-ray scattering. Structure 13, 183-195.

DeLaBarre, B., and Brunger, A.T. (2003). Complete structure of p97/valosin-containing protein reveals communication between nucleotide domains. Nat Struct Biol 10, 856-863.

DeLaBarre, B., and Brunger, A.T. (2005). Nucleotide dependent motion and mechanism of action of p97/VCP. J Mol Biol 347, 437-452.

DeLaBarre, B., Christianson, J.C., Kopito, R.R., and Brunger, A.T. (2006). Central pore residues mediate the p97/VCP activity required for ERAD. Mol Cell 22, 451-462.

Dettmer, J., Hong-Hermesdorf, A., Stierhof, Y., and Schumacher, K. (2006). Vacuolar H+-ATPase activity is required for endocytic and secretory trafficking in Arabidopsis. Plant Cell 18, 715-730.

Dharmasari, N., Dharmasari, S., and Estelle, M. (2005). The F-box protein TIR1 is an auxin receptor. Nature 435, 441-445.

Dhonukshe, P., Mathur, J., Hülskamp, M., and Gadella, T.J. (2005). Microtubule plus-ends reveal essential links between intracellular polarization and localized modulation of endocytosis during division-plane establishment in plant cells. BMC Biol 3.

Dhonushke, P., Aniento, F., Hwang, I., Robinson, D., Mravec, J., Stierhof, Y., and Friml, J. (2007). Clathrin-mediated constitutive endocytosis of PIN auxin efflux carriers in Arabidop-

sis. Curr Biol 17, 520-527.

Doelling, J., Yan, N., Kurepa, J., Walker, J., and Vierstra, R. (2001). The ubiquitin-specific protease UBP14 is essential for early embryo development in Arabidopsis thaliana. Plant J 27, 393-405.

Dreveny, I., Kondo, H., Uchiyama, K., Shaw, A., Zhang, X.D., and Freemont, P.S. (2004). Structural basis of the interaction between the AAA ATPase p97/VCP and its adaptor protein p47. Embo J 23, 1030-1039.

Edward, J.T. (1970). Molecular volumes and Stokes-Einstein equation. J Chem Educ 47, 261-&.

Feiler, H.S., Desprez, T., Santoni, V., Kronenberger, J., Caboche, M., and Traas, J. (1995). The higher-plant Arabidopsis thaliana encodes a functional CDC48 homolog which is highly expressed in dividing and expanding cells. Embo J 14, 5626-5637.

Field, K.A., Holowka, D., and Baird, B. (1995). Fc epsilon RI-mediated recruitment of p53/56lyn to detergent-resistant membrane domains accompanies cellular signaling. Proc Nat Acad Sci 92, 9201-9205.

Gampala, S., Kim, T.-W., He, J.-X., Tang, W., Deng, Z., Bai, M.-Y., Guan, S., Lalonde, S., Sun, Y., Gendron, J., et al. (2007). An essential role for 14-3-3 proteins in brassinosteroid signal transduction in Arabidopsis. Dev Cell 13, 177-189.

Gagnon, E., Duclos, S., Rondeau, C., Chevet, E., Cameron, P.H., Steele-Mortimer, O., Paiement, J., Bergeron, J.J.M., and Desjardins, M. (2002). Endoplasmic Reticulum-Mediated Phagocytosis Is a Mechanism of Entry Macrophages. Cell 110, 119-131.

Geldner, N. (2004). The plant endosomal system--its structure and role in signal transduction and plant development. Planta 219, 547-560.

Geldner, N., Anders, N., Wolters, H., Keicher, J., Kornberger, W., Muller, P., Delbarre, A., Ueda, T., Nakano, A., and Jurgens, G. (2003). The Arabidopsis GNOM ARF-GEF Mediates Endosomal Recycling, Auxin Transport and Auxin-Dependent Plant Growth. Cell 112, 219-230.

Geldner, N., Friml, j., Stierhof, Y., Jurgens, G., and Palme, K. (2001). Auxin inhibitors block PIN1 cycling and vesicle trafficking. Nature 413, 425-428.

Geldner, N., and Jurgens, G. (2006). Endocytosis in signalling and development. Curr Opin in Plant Biol 9, 589-594.

Geldner, N., Hyman, D.L., Wang, X., K., S., and Chory, J. (2007). Endosomal signalling of plant steroid receptor kinase BRI1. Genes Dev 21, 1598-1602.

Gifford, M.L., Robertson, F.C., Soares, D.C., and Ingram, G.C. (2005). ARABIDOPSIS CRINKLY4 function, internalization, and turnover are dependent on the extracellular crinkly repeat domain. Plant Cell 17, 1154-1166.

Gillooly, D., Morrow, J., Lindsay, M., Gould, R., Bryant, N., Gaullier, J., Parton, R., and Stenmark, H. (2000). Localization of phosphatidylinositol 3-phosphate in yeast and mammalian cells. Embo J 19, 4577-4588.

Gomez-Gomez, L., Bauer, Z., and Boller, T. (2001). Both the extracellular leucine-rich repeat

domain and the kinase activity of FSL2 are required for flagellin binding and signaling in Arabidopsis. Plant Cell 13, 1155-1163.

Gomord, V., Denmat, L.-A., Fitchette-Laine, A.C., Satiat-Jeunemaitre, b., Hawes, C., and Faye, L. (1997). The C-terminal HDEL sequence is sufficient for retention of secretory proteins in the endoplasmic reticulim (ER) but promotes vacuolar targeting of proteins that escape the ER. The Plant Journal 11, 313-325.

Gray, W., Kepinski, S., D, R., Leyser, O., and Estelle, M. (2001). Auxin regulates SCF(TIR1)-dependent degradation of AUX/IAA proteins. Nature 414, 271-276.

Griffiths, J., Murase, K., Rieu, I., Zentella, R., Zhang, Z., OPowers, S., Gong, F., Phillips, A., P, H., Sun, T., et al. (2006). Genetic characterization and functional analysis of the GID1 gibberellin receptors in Arabidopsis. Plant Cell 18, 3399-3414.

Haglund, K., Di Fiore, P., and Dikic, i. (2003). Distinct monoubiquitin signals in receptor endocytosis. Trends Biochem Sci 28, 598-603.

Halawani, D., and Latterich, M. (2006). p97: The cell's molecular purgatory? Mol Cell 22, 713-717.

He, K., Goa, X., Yuan, T., Lin, H., Asami, T., Yoshida, S., Russel, S., and Li, J. (2007). BAK1 and BKK1 Regulate Brassinosteroid-Dependent Growth and Brassinosteroid-Independent Cell-Death Pathways. Curr Biol 17, 1109-1115.

Hecht, V., Vielle-Calzada, J.P., Hartog, M.V., Schmidt, E.D., Boutilier, K., Grossniklaus, U., and de Vries, S.C. (2001). The Arabidopsis SOMATIC EMBRYOGENESIS RECEPTOR KINASE 1 gene is expressed in developing ovules and embryos and enhances embryogenic competence in culture. Plant Physiol 127, 803-816.

Hetzer, M., Meyer, H., Walther, T., Bilbao-Cortes, D., Warren, G., and Mattaj, I. (2001). Distinct AAA-ATPase p97 complexes function in discrete steps of nuclear assembly. Nat Cell Biol 12, 1086-1091.

Hewitt, E., Duncan, L., Mufti D, Baker, J., Stevenson, P., and Lehner, P. (2002). Ubiquitylation of MHC class I by the K3 viral protein signals internalization and TSG101-dependent degradation. Embo J 21, 2418-2429.

Hicke, L. (1997). Ubiquitin-dependent internalization and down-regulation of plasma membrane proteins. Faseb J 11, 1215-1226.

Hicke, L., and Dunn, R. (2003). Regulation of membrane protein transport by ubiquitin and ubiquitin-binding proteins. Annu Rev Plant Physiol Plant Mol Biol 19, 141-172.

Hink, M.A., Bisseling, T., and Visser, A.J.W.G. (2002). Imaging protein-protein interactions in living cells. Plant mol Biol 50, 871-883.

Huyton, T., Pye, V.E., Briggs, L.C., Flynn, T.C., Beuron, F., Kondo, H., Ma, J.P., Zhang, X.D., and Freemont, P.S. (2003). The crystal structure of murine p97/VCP at 3.6 angstrom. Journal of Structural Biology 144, 337-348.

Indig, F.E., Partridge, J.J., von Kobbe, C., Aladjem, M.I., Latterich, M., and Bohr, V.A. (2003). Werner syndrome protein directly binds to the AAA ATPase p97/VCP in an ATP-dependent fashion. Journal of Structural Biology 146, 251-259.

Jarosch, E., Taxis, C., Volkwein, C., Bordallo, J., Finley, D., Wolf, D.H., and Sommer, T. (2002). Protein dislocation from the ER requires polyubiquitination and the AAA-ATPase Cdc48. Nat Cell Biol 4, 134-139.

Jeong, S., Trotochaud, A., and Clark, S. (1999). The Arabidopsis CLAVATA2 gene encodes a receptor-like protein required for the stability of the CLAVATA1 receptor-like kinase. Plant Cell 11, 1925-1934.

Jurado, S., Díaz-Triviño, S., Abraham, Z., Manzano, C., Gutierrez, C., and del Pozo, C. (2008). SKP2A, an F-box protein that regulates cell division, is degraded via the ubiquitin pathway. Plant J 53, 828-841.

Karlova, R., Boeren, S., Russinova, E., Aker, J., Vervoort, J., and de Vries, S. (2006). The Arabidopsis SOMATIC EMBRYOGENESIS RECEPTOR-LIKE KINASE1 protein complex includes BRASSINOSTEROID-INSENSITIVE1. Plant Cell 18, 626-638.

Karlova, R., and de Vries, S.C. (2006). Advances in understanding brassinosteroid signaling. Sci STKE 2006, pe36.

Karlova, R., Boeren, S., van Dongen, W., Kwaaitaal, M., Aker, J., Vervoort, J., and de Vries, S.C (2008). Identification of in vitro phosphorylation sites in the Arabidopsis thaliana Somatic Embryogenesis Receptor-like Kinases. Proteomics, In Press.

Katzmann, D., Babst, M., and Emr, S. (2001). Ubiquitin-dependent sorting into the multivesicular body pathway requires the function of a conserved endosomal protein sorting complex, ESCRT-I. Cell 106, 145-155.

Katzmann, D., Odorizzi, G., and Emr, S. (2002). Receptor downregulation and multivesicular-body sorting. Nat Rev Mol Cell Biol 3, 893-905.

Kauschmann, A., Jessop, A., Koncz, C., Szekeres, M., Willmitzer, L., and Altmann, T. (1996). Genetic evidence for an essential role of brassinosteroids in plant development. Plant J 9, 701–713.

Kemmerling, B., Schwedt, A., Rodriquez, P., Mazzotta, S., Frank, M., Qamar, S., T, M., Betsuyaku, S., Parker, J., Mussig, C., et al. (2007). The BRI1-Associated Kinase 1, BAK1,has a Brassinolide-Independent Role in Plant Cell-Death Control. Curr Biol 17, 1116-1122.

Kepinski, S., and Leyser, O. (2005). The Arabidopsis F-box protein TIR1 is an auxin receptor. Nature 435, 446-451.

Kinoshita, T., Caño-Delgado, A., Seto, H., Hiranuma, S., Fujioka, S., Yoshida, S., and Chory, J. (2005). Binding of brassinosteroids to the extracellular domain of plant receptor kinase BRI1. Nature 433.

Kurepa, J., and Smalle, J. (2008). Structure, function and regulation of plant proteasomes Biochimie 90, 324-335.

Kwaaitaal, M.A., de Vries, S.C., and Russinova, E. (2005). Arabidopsis thaliana Somatic Embryogenesis Receptor Kinase 1 protein is present in sporophytic and gametophytic cells and undergoes endocytosis. Protoplasma 226, 55-65.

Lafont, F., and Simons, K. (2001). Raft-partitioning of the ubiquitin ligases Cbl and Nedd4 upon IgE-triggered cell signaling. PNAS 98, 3180-3184.

Latterich, M., Frohlich, K.U., and Schekman, R. (1995). Membrane fusion and the cell cycle - CDC48p participates in the fusion of ER membranes. Cell 82, 885-893.

Lam, B., Sage, T., Bianchi, F., and Blumwald, E. (2001). Role of SH3 domain-containing proteins in clathrin-mediated vesicle trafficking in Arabidopsis. Plant Cell 13, 2499-2512.

Lam, S., Tse, Y., Robinson, D., and Jiang, L. (2007). Tracking down the elusive early endosome. Trends Plant Sci 12, 497-505.

Latterich, M., Frohlich, K.U., and Schekman, R. (1995). Membrane fusion and the cell cycle - CDC48p participates in the fusion of ER membranes. Cell 82, 885-893.

Lei, J., and M, Martinez.-Moczygemba. (2008). Separate endocytic pathways regulate IL-5 receptor internalization and signaling. J Leukoc Biol In Press.

Li, J., and Chory, J. (1997). A putative leucine-rich repeat receptor kinase involved in brassinosteroid signal transduction. Cell 90, 929-938.

Li, J., Wen, J., Lease, K.A., Doke, J.T., Tax, F.E., and Walker, J.C. (2002). BAK1, an Arabidopsis LRR receptor-like protein kinase, interacts with BRI1 and modulates brassinosteroid signaling. Cell 110, 213-222.

Livnah, O., Stura, E., Middleton, S., Johnson, D., Jolliffe, L., and Wilson, I. (1999). Crystallographic evidence for preformed dimers of erythropoietin receptor before ligand activation. Science 283, 987-990.

Lowe, E., Doherty, T., Karahashi, H., and Arditi, m. (2006). Ubiquitination and de-ubiquitination: role in regulation of signaling by Toll-like receptors. 12 12, 337-345.

Machen, T., Leigh, M., Taylor, C., Kimura, T., Asano, S., and Moore, H. (2003). pH of TGN and recycling endosomes of H+/K+-ATPase-transfected HEK-293 cells: implications for pH regulation in the secretory pathway. Am J Physiol Cell Physiol 285, C205-214.

Madeo, F., Schlauer, J., Zischka,H., Mecke, D., and Frohlich, E. (1998). Tyrosine phosphorylation regulates cell cycle-dependent nuclear localization of Cdc48p. Mol Biol Cell 1, 131-141.

Mandava, N. (1988). Plant Growth-Promoting Brassinosteroids. Annual Review of Plant Physiology and Plant Molecular Biology 39, 23-52.

Maor, R., Jones, A., Nühse, T., David J. Studholme, D., Peck, S., and Shirasu, K. (2007). Multidimensional Protein Identification Technology (MudPIT) Analysis of Ubiquitinated Proteins in Plants. Molecular and Cellular Proteomics 6, 601=610.

McPherson, P., Kay, B., and Hussain, N. (2001). Signaling on the Endocytic Pathway. Traffic 2, 375-384.

Meseth, U., Wohland, T., Rigler, R., and Vogel, H. (1999). Resolution of fluorescence correlation measurements. Biophys J 76, 1619-1631.

Meyer, H.H., Shorter, J.G., Seemann, J., Pappin, D., and Warren, G. (2000). A complex of mammalian Ufd1 and Npl4 links the AAA-ATPase, p97, to ubiquitin and nuclear transport pathways. Embo J 19, 2181-2192.

Meyer, H.H., Wang, Y.Z., and Warren, G. (2002). Direct binding of ubiquitin conjugates by the mammalian p97 adaptor complexes, p47 and Ufd1-Npl4. Embo J 21, 5645-5652.

Miaczynska, M., Pelkmans, L., and Zerial, M. (2004). Not just a sink: endosomes in control of signal transduction. Curr Opin Cell Biol 16, 400-406.

Mukhopadhyay, D., and Riezman, H. (2007). Proteasome-Independent Functions of Ubiquitin in Endocytosis and Signaling. Science 315, 201-205.

Mullaly, J.E., Chernova, T., and Wilkinson, K.D. (2006). Doa1 is a Cdc48 adapter that possesses a novel ubiquitin binding domain. Mol Cell Biol 3, 822-830.
Müller, J., Mettbach, U., Menzel, D., and Samaj, J. (2007). Molecular Dissection of Endosomal Compartments in Plants. Plant Physiol 145, 293-304.

Müller, J., Piffanelli, P., Devoto, A., Miklis, M., Elliott, C., Ortmann, B., Schulze-Lefert, P., and Panstruga, R. (2005). Conserved ERAD-Like Quality Control of a Plant Polytopic Membrane Protein. Plant Cell 17, 149-163.

Nam, K.H., and Li, J. (2002). BRI1/BAK1, a receptor kinase pair mediating brassinosteroid signaling. Cell 110, 203-212.

Nirmala, J., Dahl, S., Steffenson, B., Kannangara, C., von Wettstein, D., Chen, X., and Kleinhofs, A. (2007). Proteolysis of the barley receptor-like protein kinase RPG1 by a proteasome pathway is correlated with Rpg1-mediated stem rust resistance. PNAS 104, 10276-10281.

Nougalli Tonaco, I.A., Borst, J.W., de Vries, S.C.R., E., Angenent, G.C., and Immink, R.G.H. (2005). In vivo imaging of MADS-box transcription factor interactions. J Exp Botany 57, 33-42.

Oliviusson, P., Heinzerling, O., Hillmer, S., Hinz, G., Tse, Y., Jiang, L., and Robinson, D. (2006). Oliviusson P, Heinzerling O, Hillmer S, Hinz G, Tse YC, Jiang L, Robinson DG. Plant Cell 18, 1239-1252.

Osten, p., Srivastava, S., Inman, G.J., Vilim, F.S., Khatri, l., Lee, l.m., States, B.A., Einheber, S., Milner, T.A., and Hanson, P.I. (1998). The AMPA receptor GluR2 C terminus can mediate a reversible, ATP-dependent interaction with NSF and alpha- and beta-SNAPs. Neuron 21, 99-110.

Paciorek, T., Zazimalova, E., Ruthardt, N., Petrasek, J., Stierhof, Y., Kleine-Vehn, j., DA, M., Emans N, Jurgens, G., Geldner, N., et al. (2005). Auxin inhibits endocytosis and promotes its own efflux from cells. Nature 435, 1251-1256.

Peng, J., Elias, J.E., Thoreen, C.C., Licklider, L.J., and Gygi, S.P. (2003). Evaluation of multidimensional chromatography coupled with tandem mass spectrometry (LC/LC-MS/MS) for large-scale protein analysis: the yeast proteome. J Proteome Res 2, 43-50.

Pleasure, I.T., Black, M.M., and Kee, J.H. (1993). Vasolin-containing protein, VCP, is a ubiquitous clathrin-binding protein. Nature 365, 459-462.

Pye, V.E., Dreveny, I., Briggs, i.C., Sands, C., Beuron, F., Zhang, X., and Freemont, p.S. (2006). Going through the motions: The ATPase cycle of p97. Journal of Structural biology 156, 12-58.

Rabouille, C., Kondo, H., Newman, R., Hui, N., Freemont, P., and Warren, G. (1998). Syntaxin 5 is a common component of the NSF- and p97-mediated reassembly pathways of Golgi cisternae from mitotic Golgi fragments in vitro. Cell 92, 603-610.

Rancour, D.M., Dickey, C.E., Park, S., and Bednarek, S.Y. (2002). Characterization of AtCDC48. Evidence for multiple membrane fusion mechanisms at the plane of cell division in plants. Plant Physiol 130, 1241-1253.

Rancour, D.M., Park, S., Knight, S.D., and Bednarek, S.Y. (2004). Plant UBX domain-containing protein 1, PUX1, regulates the oligomeric structure and activity of arabidopsis CDC48. J Biol Chem 279, 54264-54274.

Reggiori, F., and Pelham, H. (2001). Sorting of proteins into multivesicular bodies: ubiquitin-dependent and -independent targeting. EMBO J 20, 5176-5186.

Rienties, I.M., Vink, J., Borst, J.W., Russinova, E., and Vries, S.C. (2005). The Arabidopsis SERK1 protein interacts with the AAA-ATPase AtCDC48, the 14-3-3 protein GF14lambda and the PP2C phosphatase KAPP. Planta 221, 394-405.

Rigler, R., Mets, U., Widengren, J., and Kask, P. (1993). Fluorescence correlation spectroscopy with high count rate and low background - Analysis of translational diffusion. Eur Biophys J Biophys Lett 22, 169-175.

Robatzek, S., Chinchilla, D., and Boller, T. (2006). Ligand-induced endocytosis of the pattern recognition receptor FLS2 in Arabidopsis. Genes Dev 20, 537-542.

Robinson, D., Albrecht, S., and Moriysu, Y. (2004). The V-ATPase inhibitors concanamycin A and bafilomycin A lead to Golgi swelling in tobacco BY-2 cells. Protoplasma 224, 255-260

Robinson, L.J., Aniento, F., and Gruenenberg, J. (1997). NSF is required for transport from early to late endosomes. J Cell Science 110, 2079-2087.

Russinova, E., Borst, J.W., Kwaaitaal, M., Cano-Delgado, A., Yin, Y.H., Chory, J., and de Vries, S.C. (2004). Heterodimerization and endocytosis of Arabidopsis brassinosteroid receptors BRI1 and AtSERK3 (BAK1). Plant Cell 16, 3216-3229.

Rumpf, S., and Jentsch, S. (2006). Functional division of substrate processing cofactors of the ubiquitin-selective Cdc48 chaperone. Mol Cell 21, 261-269.

Samaj, J., Read, N., Volkmann, D., Menzel, D., and Baluska, F. (2005). The endocytic network in plants. Trend Cell Biol 15, 425-433.

Samaj, J., Müller, J., Beck, M., Böhm, N., and D, M. (2006). Vesicular trafficking, cytoskeleton and signalling in root hairs and pollen tubes. Trends Plant Sci 11, 594-600.

Schuberth, C., and Buchberger, A. (2005). Membrane-bound Ubx2 recruits CDC48 to ubiquitin ligases and their substrates to ensure efficient ER-associated protein degradation. Nat Cell Biol 7, 999-U102.

Schuberth, C., Richly, H., Rumpf, S., and Buchberger, A. (2004). Shp1 and Ubx2 are adaptors of CDC48 involved in ubiquitin-dependent protein degradation. Embo Reports 5, 818-824.

Schubert, U., Anton, L., Gibbs, J., Norbury, C., Yewdell, J., and Bennink, J. (2000). Rapid degradation of a large fraction of newly synthesized proteins by proteasomes. Nature 404, 770-774.

Shah, K., Gadella, T.W., Jr., van Erp, H., Hecht, V., and de Vries, S.C. (2001a). Subcellular localization and oligomerization of the Arabidopsis thaliana somatic embryogenesis receptor kinase 1 protein. J Mol Biol 309, 641-655.

Shah, K., Vervoort, J., and de Vries, S.C. (2001b). Role of threonines in the Arabidopsis thaliana somatic embryogenesis receptor kinase 1 activation loop in phosphorylation. J Biol Chem

276, 41263-41269.

Shah, K., Russinova, E., Theodorus W.J. Gadella, J., Willemse, J., and Vries, S.C.d. (2002). The Arabidopsis kinase-associated protein phosphatase controls internalization of the somatic embryogenesis receptor kinase 1. Genes Dev 16, 1707-1720.

Sheen, J. (2001). Signal transduction in maize and Arabidopsis mesophyll protoplasts. Plant Physiol 127, 1466-1475.

Shenoy, S. (2007). Seven-transmembrane receptors and ubiquitination. Circ Res 100, 1142-1154.

Shenoy, S., and Lefkowitz, R. (2003). Multifaceted roles of beta-arrestins in the regulation of seven-membrane-spanning receptor trafficking and signalling. Biochem J 375, 503-515.

Shevchenko, A., Wilm, M., Vorm, O., and Mann, M. (1996). Mass spectrometric sequencing of proteins silver-stained polyacrylamide gels. Anal Chem 68, 850-858.

Shtiegman, K., and Yarden, Y. (2003). The role of ubiquitylation in signaling by growth factors: implications to cancer. Semin Cancer Biol 13, 29-40.

Song, C.C., Wang, Q., and Li, C.C.H. (2003). ATPase activity of p97-valosin-containing protein (VCP) - D2 mediates the major enzyme activity, and D1 contributes to the heat-induced activity. J Biol Chem 278, 3648-3655.

Spitzer, C., Schellmann, S., Sabovljevic, A., Shahriari, M., Keshavaiah, C., Bechtold, N., Herzog, M., Müller, S., Hanisch, F., and M, H. (2006). The Arabidopsis elch mutant reveals functions of an ESCRT component in cytokinesis. Development 133, 4679-4689.

Stasolla, C., Bozhkov, P., Chu, T., Van Zyl, L., Egertsdotter, U., Suarez, M., Craig, D., Wolfinger, R., Von Arnold, S., and Sederoff, R. (2004). Variation in transcript abundance during somatic embryogenesis in gymnosperms. Tree Physiol 24, 1073-1085.

Staub O, Gautschi I, Ishikawa T, Breitschopf K, Ciechanover A, Schild L, and D, R. (1997). Regulation of stability and function of the epithelial Na+ channel (ENaC) by ubiquitination. Embo J 16, 6325-6336.

Suty, L., Lequeu, J., Lançon, A., Etienne, P., Petitot, A., and Blein, J. (2003). Preferential induction of 20S proteasome subunits during elicitation of plant defense reactions: towards the characterization of "plant defense proteasomes". Int J Biochem Cell Biol 35, 637-650.

Szekeres, M., Németh, K., Koncz-Kálmán, Z., Mathur, J., Kauschmann, A., Altmann, T., Rédei, G., Nagy, F., Schell, J., and Koncz, C. (1996). Brassinosteroids rescue the deficiency of CYP90, a cytochrome P450, controlling cell elongation and de-etiolation in Arabidopsis. cell 85, 171-182.

Takano, J., Miwa, K., Yuan, L., von Wirén, N., and Fujiwara, T. (2005). Endocytosis and degradation of BOR1, a boron transporter of Arabidopsis thaliana, regulated by boron availability. PNAS 102, 12276-12281.

Tang, G., Hardin, S., Dewey, R., and Huber, S. (2003). A novel C-terminal proteolytic processing of cytosolic pyruvate kinase, its phosphorylation and degradation by the proteasome in developing soybean seeds. Plant J 34, 77-93.

Tse, Y., Mo, B., Hillmer, S., Zhao, M., Lo, S., Robinson, D., and Jiang, L. (2004). Identifica-

tion of multivesicular bodies as prevacuolar compartments in Nicotiana tabacum BY-2 cells. Plant Cell 16, 672-693.

Uchiyama, K., and Kondo, H. (2005). p97/p47-mediated biogenesis of Golgi and ER. J Biochem 137, 115-119.

Ueda, T., Yamaguchi, M., Uchimiy, A.H., and Nakano, A. (2001). Ara6, a plant-unique novel Rab GTPase, functions in the endocytic pathway of Arabidopsis thaliana. The EMBO Journal 20, 4730-4741.

Uemura, T., Ueda T, Ohniwa RL, Nakano A, Takeyasu K, and MH., S. (2004). Systematic analysis of SNARE molecules in Arabidopsis: dissection of the post-Golgi network in plant cells. Cell Struct Funct 29, 49-65.

Vacca, R., Valenti, D., Bobba, A., de Pinto, M., Merafina, R., De Gara, L., Passarella, S., and Marra, E. (2007). Proteasome function is required for activation of programmed cell death in heat shocked tobacco Bright-Yellow 2 cells. FEBS Lett 581, 917-922.

Varghese, B., Barriere, H., Carbone, C., Banerjee, A., Swaminathan, G., Plotnikov, A., Xu, P., Peng, J., Goffin, V., Lukacs, G., et al. (2008). Polyubiquitination of prolactin receptor stimulates its internalization, post-internalization sorting, and degradation via the lysosomal pathway. Mol Biol Cell In Press.

van Bokhoven, H., Verve, r.J., Wellink, J., and van Kammen, A. (1993). Protoplasts transiently expressing the 200K coding sequence of cowpea mosaic virus B-RNA support replication of M-RNA. J Gen Virol 74, 2233-2241.

Van kuppeveld, F.J.M., Melchers, W.J.G., Willems, P.H.G.M., and Gadella Jr, T.W.J. (2002). Homomultimerization of the coxsackievirus 2B protein in living cells visualized by fluorescence resonance energy transfer microscopy. Journal of virology 76, 9446-9456.

Vermeer, J., van Leeuwen, W., Tobena-Santamaria, R., Laxalt, A., Jones, D., Divecha, N., Gadella, T.J., and Munnik, T. (2006). Visualization of PtdIns3P dynamics in living plant cells. Plant J 47, 687-700.

Vert, G., and Chory, J. (2006). Downstream nuclear events in brassinosteroid signalling. Nature 441, 96-100.

Wang, Q., Song, C.C., and Li, C.C.H. (2003a). Hexamerization of p97-VCP is promoted by ATP binding to the D1 domain and required for ATPase and biological activities. Biochem Biophys Res Commun 300, 253-260.

Wang, Q., Song, C.C., Yang, X.Y., and Li, C.C.H. (2003b). D1 ring is stable and nucleotide-independent, whereas D2 ring undergoes major conformational changes during the ATPase cycle of p97-VCP. J Biol Chem 278, 32784-32793.

Wang, Q., Song, C.C., and Li, C.C.H. (2004). Molecular perspectives on p97-VCP: progress in understanding its structure and diverse biological functions. Journal of Structural Biology 146, 44-57.

Wang, X., and Chory, J. (2006). Brassinosteroids regulate dissociation of BKI1, a negative regulator of BRI1 signaling, from the plasma membrane. Science 313, 1118-1122.

Wang, X., Li, X., Meisenhelder, J., Hunter, T., Yoshida, S., Asami, T., and Chory, J. (2005). Autoregulation and Homodimerization Are Involved in the Activation of the Plant Steroid

Receptor BRI1. Dev Cell 8, 855-865.

Wang, X., Goshe, M.B., Soderblom, E.J., Phinney, B.S., Kuchar, J.A., Li, J., Asami, T., Yoshida, S., Huber, S.C., and Clouse, S.D. (2005). Identification and Functional Analysis of in Vivo Phosphorylation Sites of the Arabidopsis BRASSINOSTEROID-INSENSITIVE1 Receptor Kinase. Plant Cell 17, 1685-1703.

Warren, C., and Landgraf, R. (2006). Signaling through ERBB receptors: multiple layers of diversity and control. Cell Signal 18, 923-933.

Weijers, D., Schlereth, A., Ehrismann, J., Schwank, G., Kientz, M., and Jürgens, G. (2006). Auxin Triggers Transient Local Short ArticleSignaling for Cell Specificationin Arabidopsis Embryogenesis. Developmental Cell 10, 265-270.

Wojcik, C., and DeMartino, G.N. (2003). Intracellular localization of proteasomes. . The International Journal of Biochemistry and Cell Biology, 35, 579-589.

Woodman, P.G. (2003). p97, a protein coping with multiple identities. J Cell Sci 116, 4283-4290.

Yen, C.-H., yang, Y.-C., Ruscetti, S.K., Kirken, R.A., Dai, R.M., and Li, C.-C.H. (2000). Involvement of the Ubiquitin-Proteasome Pathway in the Degradation of Nontyrosine Kinase-Type Cytokine Receptors of IL-9, IL-2, and Erythropoietin. The Journal of Immunology 165 6372-6380.

Zhang, L., Ashendel, C.L., Becker, G.W., and Morre, D.J. (1994). Isolation and characterization of the principal ATPase associated with transitional endoplasmic reticulum of rat liver. J Cell Biol 127, 1871-1883.

Zhang, X.D., Shaw, A., Bates, P.A., Newman, R.H., Gowen, B., Orlova, E., Gorman, M.A., Kondo, H., Dokurno, P., Lally, J., et al. (2000). Structure of the AAA ATPase p97. Mol Cell 6, 1473-1484.

Nederlandse samenvatting

Om zich aan te kunnen passen aan veranderende omstandigheden tijdens hun leven, moeten planten signalen kunnen opvangen van buitenaf. Deze signalen worden opgevangen door "receptoren", eiwitten met een extracellulair gedeelte aan de buitenkant van de cel, een transmembraan domein door het plasmamembraan (PM) en een intracellulair gedeelte dat het signaal door middel van interacties met andere eiwitten kan doorgeven. De receptoren beschreven in dit proefschrift, zijn betrokken bij de signaleringsroute van de brassinosteroïd-hormonen. Deze worden door de planten zelf geproduceerd en ook herkend. Binding van een dergelijk hormoon aan het extracellulaire domein van de brassinosteroïd receptor BRI1 (Brassinosteroid insensitive 1) leidt uiteindelijk tot stimulatie van cel verlenging, blad ontrolling, xyleem differentiatie en celdeling, en tot remming van wortel verlenging, radiale stam expansie en anthocyaan biosynthese. Andere processen waarbij de brassinosteroïd signalering een rol speelt zijn de timing van de bloei en bladafval, blad ontwikkeling en resistentie tegen stres en de controle over cel dood.

De hoofdreceptor voor brassinosteroïden in Arabidopsis, ofwel de zandraket, is dus BRI1 maar andere, co-receptoren, zijn ook vereist voor de signalering. Deze receptoren, SERK1 en SERK3 (Somatic embryogenesis receptor-like kinase), dimerizeren met BRI1 na het binden van brassinolide (BL), de sterkste van de brassinosteroïd-hormonen, aan de BRI1 receptor. Daarop phosphoryleren de receptoren elkaar en wordt er uiteindelijk via een nog onbekende route een signaal afgegeven aan transcriptiefactoren in de kern die leiden tot gen-transcriptie, waarop eiwitten geproduceerd worden die een bepaalde reactie teweeg brengen in de cel.

Na de signaal-overdracht, moet het signaal ook weer worden afgezet, om te voorkomen dat er uiteindelijk teveel of te weinig van een bepaald eiwit wordt gemaakt en er over-stimulatie plaatsvindt. Daarvoor moeten de receptoren eerst naar binnen worden gebracht, ofwel geïnternaliseerd worden. Er zijn verschillende manieren om het signaal af te zetten. De eerste is de afbraak van de receptoren in het proteasoom. Het proteasoom is de verbrandingsoven van de cel; een complex van eiwitten die een signaal herkennen op eiwitten die moeten worden afgebroken. Receptoren en andere eiwitten die moeten worden afgebroken moeten dit herkenningssignaal, het eiwitje ubiquitine, meekrijgen om herkend te worden door het proteasoom. Een andere methode om het signaal van de receptor af te zetten is doordat de vroege endosomen, de blaasjes waarin de receptoren terecht komen na internalizatie, fuseren met andere latere endosomen, om vervolgens in een groot organel terecht te komen (MVB of multi-vesicular body) met onder andere lysozym bevattende blaasjes. Fusie daarmee bewerkstelligt de afbraak van de receptoren.

De keuze voor afbraak in het proteasoom of in de lysosomen wordt bepaald door de lengte van het ubiquitine-eiwit. Eén ubiquitine-eiwit leidt naar de endosomale route, een keten van ubiquitines leidt naar de proteasoom-route. Er zijn ook nog verschillende ontsnappings-routes mogelijk. Vanaf de vroege endosomen kunnen de receptoren teuggezet worden op het plasma-membraan voor hergebruik. Vanaf de MVB kunnen ze ook via het trans golgi netwerk (TGN), waarin eiwitten terecht komen die nieuw geproduceerd zijn en op weg zijn naar allerlei locaties in de cel, terecht komen op het PM.

Het onderzoek beschreven in het eerste deel van dit proefschrift behandelt de communicatie,

of interactie, tussen SERK1 en het CDC48A-eiwit dat een rol speelt bij het opruimen van eiwitten die mis-gevouwen uit het ER (endoplasmatisch reticulum) komen. In het tweede deel wordt beschreven wat er gebeurt met BRI1 en de co-receptoren SERK1 en SERK3 nadat signalering heeft plaatsgevonden.

In hoofdstuk **2** wordt de interactie beschreven tussen SERK1 en het eiwit CDC48A, dat gevonden werd in voorgaand onderzoek tijdens een twee-hybride screen in gist en in een eiwit-complex geïsoleerd uit zaailingen van Arabidopsis, tesamen met de fosfatase KAPP en een 14-3-3 eiwit. KAPP defosforyleert SERK1 en co-localiseert met SERK1 in endosomen. Van CDC48 eiwitten is beschreven dat ze een rol spelen in endoplasmic reticulum-geassocieerde degradatie (ERAD) van eiwitten. Ze leiden deze eiwitten m.b.v ubiquitine-herkennende helper-eiwitten naar het proteasoom. De conformatie-verandering die CDC48A ondergaat na het binden en de hydrolyse van ATP, levert de energie om ERAD substraten uit het ER te trekken en ze naar het proteasoom te leiden.

We hebben gevonden dat SERK1 en CDC48A een interactie aangaan in domeinen aan de PM die co-localizeren met ER-markers, en veronderstellen dat dit de functie van deze interactie is. Met behulp van FRET-FLIM konden we vaststellen dat SERK1 een interactie aangaat met zowel het N-terminale als het C-terminale domein van CDC48A. Deze interacties aan beide zijden van het CDC48A eiwit zouden verschillende functies in de cel kunnen vertegenwoordigen.

Ten eerste zou proteasoom-afhankelijke afbraak van SERK1 receptoren een manier kunnen zijn om hun activiteit te reguleren, analoog aan de Interleukine (IL-2 en IL-3) en de Erythropoietin receptoren die binden aan de CDC48 homoloog VCP in zoogdiercellen wat tot degradatie in het proteasoom leidt. Een andere al genoemde functie is de rol van CDC48A in de kwaliteitscontrole van SERK eiwitten die uit het ER komen. Als deze niet goed gevouwen zijn worden ze uit het ER getrokken, ge-ubiquitineerd en naar het proteasoom gedirigeerd. Ter illustratie: maar liefst 30% van de nieuw geproduceerde eiwitten bevatten peptides afkomstig van afgebroken misgevouwen eiwitten.

In hoofdstuk **3** wordt nader ingegaan op de interactie tussen SERK1 en CDC48A. CDC48 eiwitten komen namelijk voor in monomere of hexamere (enkelvoudige of zesvoudige) vorm, maar alleen de laatste vorm is actief. De vraag was dus of SERK1 een interactie zou aangaan met de monomere of de hexamere vorm van CDC48A, waardoor de relevantie van het voorgaande hoofdstuk zou kunnen worden bevestigd. Door aan een van de monomeren een blauw en een andere een geel fluorescent eiwit te koppelen, kon d.m.v Förster resonance energy transfer (FRET) energie-overdracht gemeten worden tussen de verschillende monomeren in de hexameer, als dit de overheersende vorm is in cellen. Dat bleek inderdaad het geval, en dit kon bovendien m.b.v natieve gel-electroforese bevestigd worden. Met behulp van fluorescente correlatie spectroscopie (FCS) kan de snelheid van diffusie van fluorescente moleculen worden bepaald, die voor het CDC48A eiwit veel groter bleek te zijn dan berekend voor de hexameer alleen. Daarom concludeerden we dat CDC48A in een veel groter complex van eiwitten, bijvoorbeeld onder andere met het SERK-eiwit, in de cel voorkomt. Door deletie van het domein dat waarschijnlijk verantwoordelijk is voor de interactie met andere eiwitten, ging

de diffusiesnelheid omhoog. Ook een mutatie in CDC48A waardoor de ATPase activiteit verminderd wordt, leverde een hogere diffusiesnelheid op. Dit samen leidde tot de conclusie dat er in deze gevallen een kleiner eiwit-complex wordt gevormd dat sneller beweegt in het cytoplasma.

In hoofdstuk **4** wordt de endosomale route na signalering bestudeerd in worteltips. Met behulp van een transgene lijn waarin BRI1 gekoppeld is aan GFP en de co-receptor SERK3 gekoppeld aan een HA-vlag, wordt na fixatie van de worteltips en kleuring met antibodies tegen GFP en HA, vastgesteld dat over-expressie van SERK3 leidt tot verhoogde endocytose van BRI1. Dit leidt echter niet tot verhoogde brassinosteroïd signalering mogelijk omdat SERK1 niet in voldoende mate aanwezig is. Daarop werd BRI1-GFP gekruist in lijnen waarin een of beide van de coreceptoren SERK1 en SERK3 gemuteerd waren (genoemd *sk1sk3*), om te zien of dit een verandering van distributie van BRI1 aan de PM of het cytoplasma te zien zou geven. *Sk1sk3* is ongevoelig voor de brassinosteroïde BL, en BRI1-GFP in deze lijn herstelde dit slechts met 15%, mogelijk omdat de homodimere BRI1 receptoren ook kunnen signaleren. BRI1-GFP in wildtype achtergrond bleek namelijk hypersensitief voor BL te zijn. Dit gebeurt waarschijnlijk alleen als de hoeveelheid BRI1 receptor hoger is dan die van de co-receptoren en het systeem uit balans is.

Het ontbreken van de co-receptoren bleek echter geen effect te hebben op de distributie van BRI1-GFP over de PM en het cytoplasma. Wel bleek de totale hoeveelheid BRI1 eiwit lager te zijn de mutante lijnen. De veronderstelling was dat SERK1 en SERK3 het BRI1 signalerings-complex stabiliseren en daarmee de signaleringstijd verlengen. Het ontbreken van de SERK receptoren maakt BRI1 instabiel en meer gevoelig voor degradatie. Meer SERK3 leidde echter ook tot verhoogde endocytose. De veronderstelling is dat endocytose is verhoogd zowel in geval van over- als onder-expressie van de co-receptoren, maar dat in het laatste geval de degradatie-route verschuift van recycling naar degradatie in het proteasoom. SERK1 en SERK3 dragen mogelijk bij aan de stabilisatie van de BRI1-receptor.

In hoofdstuk **5** wordt de rol van de co-receptoren nader bestudeerd. SERK3 blijkt slechts voor een gedeelte een interactie aan te gaan met BRI1, namelijk alleen met die portie die gevoelig is voor de toxine brefeldin A (BFA). BFA wordt gebruikt om recycling van membraan-eiwitten te blokkeren zodat deze zich ophopen in endosomale compartimenten (zogenaamde BFA compartimenten). Voor de recycling van receptoren terug naar de PM zijn ARF-GEF eiwitten (ADP ribosylation factor-guanine exchange factors) betrokken, die door BFA specifiek geblokkeerd worden. Toegepast op transgene worteltips met SERK3 en BRI1-GFP, kon worden vastgesteld dat er van BRI1 veel meer in de BFA compartimenten terechtkomt dan van SERK3, hoewel de expressie van SERK3 aan het membraan even hoog is. De veronderstelling is dat van SERK3 slechts een klein deel over deze BFA gevoelige route recycled, en dat de rest een BFA-ongevoelige route neemt. De SERK3 receptor signaleert met verschillende andere partners, die onder andere een rol spelen in controle over cel-dood en immuniteit tegen pathogenen. Bij deze signalerings routes zouden andere ARF-GEFs betrokken kunnen zijn voor recycling van de SERK3 receptor.

Sk1sk3 mutante zaailingen zijn ongevoelig voor BL. Tot onze verrassing bleek bovendien dat

in met BFA behandelde BRI1-GFP zaailingen de brassinosteroïd signalering ook aanstond, terwijl dit in *sk1sk3* mutanten nauwelijks het geval was. Dit toont aan dat voor signalering SERK1 en SERK3 nodig zijn en dat deze vrijwel uitsluitend plaatsvindt vanaf de endosomale compartimenten en dus mogelijk niet vanaf de PM. BRI1-GFP alleen kan ook in mindere mate als homodimeer signaleren en dit wordt verhoogd wanneer met BFA de recycling en degradatie van BRI1 geblokkeerd wordt.

Perspectief

Het in dit proefschrift beschreven onderzoek heeft nader inzicht opgeleverd in de routes die membraan receptoren volgen na de signaal-transductie. CDC48A speelt mogelijk een rol in het reguleren van de SERK1 activiteit door afbraak van SERK1 naar het proteasoom te beïnvloeden, of bij de kwaliteitscontrole van nieuw gesynthetiseerde SERK1 eiwitten. SERK1 en SERK3 zijn van belang voor de signalering van de BRI1-receptor, maar niet voor het proces van endocytose van de BRI1-receptor op zich. De aan- of afwezigheid van de co-receptoren bepaalt waarschijnlijk wel of en hoeveel van de BRI1 receptoren worden teruggezet op de PM of naar degradatie in het proteasoom wordt geleid. De hoeveelheden van de verschillende receptoren in het BRI1-receptor complex zijn mogelijk van belang voor de signalering en het lot van de receptoren na signalering. Verder onderzoek zal daarop het antwoord moeten geven.

List of publications

Aker J, Wijdeven R, Borst JW, and de Vries SC (2008). The SERK1 and SERK3/BAK1 co-receptors are required for BRI1 endosomal signaling. In preparation.

Borst JW, Laptenok SP, Westphal AH, Kühnemuth R, Hornen H, Visser NV, Kalinin S, **Aker J,** van Hoek A, Seidel, CAM, Visser, AJWG. (2008). Structural changes of Yellow Cameleon domains observed by quantitative FRET analysis and polarized fluorescent correlation spectroscopy. *Biophys J.* In Press.

Karlova R, Boeren S, van Dongen W, Kwaaitaal M, **Aker J**, Vervoort J and de Vries SC (2008). Identification of in vitro phosphorylation sites in the Arabidopsis thaliana Somatic Embryogenesis Receptor-like Kinases. *Proteomics*, In Press.

Aker J and de Vries SC (2008). Plasma Membrane Receptor Complexes. *Plant Physiol.* Vol. 147, pp 1560-1564.

Aker J, Hesselink R, Engel R, Karlova, R, Borst, JW, Visser AJ and de Vries SC (2007). In vivo Hexamerisation and Characterization of the Arabidopsis AAA ATPase CDC48A complex using Förster Resonance Energy Transfer-Fluorescenc Lifetime Imaging Microscopy and Fluorescence Correlation Spectroscopy. *Plant Physiol.* Vol. 145, pp. 339-350.

Aker J, Borst JW, Karlova R, and de Vries SC (2006). The Arabidopsis thaliana AAA protein CDC48A interacts in vivo with the Somatic Embryogenesis Receptor-like Kinase 1 receptor at the plasma membrane. *Journal of Structural Biology* Vol. 156(1) 62-71.

Karlova R, Boeren S, Russinova J, Albrecht C, **Aker J,** Vervoort J and de Vries, SC (2006). The Arabidopsis SOMATIC EMBRYOGENESIS RECEPTOR-LIKE KINASE1 protein complex includes BRASSINOSTEROID-INSENSITIVE1. *Plant Cell* 18, 626-638.

van der Wal-Aker, J, Habets R, Várnai P, Balla T, and Jalink K (2001). Monitoring Agonist-induced Phospholipase C Activation in Live Cells by Fluorescence Resonance Energy Transfer. *J. Biol. Chem*., Vol. 276, Issue 18, 15337-15344.

van der Hoeven PC, **van der Wal J**, Ruurs P, Van Dijk MC, van Blitterswijk WJ. (2000). 14-3-3 isotypes facilitate coupling of protein kinase C-zeta to Raf-1: negative regulation by 14-3-3 phosphorylation. *Biochem J.* Vol 345 Pt 297-306.

Van Der Hoeven PC, **van der Wal J,** Ruurs P, Van Blitterswijk WJ.(2000). Protein kinase C activation by acidic proteins including 14-3-3. *Biochem J.* Vol. 347 Pt 3:781-5.

Houssa B, Schaap D, **van der Wal J**, Goto K, Kondo H, Yamakawa A, Shibata M, Takenawa T, van Blitterswijk WJ (1997). Cloning of a novel human diacylglycerol kinase (DGKtheta) containing three cysteine-rich domains, a proline-rich region, and a pleckstrin homology domain with an overlapping Ras-associating domain. *J Biol Chem*.Vol. 272(16):10422-8.

Schaap D, **van der Wal J**, van Blitterswijk WJ (1994). Consensus sequences for ATP-binding sites in protein kinases do not apply to diacylglycerol kinases. *Biochem J.* Vol. 304 (2): 661-2.

Schaap D, **van der Wal J**, Howe LR, Marshall CJ, van Blitterswijk WJ. (1993). A dominant-negative mutant of raf blocks mitogen-activated protein kinase activation by growth factors and oncogenic p21ras. *J Biol Chem*. Vol. 268 (27):20232-6.

Schaap D, **van der Wal J**, van Blitterswijk WJ, van der Bend RL, Ploegh HL (1993). Diacylglycerol kinase is phosphorylated in vivo upon stimulation of the epidermal growth factor receptor and serine/threonine kinases, including protein kinase C-epsilon. *Biochem J.* Vol. 289 (3): 875-81.

Roelofs H, Tasseron-de Jong JG, **van der Wal-Aker J**, Rodenburg RJ, van Houten GB, van de Putte P, Giphart-Gassler M (1992). Gene amplification in a human osteosarcoma cell line results in the persistence of the original chromosome and the formation of translocation chromosomes. *Mutat Res*. Vol. 276(3):241-60.

Schaap D, de Widt J, **van der Wal J,** Vandekerckhove J, van Damme J, Gussow D, Ploegh HL, van Blitterswijk WJ, van der Bend RL (1990). Purification, cDNA-cloning and expression of human diacylglycerol kinase. *FEBS Lett.* Vol. 275(1-2):151-8.

Tasseron-de Jong JG, **Aker J**, den Dulk H, van de Putte P, Giphart-Gassler M (1989). Cytosine methylation in the EcoRI site of active and inactive herpesvirus *Biochim Biophys Acta*. Vol. 1008(1):62-70.

Tasseron-de Jong JG, **Aker J,** Giphart-Gassler M (1988). The ability of the restriction endonuclease EcoRI to digest hemi-methylated versus fully cytosine-methylated DNA of the herpes tk promoter region. *Gene.* Vol. 74(1):147-9.

Dankwoord

Dit was het dan. De klus is geklaard. Maar niet zonder de hulp van de mensen die ik hierbij wil bedanken. Het lijkt nog maar kort geleden dat ik in een lege kamer werd gestald met een oude, door Sacco afgedankte computer, met de opdracht me in te lezen in het onderwerp. Het onderwerp was me bekend maar het project waar ik aan zou werken? Het was me niet helemaal duidelijk en ik vroeg me af waar ik in hemelsnaam aan begonnen was. Gelukkig kwam na 2 weken Rumyana met haar spullen onder de arm mijn kamer bevolken. Ze was ook pas begonnen en zat bij Sophia, maar was verzocht te verhuizen naar mij omdat wij in dezelfde groep zouden werken. Al snel bleek dat we gelijkgestemde zielen waren en zij veel voor mij ging betekenen. Maar daarover later meer. Allereerst wil ik hierbij Sacco de Vries bedanken voor de kans die hij mij gegeven heeft om in zijn groep promotieonderzoek te doen. Ik heb veel geleerd en ben je daarvoor dankbaar. De vonken die soms van onze dinsdagse werkbesprekingen afspatten zorgden voor sprongen voorwaarts in mijn onderzoek. Ik kijk terug op een goede tijd en bedank je voor jouw vertrouwen.

Jan Willem, jou wil ik bedanken voor je praktische adviezen en hulp bij metingen voor dit proefschrift. Ondanks de "files" voor jouw kamer in de morgen, had je toch vaak tijd om even te buurten als ik je kamer in kwam met een kop koffie en een vraag. Zelfs door de muur heen hield je me op de hoogte van de nieuwste artikelen en andere zaken. Ik ga je missen in mijn nieuwe baan en hoop dat we contact zullen houden. Willy, hoewel ik je de laatste tijd niet zoveel heb gezien door jouw bezigheden elders, was je voor mij vooral van belang bij de aanvang van mijn onderzoek. Jij hebt me wegwijs gemaakt op de afdeling en hebt, hoewel je het er niet zo mee eens was, tóch met mij de grote slagerskoelkast in het VMT-lab schoon gemaakt omdat ik hem te vies vond om er mijn bacterieplaten in te stallen. Adrie, jij hebt mij geïntroduceerd in de wereld van de FCS en was altijd bereid om mij te helpen. Ook was je bereid om met mij zitting te nemen in de borrelcommissie ofwel de LQFDC (laboratory of Quantitative Food and Drink Consumption), nadat Vief en Mark vertrokken waren.

Mijn labgenote Cathy, hoewel mijn buur op de lab-bench, heb ik je eigenlijk veel te weinig gesproken. Ik had meer moeten profiteren van jouw kennis en ervaring. Mark K.; jij was altijd bereid te helpen als je dat kon en was een rots in de branding als enige heer op het lab. Jenny, I appreciate your help with constructs and your worries about the genetic part of my research. You urged me from the beginning to start transform plants. In my last year I fully understood why.

Rumyana, my greatest thanks are for you. You were my roommate, my lab mate and my soul mate. Thanks for all the occasions we discussed our research, our worries, our hopes and disappointments. We had lots of fun during all the lunches we took, in the beginning at the chemistry building, and later in the Biotechnion. We never lacked subjects to talk about. I enjoyed your company and spirit during all the conferences and courses we went together. Thanks for all this. Ed, Sanne, Nienke and I would love to visit you and your family in Bulgaria in the future, after all I heard about your country. I wish you all the best and I am convinced that you await a bright future in Science. Isabella, I enjoyed your company in Madison, USA, and during all the social events we had. I will always remember your hospitality in Sienna when

I visited you there together with Rumyana.

Nicole, dank voor jouw gezelschap tijdens de vele koffiepauzes. Jij ging gelijk op met jouw promotieonderzoek en het was altijd leuk om de wederzijdse vorderingen door te nemen. Bedankt dat jij mijn paranimf wilde zijn, en veel succes in de toekomst.

Mijn studenten Karin, Lucas, Renske, Thierry en Ruud hebben allen in meer of mindere mate bijgedragen aan het tot stand komen van dit proefschrift; bedankt daarvoor. Alle andere collega's van Biochemie; bedankt voor jullie interesse, hulp en gezelligheid. Ik heb een bijzonder leuke tijd gehad en zal jullie missen. Ook Laura bedankt voor jouw luisterend oor en efficiënte afhandeling van allerlei administratieve zaken. Marijke, ik zal onze gesprekken missen, maar we zien elkaar vast nog wel op de school van onze kinderen of in een of andere tuin. Ellen; de vrijdagse wandelingen in het Bennekomse bos hielpen mij de zaken weer op een rijtje te zetten en Nicoline; jou nuchterheid en relativeringsvermogen maakten het leven weer simpel. Jépé, Petra en Hans, Monique en Robbert (Komt die beloofde speech er echt?), Jeffrey en Christine, Connie en Leo, Petra en Peter, Corina en Daan, Karin en Chinedu, Lidwien, dank voor jullie langdurige vriendschap en steun. Johan en Elly, jullie vriendschap is mij zeer dierbaar en onze genuttigde wijntjes van tijd tot tijd hielpen mij even het onderzoek op de achtergrond te schuiven. Al mijn vrienden en vriendinnen die ik hier niet met name genoemd heb wil ik bedanken voor hun belangstelling en vriendschap. Rest mij nog te bedanken de leden van de badmintonclub die belangstelling toonden in mijn onderzoek.

Mijn zussen Ina en Trudy, broers Ton, André, Jan en Jeroen, zwager Ruud en schoonzussen Monique, Miranda en Fatima; onze talrijke gezellige familiebijeenkomsten hielpen mij te relaxen en het onderzoek te relativeren. Dit geldt natuurlijk ook voor de schoonzussen en zwagers Ed, Lily, Tom, Desirée, Frank en Helga. Dank ook aan mijn dochters Sanne en Nienke, die altijd bereid waren de puntjesdozen te vullen als ik op zondag naar het lab moest om kolonies aan te prikken, en die nog blijer waren dan ik wanneer een artikel geaccepteerd was. Jullie begrip als ik weer eens 's avonds moest werken en Nienke's hulp bij het opschrijven van de eindeloze wortel lengtemetingen, vaak in het weekend, zal ik nooit vergeten.

Mam, bedankt voor jouw belangstelling en zorg. Je vroeg je af of het niet allemaal te zwaar was voor mij en vond eigenlijk dat ik wel genoeg had geleerd, maar bent tegelijkertijd heel trots. Jammer dat pap dit niet meer samen met jou mag meemaken. Jopie, jouw steun en belangstelling waren belangrijk voor mij.

En dan Ed. Zonder jou was ik hier nooit aan begonnen. Jij stimuleerde mij om verder te studeren toen ik spijt had dat ik dat nooit gedaan had. Vervolgens stimuleerde je mij om een promotieonderzoek te gaan doen en deed zelf een stapje terug. Jouw liefde, belangstelling en zorg maakten dat ik het heb volbracht. Jouw heerlijke maaltijden elke dag en de zorg voor Sanne en Nienke zorgden dat ik met een gerust hart laat thuis kon komen om mijn FCS metingen of andere experimenten af te maken. Je zorgde altijd dat de koelkast vol lag als je zelf weer eens voor een week naar Italië moest, om het mij makkelijker te maken. Ik hoop dat ik in de toekomst meer voor jou kan doen. Ik koester me in jouw warmte en zeg met Neil Diamond; "You're the best part of me".

Curriculum Vitae

José Aker werd geboren op 3 februari 1963 te Ursem (N.H.). Op 5 jarige leeftijd verhuisde zij naar Zwaagdijk-West. In juni 1982 behaalde zij het Atheneum B diploma aan het St. Werenfridus Lyceum te Hoorn. In juni 1986 behaalde zij het diploma van de Hogere Laboratorium School, richting Botanie, aan het Ir. W. van den Broek Instituut te Amsterdam. Vervolgens was zij werkzaam als analist bij het Academisch Ziekenhuis Leiden (het huidige LUMC), bij de afdeling Moleculaire Genetica o.l.v Prof. Piet van der Putte. Hier verrichtte zij onderzoek naar de methylering en amplificatie van het eiwit thymidine kinase, onder begeleiding van Dr. Judith Tasseron-de Jong. In 1990 verplaatste zij haar werkterrein naar Het Nederlands Kanker Instituut te Amsterdam, om in de groep van Dr. Wim van Blitterswijk op de afdeling Cellulaire Biochemie o.l.v. van Prof. Dr. Wouter Moolenaar, te gaan werken. Hier verrichtte zij onderzoek naar het enzym Diacyl Glycerol kinase onder begeleiding van Dr. Dick Schaap en vervolgens naar de rol van 14-3-3 eiwitten in signalering onder begeleiding van Dr. Paul van der Hoeven. In 1996 werd het Pedagogisch Didactisch Diploma behaald aan de Pedagogisch Technisch Hogeschool Nederland, vestiging Amsterdam. In 1997 werd zij analist in de groep van Dr. Kees Jalink op de afdeling Celbiologie o.l.v. Dr. Ed Roos, waar zij geavanceerde microscopische technieken gebruikte om interacties tussen fluorescent gelabelde eiwitten te meten. In 2002 en 2003 heeft zij Medische Biologie gestudeerd aan de Vrije Universiteit van Amsterdam, waarvoor zij het hoofdvak Immunologie volgde bij de afdeling Experimentele Immuno-hematologie, onderdeel van Sanquin te Amsterdam, o.l.v Dr. Dirk Roos. Daar heeft zij de signalerings routes in de transendothele migratie van leukocyten bestudeerd onder begeleiding van Dr. Jaap van Buul en Dr. Peter Hordijk. In augustus 2003 werd zij aangesteld als wetenschappelijk medewerker bij de afdeling Biochemie van de Wageningse Universiteit, o.l.v. Prof. Dr. Sacco de Vries, waar zij de rol van de co-receptoren in het BRI1-SERK signalerings complex heeft bestudeerd. De resultaten daarvan hebben geleid tot dit proefschrift. Vervolgens is zij aangesteld per augustus 2008, als docent bij het Rijnijssel College te Arnhem.

Education Statement of the Graduate School
Experimental Plant Sciences

Issued to: **José Aker**
Date: **8-Oct-08**
Group: **Laboratory of Biochemistry, Wageningen University**

1) Start-up phase		*date*	*cp*
►	**First presentation of your project**		
	Arabidopsis protoplasts as a modelsystem for endocytosis	April 18, 2004	1.5
►	**Writing or rewriting a project proposal**		
►	**Writing a review or book chapter**		
	Plasma membrane receptor complexes, Update - Plant Physiology 147 (2008), pp. 01-05	Aug 2008	6.0
►	**MSc courses**		
►	**Laboratory use of isotopes**		
	Subtotal Start-up Phase		7.5

2) Scientific Exposure		*date*	*cp*
►	**EPS PhD student days**		
	VU, Amsterdam	Jun 03, 2004	0.3
	RU, Nijmegen	Jun 20, 2005	0.3
	WU, Wageningen	Sep 18, 2006	0.3
	WU, Wageningen	Sep 13, 2007	0.3
►	**EPS theme symposia**		
	EPS Theme 1 symposium Developmental Biology of Plants, Wageningen University	Feb 17, 2004	0.3
	EPS Theme 1 symposium Developmental Biology of Plants, Leiden University	Apr 26, 2005	0.3
►	**NWO Lunteren days and other National Platforms**		
	NWO chemische wetenschappen; Lipids and biomembranes, Lunteren	Mar 08-09, 2004	0.6
	NWO chemische wetenschappen; Lipids and biomembranes, Lunteren	Mar 14-15, 2005	0.6
	NWO chemische wetenschappen; Lipids and biomembranes, Lunteren	Mar 06-07, 2006	0.6
	NWO chemische wetenschappen; Lipids and biomembranes, Lunteren	Mar 05-06, 2007	0.6
	NWO chemische wetenschappen; studiegroep Protein Research, Lunteren	Dec 12-13, 2005	0.6
	NWO chemische wetenschappen; studiegroep Protein Research, Lunteren	Dec 11-12, 2006	0.6
	ALW-EPS Lunteren	Apr 05-06, 2004	0.6
	ALW-EPS Lunteren	Apr 04-05, 2005	0.6
	ALW-EPS Lunteren	Apr 03-04, 2006	0.6
	ALW-EPS Lunteren	Apr 02-03, 2007	0.6
	ALW-EPS Lunteren	Apr 07-08, 2008	0.6
►	**Seminars (series), workshops and symposia**		
	Adv. Microscopy day, UVA, Amsterdam	Mar 30, 2004	0.3
	Flying seminar Steven Clark	Jun 28, 2004	0.1
	Flying seminar Philip Benfey	Sep 29, 2005	0.1
	Flying seminar Joseph Ecker	Oct 25, 2005	0.1
	Seminar Biochemistry, Jiri Friml	Jun 14, 2006	0.1
	Seminar Biochemistry, D. Chinchilla	Apr 24, 2008	0.1
	Seminar Biochemistry, N. Geldner	Jun 29, 2008	0.1
	Seminar Biochemistry, Jan Lohman	Jun 26, 2008	0.1
►	**Seminar plus**		
	Flying seminar Steven Clark	Jun 28, 2004	0.1
	Seminar Biochemistry, D. Chinchilla	Apr 24, 2008	0.1
	Seminar Biochemistry, N. Geldner	Jun 29, 2008	0.1
	Seminar Biochemistry, Jan Lohman	Jun 26, 2008	0.1
►	**International symposia and congresses**		
	EPSO conf. Italy	Oct 10-14, 2004	1.5
	Arabidopsis conf. Madison, USA	Jun 15-19, 2005	1.5
	6th International conf. on AAA proteins, Graz, Austria	Sep 14-18, 2005	1.5
	Arabidopsis conf. Beijing, China	Jun 20-23, 2007	1.2
	Plant Cell Biology Conf, Cologne, Germany	Sep 05-06, 2007	0.6
	ELSYS conf. Enschede, The netherlands	Feb 24-26, 2008	0.9
►	**Presentations**		
	Meeting with group Angenent at PRI, oral	Feb 15, 2005	0.7
	Arabidopsis conf. Madison, USA, poster	Jun 15-19, 2005	
	6th International conf. on AAA proteins, Graz, Austria, poster plus oral	Sep 14-18, 2005	1.4
	Advanced course on digital microscopy, Heidelberg, Germany, oral	Oct 01-06, 2006	0.7
	NWO chemische wetenschappen; studiegroep Protein Research, Lunteren, poster plus oral	Dec 11-12, 2006	1.4
	ALW-EPS Lunteren, poster plus oral	Apr 02-03, 2007	1.4
	ALW-EPS Lunteren, poster,	2004,2005,2006	2.1
	Arabidopsis conf. Beijing, China, poster	Jun 20-23, 2007	
	Meeting with group Angenent PRI, oral	Jun 28, 2008	0.7
	ELSYS conf. Enschede, The Netherlands, poster plus oral	Feb 24-26, 2008	1.4
►	**IAB interview**	Sep 18, 2006	0.7
►	**Excursions**		
	Subtotal Scientific Exposure		27.5

3) In-Depth Studies		*date*	*cp*
►	**EPS courses or other PhD courses**		
	Bioinformation -Technology-1, VLAG, Wageningen	Dec 8-16, 2004	2.1
	Summerschool EPS Signaling and development	Jun 19-21, 2006	0.9
	Advanced course on digital microscopy, Heidelberg, Germany	Oct 01-06, 2006	1.8
►	**Journal club**		
	Literature, Biweekly at Biochemistry, oral once per year	2004-2008	3.0
►	**Individual research training**		
	Subtotal In-Depth Studies		7.8

4) Personal development		*date*	*cp*
►	**Skill training courses**		
	Techniques for writing and presenting a Scientific paper	Nov 22-25, 2004	1.2
►	**Organisation of PhD students day, course or conference**		
►	**Membership of Board, Committee or PhD council**		
	Subtotal Personal Development		1.2

TOTAL NUMBER OF CREDIT POINTS*		**44.0**

* A credit represents a normative study load of 28 hours of study